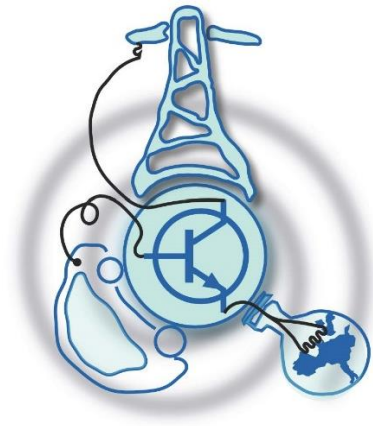


Modelling for Integration in Electricity Grids with Advanced Grid Code Requirements and Study the Viability of DC-DC BESS of a Solar PV Power Plant

by

Danial Saleem



Submitted to the Department of Electrical Engineering, Electronics, Computers and Systems in partial fulfilment of the requirements for the degree of Erasmus Mundus Masters Course in Sustainable Transportation and Electrical Power Systems at the
UNIVERSITY OF OVIEDO

September 2017

© University of Oviedo 2017. All rights reserved.

Author.....

Certified by.....

Ms. Mireia Barenys Espadaler & Mr. David Novak

Gamesa Electric Spain

Certified by.....

Dr. Pablo García Fernández

University of Oviedo

Modelling for Integration in Electricity Grids with Advanced Grid Code Requirements and Study the Viability of DC-DC BESS of a Solar PV Power Plant

by

Danial Saleem

Submitted to the Department of Electrical Engineering, Electronics, Computers and Systems on September 5, 2017, in partial fulfilment of the requirements for the degree of Erasmus Mundus Master Course in Sustainable Transportation and Electrical Power Systems

Abstract

This Master Thesis focuses on solar PV (Photovoltaic) plant integration in electrical power systems and the problem of power variability from a solar PV power plant. It presents an analysis to test the grid interconnectivity of Gamesa Solar PV inverter model by performing load flow, short circuit and dynamic stability studies. It evaluates the compliance of the PV inverter for Mexican Grid Code requirements of LVRT/HVRT (Low Voltage Ride Through/ High Voltage Ride Through), frequency response and active power regulation.

To accommodate the effect of spatial and temporal diversification on the measured irradiance data from a single sensor, different methodologies are compared, with WVM (Wavelet Variability Model) methodology being selected for further analysis. It studies the power ramping issue in a solar PV plant and evaluates the feasibility of DC coupled BESS (Direct Current Coupled Battery Energy Storage System) to minimize the power ramp-down problem. It also determines the economic viability and best design size for this DC coupled BESS.

Thesis Supervisor: Ms. Mireia Barenys

Title: Head of Control and Modelling section, Gamesa Electric Spain.

Thesis Co-Supervisor: Dr. Pablo García Fernández

Title: Associate Professor, University of Oviedo

ACKNOWLEDGEMENTS

I am thankful to the team of Gamesa Electric Spain (Mr. Andres Agudo Araque, Ms. Mireia Barenys Espadaler, Mr. David Novak and Mr. Miguel Ochoa Giménez) and the complete faculty of electrical engineering, University of Oviedo. First of all I would like to express my sincere gratitude to the thesis supervisor, Ms. Mireia Barenys and to Mr. David Novak from Gamesa Electric Spain for their support and continuous guidance without which this dissertation would have not been possible.

I am also very thankful to Dr. Pablo García Fernández for guiding me throughout the thesis. I would like to extend my appreciation to all my professors from University of Oviedo, ISEC Coimbra and University of Nottingham for providing me the basic knowledge to perform this research.

Contents

Chapter 1 Introduction.....	1
1.1 Research Objectives	1
1.2 Research Methodology.....	1
1.3 Thesis Overview.....	2
Chapter 2 Modelling of Gamesa Solar PV Power Plant and Associated Technical Studies	3
2.1 Introduction	3
2.2 Preparation of PSS/E Base Case	3
2.3 Integration of Gamesa Solar PV Power Plant and Associated Technical Studies	5
2.3.1 Modelling of Gamesa Solar Power Plant.....	5
2.3.2 Load Flow Analysis	7
2.3.3 Short Circuit Analysis.....	8
2.3.4 Transient Stability Analysis.....	9
2.3.4.1 Observations and Comments on Stability Analysis	15
2.3.4.2 Verification Using IEEE-14 Bus System.....	15
Chapter 3 Grid Code Compliance of Gamesa Solar PV Power Plant Model	20
3.1 Introduction	20
3.2 LVRT/HVRT Studies.....	20
3.2.1 Zero-voltage fault for 400 msec (0.40 sec).....	22
3.2.2 0.45 p.u. voltage fault for 600 msec (0.60 sec).....	22
3.2.3 0.7 p.u. voltage fault for 700 msec (0.70 sec).....	24
3.3 Frequency Response and Active Power Regulation	25
Chapter 4 Methodologies for Solar PV Plant Output Patterns and Ramp-Down Analysis	31
4.1 Introduction	31
4.2 PV Plant Dimensioning.....	31
4.2.1 Data Inputs	31
4.2.2 Design Calculations	32
4.2.3 PV Plant Dimensions Calculations	32
4.3 Categorization of Solar Days	33
4.4 Power Production Calculations	34
4.4.1 Data Inputs	35
4.4.1.1 Solar Irradiation and Temperature	35
4.4.1.2 PV Panel Parameters.....	35
4.4.1.3 Efficiencies	35
4.4.2 Equations.....	35
4.5 Methodologies for Power Output Profile Determination.....	36
4.5.1 Single-section & N-section Methods	36
4.5.1.1 Cloud Movement Modelling for the PV Plant in N-section method	36
4.5.2 WVM Method.....	38
4.5.2.1 Introduction.....	38
4.5.2.2 WVM Methodology	39
4.5.2.2.1 GHI Normalization.....	39

4.5.2.2.2	Wavelet Decomposition	40
4.5.2.2.3	Distances Computation	41
4.5.2.2.4	Correlations	42
4.5.2.2.5	Variability Reduction	43
4.5.2.2.6	Inverse Wavelet Transform:	44
4.5.2.3	Procedure to Use WVM Toolbox	44
4.5.2.4	Inputs Used in the Program	45
4.5.2.4.1	Sensor Inputs: [20]	46
4.5.2.4.2	Solar Plant Inputs:	46
4.5.2.4.3	Cloud Input:	46
4.5.2.4.4	Irradiance and Temperature Inputs:	46
4.5.2.4.5	Timestamps:	46
4.5.2.5	WVM Toolbox Explanation	46
4.5.2.6	Input Flow Diagram	49
4.5.3	Comparison of Three Methods for Power Patterns	51
4.6	Power Ramp-Down Analysis	52
4.6.1	PV Plant Power Ramp-Down literature review	52
4.6.2	Power Ramp-Downs Sensitivity Analysis for N-sections Method	53
4.6.3	Comparison of Three Methods for Power Ramps	56
4.6.4	Conclusions	58
Chapter 5 Sizing and Economic Viability of DC-DC BESS		59
5.1	Introduction	59
5.2	Literature Review of BESS for Solar PV Installations	60
5.3	Topology of DC BESS	62
5.4	Assumptions	62
5.5	Methodology	63
5.6	Comparison of the two Approaches	66
5.7	Sizing the DC-BESS	67
5.8	Battery Degradation Considerations	69
5.9	Distribution Plots	70
5.10	Economic Analysis	72
Chapter 6 Conclusion		76
6.1	Conclusions	76
6.2	Future Work	77

List of Figures

Figure 2.1. IEEE 118-bus Test System.....	5
Figure 2.2. Plots for Analysis No.1.....	11
Figure 2.3. Plots for Analysis No.2.....	12
Figure 2.4. Plots for Analysis No.3.....	13
Figure 2.5. Plots for Analysis No.4.....	14
Figure 2.6. IEEE-14 bus system [6].....	16
Figure 2.7. Active Power Plot for Stability Analysis with IEEE-14 bus system.....	17
Figure 2.8. Reactive Power Plot for Stability Analysis with IEEE-14 bus system	17
Figure 2.9. Bus Voltage Plot for Stability Analysis with IEEE-14 bus system.....	18
Figure 2.10. Frequency Plot for Stability Analysis with IEEE-14 bus system.....	18
Figure 3.1. Plot for Grid Code Compliance for LVRT/HVRT – Plotted for 10 seconds	21
Figure 3.2. Plot for Grid Code Compliance for LVRT/HVRT – Plotted for 1 second.....	21
Figure 3.3. Zero-voltage fault for 400 msec (0.4 sec)	22
Figure 3.4. 0.45 p.u. voltage fault for 600 msec (0.6 sec)	23
Figure 3.5. Voltage response from Bus # 13	23
Figure 3.6. 0.7 p.u. voltage fault for 700 msec (0.7 sec)	24
Figure 3.7. Voltage response from Bus # 33	25
Figure 3.8. Plots for Case A.....	27
Figure 3.9. Plots for Case B	28
Figure 3.10. Plots for Case C	29
Figure 4.1. Distribution Plot for DARR Categories	33
Figure 4.2. Comparison of Irradiance for Cat.1 and Cat.5 Solar Days.....	34
Figure 4.3. Simplified Cloud Movement Modelling (Position at t = 0)	37
Figure 4.4. Solar PV power plant output for minutely irradiance data – sections’ output and total output (zoomed-in)	38
Figure 4.5. Measured and WVM-smoothed irradiance data.....	39
Figure 4.6. Wavelet Modes and Clear Sky Index Time-series for dataset of August 2016.....	41
Figure 4.7. Distance (dmn) Plot – zoomed-in.....	42
Figure 4.8. Wavelet correlation versus the distance between inverters (exponential decay model) [15].....	42
Figure 4.9. Input Flow Diagram	50
Figure 4.10. Comparison of power output from Solar PV plant for 3 methods (zoomed-in)..	52
Figure 4.11. Scenario 1 Solar Ramp outputs	54
Figure 4.12. Scenario 2 Solar Ramp outputs	54
Figure 4.13. Scenario 3 Solar Ramp outputs	55
Figure 4.14. Scenario 4 Solar Ramp outputs	55
Figure 4.15. Comparison of power ramps from Solar PV plant for 3 methods.....	56
Figure 4.16. Comparison of power ramps from Solar PV plant for 3 methods (zoomed-in) ..	56
Figure 4.17. Distribution Plot for power ramps for three methods.....	57
Figure 4.18. CDF Plot for Power Ramp Rates for three methods	58
Figure 5.1. PV plant power outputs	59
Figure 5.2. Extra Available DC Clipped Energy	60
Figure 5.3. Topology of DC Coupling for Solar PV plant [28].....	62

Figure 5.4. Power Output Plots.....	65
Figure 5.5. Comparison of the two approaches (zoomed-in).....	66
Figure 5.6. State of Charge of Battery System	70
Figure 5.7. Ramp-downs Distribution Plot.....	71
Figure 5.8. Power Distribution Plot	71
Figure 5.9. Energy-per-day Distribution Plot	72
Figure 5.10. Minimum Tariff Vs RRV Penalty Rate.....	75

List of Tables

Table 4.1. Variability Reduction for the modes of Wavelets	44
Table 5.1. Factors Calculated for BESS Approaches	67
Table 5.2. Results of Analysis – Power Ramp Calculations.....	68
Table 5.3. Factors Calculated for Battery System	69
Table 5.4. Results of Analysis – Minimum Tariff Calculations	74

List of Abbreviations

AC	Alternating current
BESS	Battery Energy Storage System
BUF	Battery Utilization Factor
CDF	Cumulative probability Distribution Function
CSI	Clear Sky Index
DARR	Daily Aggregate Ramp Rate
DC	Direct current
GHI	Global Horizontal Irradiance
HESS	Hybrid Energy Storage System
HV	High Voltage
HVRT	High Voltage Ride Through
LV	Low Voltage
LVRT	Low Voltage Ride Through
MV	Medium Voltage
MVA	Mega Volt Ampere
MVAR	Mega Volt Ampere Reactive
MWp	Mega Watt peak
NOCT	Nominal Operating Cell Temperature
NREL	National Renewable Energy Laboratory
PCC	Point of Common Coupling
PPA	Power Purchase Agreement
PPC	Power Plant Controller
PREPA	Puerto Rico Electric Power Authority
PSS	Power System Stabilizer
PSS/E	Power System Simulation for Engineering
P.U.	Per Unit
PV	Photovoltaic
ROI	Return on Investment
RRV	Ramp Rate Violation
SOC	State of Charge
STC	Standard Test Conditions

VR Variability Reduction
WVM Wavelet Variability Model

Keywords

Battery Energy Storage Systems, Daily Aggregate Ramp Rate, Gamesa, High Voltage Ride Through, Load Flow, Low Voltage Ride Through, Power Ramp Downs, Short Circuit, Solar PV Inverter, System Stability, Wavelet Variability Model.

List of Symbols

B	Susceptance
d_{mn}	Distance between sites m and n
G	Irradiance
G_{ref}	Reference irradiance at STC
E_{term}	Terminal Voltage of PV Inverter
P_{elec}	Active Power Output of PV Inverter
P_{mech}	Mechanical Power Output of PV Inverter
$P_{mp,ref}$	Maximum power of the PV module at STC
ρ	Correlation
Q_{elec}	Reactive Power Output of PV Inverter
γ	Temperature coefficient of the PV module
R	Resistance
T_a	Ambient temperature
T_{ref}	Reference ambient temperature at STC
X	Reactance

Chapter 1

Introduction

1.1 RESEARCH OBJECTIVES

The purpose of the thesis is to carry out the solar PV plant modelling for integration in electricity grids with advanced grid connection requirements and develop a technique to investigate the viability of DC-DC BESS for a solar PV power plant depending upon the factors of power ramping and economics involved. The main research questions are as follows:

- a. Will Gamesa's Solar PV model pass the general criteria of grid interconnectivity? If no, does it need any changes?
- b. Is Gamesa's Solar PV model compliant with the Mexican grid code? If no, does it need any improvements?
- c. How to determine the reliable solar output profiles based on measured one-point solar irradiance data? Is there any problem of the power ramp-downs based on the output patterns? If yes, how to mitigate it?
- d. What are the benefits of applying DC-DC BESS? Will it help to reduce the power-ramping problem? Is DC-DC BESS economically viable based on the amount of extra captured energy and avoided RRV cost? What would be the optimal rating of it?

1.2 RESEARCH METHODOLOGY

The analysis is divided into two major parts, each one being performed in a different software, PSS/E and MATLAB for first and second type of analyses respectively. It is important to mention here that the second type of analysis is performed using measured available data for 8.5 months provided by Gamesa Electric and the technique developed can be applied to evaluate feasibility of any solar PV plant with available irradiance data. The main steps followed in the thesis are as follows:

- a. Modelling of solar PV power plant for Gamesa model of an inverter in IEEE-118 bus system network using PSS/E software.

- b. Performing grid integration studies (load flow, short circuit and transient stability) for verifying the validity of the provided model.
- c. Checking the compliance of the provided model according to Mexcan grid code.
- d. Comparing different approaches (single-section, N-section and WVM) to find the solar PV plant power output patterns according to available one-point solar irradiance data.
- e. Performing power ramp-down analysis occurred due to the clouding effect in the determined solar output profiles and carrying out PV plant dimensioning.
- f. Evaluating viability and determining optimal rating of DC-DC BESS based on penalties on ramp-rate violations, ramp-down smoothing and economics of the project.

1.3 THESIS OVERVIEW

The outline of the chapters after the chapter of introduction is given below:

Chapter 2 Modelling of Gamesa Solar PV Power Plant and Associated Technical Studies

This chapter includes the detailed modelling of the solar PV power plant for Gamesa provided model using IEEE-118 bus system. Furthermore, it discusses the related technical studies (load flow, short circuit and transient stability) performed for the model.

Chapter 3 Grid Code Compliance of Gamesa Solar PV Power Plant Model

This chapter explains the compliance of the provided solar PV plant model for most of the clauses of the grid code. The two major compliances checked are HVRT/LVRT and active power & frequency regulation.

Chapter 4 Methodologies for Solar PV Plant Output Patterns and Ramp-Down Analysis

This chapter discusses the different methodologies to determine solar PV power output profile and performing power ramp-down analysis. It also includes the dimensioning of the solar PV power plant.

Chapter 5 Sizing & Economic Viability of DC-DC BESS

This chapter discusses the sizing and economic viability of DC BESS to be installed to capture the clipped energy from the solar PV power plant.

Chapter 6 Conclusion It includes the drawn conclusions and recommendations for future research.

Chapter 2

Modelling of Gamesa Solar PV Power Plant and Associated Technical Studies

2.1 INTRODUCTION

This chapter comprises two sections. The first section explains the adopted methodology to prepare the power flow base case in PSS/E using IEEE-118 bus system. The second section discusses integration of Gamesa Solar PV Power Plant and related technical studies (load flow, short circuit and transient stability).

2.2 PREPARATION OF PSS/E BASE CASE

IEEE 118 bus system is modelled using PSS/E software. The available data of IEEE bus system is a simple approximation of American Electric power system (in year 1962) [5]. This IEEE 118-bus system contains 19 generators, 35 synchronous condensers, 177 lines, 9 transformers, and 91 loads. There is no available data for the line MVA limits and their parameters. It is quite outdated and not suitable for dynamic studies. For this reason, a good modern system using some assumptions and improvements in this available IEEE 118 bus system data has been developed.

The following improvements have been applied to the base case:

- Reactive power demands have been added for most of the connected loads.
- Power system stabilizers have been added to some of the buses to improve stability of the system.
- Active and reactive power generations from some of the generators have been changed.
- Resistance (Line R), inductance (Line X) and susceptance (Charging B) have been added for the transmission lines.
- MVA limits (Rate A) have been added for the transmission lines.
- Reactive power generation limits and scheduled voltage from some of the generators have been modified so that the generators shall generate reactive power within the limits.

- Dynamic parameters have been added for the preparation of base case for stability analysis.
- Dynamic modelling of motors and synchronous condensers has been ignored and only considered for the generators.
- The limits for exciters and governors have been changed for the stability base case preparation.
- Fixed shunts have been added to improve the voltage profile of the network.
- Some of the synchronous condensers are switched off for balancing reactive power generation.
- Active and reactive power demand of the loads have been modified at few buses to improve the power flows in the case.

For preparing base load flow case, following conditions have been satisfied and checked:

- All the transmission lines are under their 100% loading limit.
- The voltages at all the buses are within the limit of 0.95p.u. to 1.05p.u.
- All the generators are generating reactive power within their specified limits.

In the base case, the total active and reactive power generation is 4182.7 MW and 1639.3 MVAR respectively out of which 112.7 MW (2.694 %) are active power losses in the system. N-1 contingency analysis has not been performed for this network and will be performed for the network after the integration of the studies solar PV power plant. The oneline diagram of the IEEE-118 bus system has been shown in Figure 2.1. The load flow modelling without GAMESA Solar PV Power Plant along with its vicinity network in PSS/E has been shown in Diagram No. 1 (attached in Appendix). The modelled 54 GAMESA Solar PV plant is switched out and the stress on the system is determined. It is clear that there are no major bottlenecks in the system.

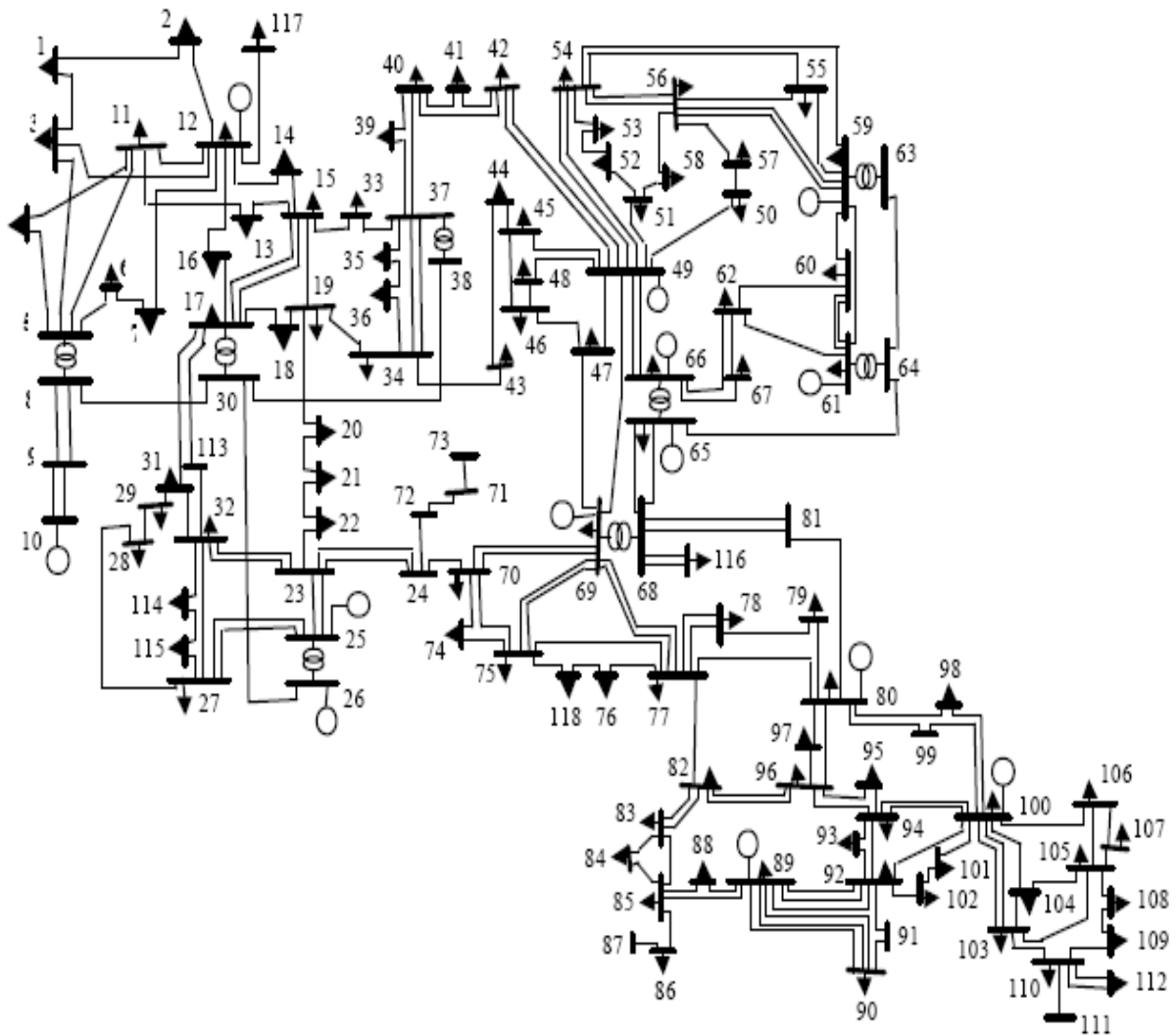


Figure 2.1. IEEE 118-bus Test System

2.3 INTEGRATION OF GAMESA SOLAR PV POWER PLANT AND ASSOCIATED TECHNICAL STUDIES

In this section, modelling of Gamesa solar power plant has been discussed along with associated technical studies (Load Flow, Short Circuit and Stability Analysis) to evaluate the impact of Gamesa solar PV plant on the system.

2.3.1 MODELLING OF GAMESA SOLAR POWER PLANT

The solar power plant has 24 solar PV inverters, each having rated output of 2.25 MW. Every two PV panel inverters are connected to 2-winding 0.66/20kV step-up transformer having 5 MVA rated power. These transformers are connected to 20kV collector bus. There are 3 collector buses each receiving output from 8 solar PV inverters. These collector buses are then connected to one MV bus at the substation. At the substation, this output has been stepped-up

using two transformers of 20/138kV 60 MVA each. To integrate this power into the grid network, the transmission line from Bus #11 to Bus #13 has been loop-in and out at 138kV Gamesa solar PV power plant substation.

Three MV collector cables of 20 kV are used in the plant connecting each group of the inverters to the MV bus at the substation.

Collector Line – 1 solar PV inverters 1-8 ($8 \times 2.25 = 18$ MW)

Collector Line – 2 solar PV inverters 9-16 ($8 \times 2.25 = 18$ MW)

Collector Line – 3 solar PV inverters 16-24 ($7 \times 2.25 = 18$ MW)

The parameters assumed for underground cable of collector lines are:

Resistance (Line R) = 0.019348 p.u.

Reactance (Line X) = 0.010905 p.u.

Charging (B) = 0.000006 p.u.

It is important to mention here that nomenclature adopted for the buses of the Solar PV power plant is as follows:

- Buses where solar PV inverters are connected having voltage level of 0.66kV and are imaginary buses: 110101, 110102, 110201, 110202, 110301, 110302,111101, 111102, 111201, 111202. (Total 24 buses)
- Buses where the output from two solar PV inverters is accumulated having voltage level of 0.66kV and are imaginary buses: 110103, 110203, 110303,111103, 111203. (Total 12 buses)
- Buses where the output from two solar PV inverters is accumulated after 0.66/20kV Step-up transformer having voltage level of 20kV and are imaginary buses: 1101, 1102, 1103,1111, 1112. (Total 12 buses)
- Collector group buses where the output from eight solar PV inverters is accumulated having voltage level of 20kV and are real buses: 99111, 99112, 99113. (Total 3 buses)
- Medium Voltage (MV) Collector Bus to receive the output from 3 collector group buses having voltage level of 20kV and is real bus: 9911
- High Voltage (HV) Bus in the substation from where the output from PV power plant is interconnected with the grid network having voltage level of 138 kV and is real bus: 110000

2.3.2 LOAD FLOW ANALYSIS

After integration of 54 MW GAMESA Solar PV power plant, Load flow analysis has been carried out for the developed IEEE-118 bus system base case. It has been assumed that the network in the vicinity of the power plant remains same till the commissioning of the said power plant. The dispatch from the conventional generators are kept same and no additional load has been added. It has been found that each transmission line is loaded under its rated power capacity and the voltage profile of all the buses (0.66 kV, 20 kV and 138 kV) is within the permissible range. Moreover, all power plants are operating within their rated range.

Additionally, the integration of this power plant improves the voltage profile in its vicinity and reduces the stress on the network. The total active and reactive power generation becomes 4181.9 MW and 1635.6 MVar respectively out of which 111.9 MW (2.675 %) are active power losses in the system. A slight improvement in the losses percentage can also be observed after the integration of the said solar PV power plant. The load flow modelling of GAMESA Solar PV Power Plant and its vicinity network in PSS/E has been shown in Diagram No. 2 (attached in Appendix).

The N-1 contingency analysis has also been performed in the close vicinity of 54 MW GAMESA Solar PV power plant and the load flow results are shown in the below mentioned diagrams attached as Appendix.

- Diagram 3: Transformer From 20kV GAMESAPV MV To 138kV GAMESAPV Switched Out (Contingency No.1)
- Diagram 4: Transmission Line From 138 kV GAMESAPV To Bus No. 11 Switched Out (Contingency No. 2)
- Diagram 5: Transmission Line From 138 kV GAMESAPV To Bus No. 13 Switched Out (Contingency No. 3)

The results indicate that all the power flows on the lines are within the nominal limits of the network and there are no limitations in terms of power transmitting capacity for normal as well as N-1 contingency condition.

2.3.3 SHORT CIRCUIT ANALYSIS

For preparing short circuit case, load flow base case has been modified and sequence (positive, negative and zero) parameters are entered in the case. The zero-sequence parameters for underground cables of collector lines are assumed equal to positive sequence parameters. Since for the transmission lines, positive and negative sequence parameters are equal, the zero-sequence parameters assumed for the transmission lines are:

- Resistance (R zero) = 0.037375 p.u.
- Reactance (X zero) = 0.168925 p.u.
- Charging (B zero) = 0 p.u.

Since the sequence data for the generators (both conventional and solar PV generators) is not available, the parameters like Zero X, Transient X, Sub-transient X, Synchronous X and Negative X (all in p.u.) are assumed to be equal to X source (p.u.). Similarly Zero R, Negative R and Positive R (all in p.u.) are assumed to be equal to 0.

Short Circuit Analysis has been carried out using the methodology of IEC 909 available in the PSS/E software. Maximum and minimum fault levels are calculated by assuming the bus voltages equal to 1.1 p.u. and 0.9 p.u. respectively i.e. 10 % above and below the nominal ones, according to IEC909. The following assumptions are used to calculate the fault currents under IEC909 standard:

- Set line charging to zero
- Set tap ratios to unity
- Set shunts to zero in positive sequence

The magnitude of short circuit levels have been calculated and plotted on the bus bars lying in the electrical vicinity of our area of interest (near 54 MW GAMESA Solar PV Power Plant). The results are shown in Diagram No. 6 and 7 for maximum and minimum short circuit levels respectively. Both single phase and three phase fault currents are mentioned in the diagrams which are shown in polar coordinates i.e. the angle and the magnitude of the current. The total fault currents are mentioned under the bus bars.

The tabular output of the short circuit calculations (both maximum and minimum) are also attached in the Appendix for the buses in the area of study i.e. near 54 MW GAMESA Solar PV Power Plant. It is the detailed output showing the contribution to the fault current from the connecting sources i.e. the transformers and lines connected to the bus. The sequence

impedances, the sequence currents and the phase currents are shown in detail for every faulted bus. It is evident that the determined maximum fault level do not exceed the short circuit rating of the equipment (assumed to be equal to 40 kA, one of the standard switchgear ratings at 138 kV) at these 138 kV substations.

2.3.4 TRANSIENT STABILITY ANALYSIS

For preparing the transient stability case, load flow base case has been modified to converted load flow case by transforming the generators and loads. The generators are modelled as current source model so that the generator dynamic models can be integrated. Similarly, since the loads are not constant power loads (as used in power flow case), the default convention has been adopted and active and reactive powers are modelled as 100% constant current and 100% constant impedance types respectively. Moreover PSS/E activities like FACT, ORDR and TYSL (required to prepare the case ready for switching studies) are performed as well. The dynamic data for all conventional generators is assumed to be same and PSS/E built-in models are used. GENROU, EXST1 and TGOV1 models are used for generator, exciter and governor respectively. For some of the generators, Power system stabilizer (PSS) has been attached and PSS/E built-in model of PSS2A is used. The parameters assumed for GENROU, EXST1, TGOV1 and PSS2A can be found in the attached stability case. It is important to mention that the dynamic modelling of motors and synchronous condensers is not considered and ‘GNET’ activity has been used for this purpose. For GAMESA solar PV inverter, the provided dynamic data has been incorporated in the stability case along with their user-defined model.

After adding dynamic data, channels have been defined to plot the outputs and snapshot file has been created. Several types of analysis have been carried out by applying different types of faults to check the transient stability of the system and 54 MW Solar PV power plant, which are:

- **Analysis Type 1, Normal Fault:** Three Phase Fault having Normal Clearing Time of 5 Cycles at 138 kV GAMESAPV (Bus No. 110000)
- **Analysis Type 2, Stuck Breaker Fault:** Three Phase Fault having Normal Clearing Time of 9 Cycles at 138 kV GAMESAPV (Bus No. 110000)
- **Analysis Type 3, Severe Fault Inside Solar PV Plant:** Three Phase Fault having Normal Clearing Time of 5 Cycles at 20 kV GAMESAMV (Bus No. 9911) along with tripping of one of the transformers

- **Analysis Type 4, Severe Fault In Close Vicinity of Solar PV Plant:** Three Phase Fault having Normal Clearing Time of 5 Cycles at 138 kV CONCORD (Bus No. 13) along with tripping of one of the associated transmission lines (Transmission line 13-15)

For each analysis type, several parameters are plotted to check the stability of the system which are:

- Active Power (MW) Output from 1 Solar PV Inverter
- Reactive Power (MVar) Output from 1 Solar PV Inverter
- Transmission Line Flows (both active and reactive power) from the solar PV plant into the grid network
- Bus bar voltages inside GAMESA Solar PV power plant and its associated substation
- Frequency of the system
- Rotor angles of the conventional generators

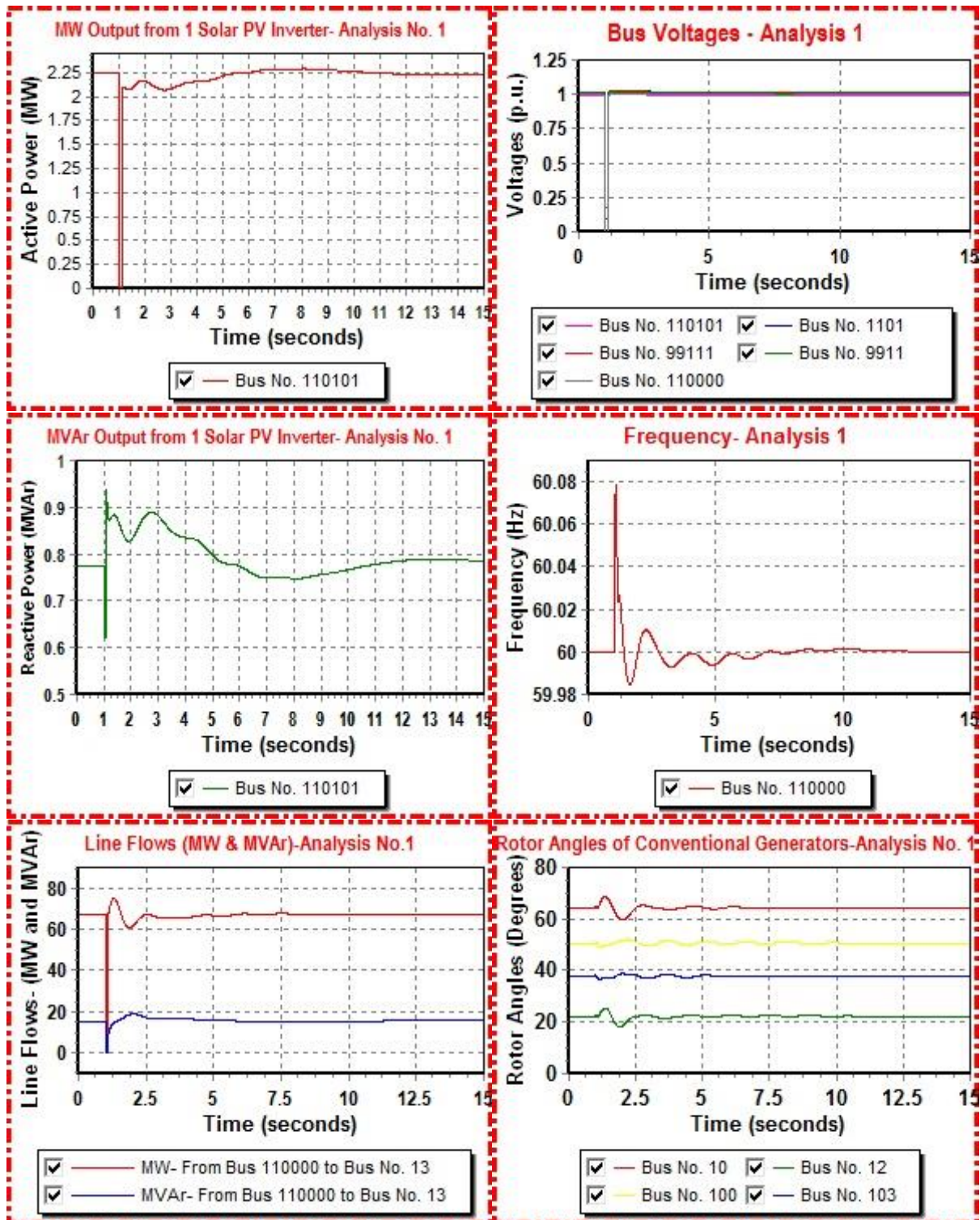


Figure 2.2. Plots for Analysis No.1

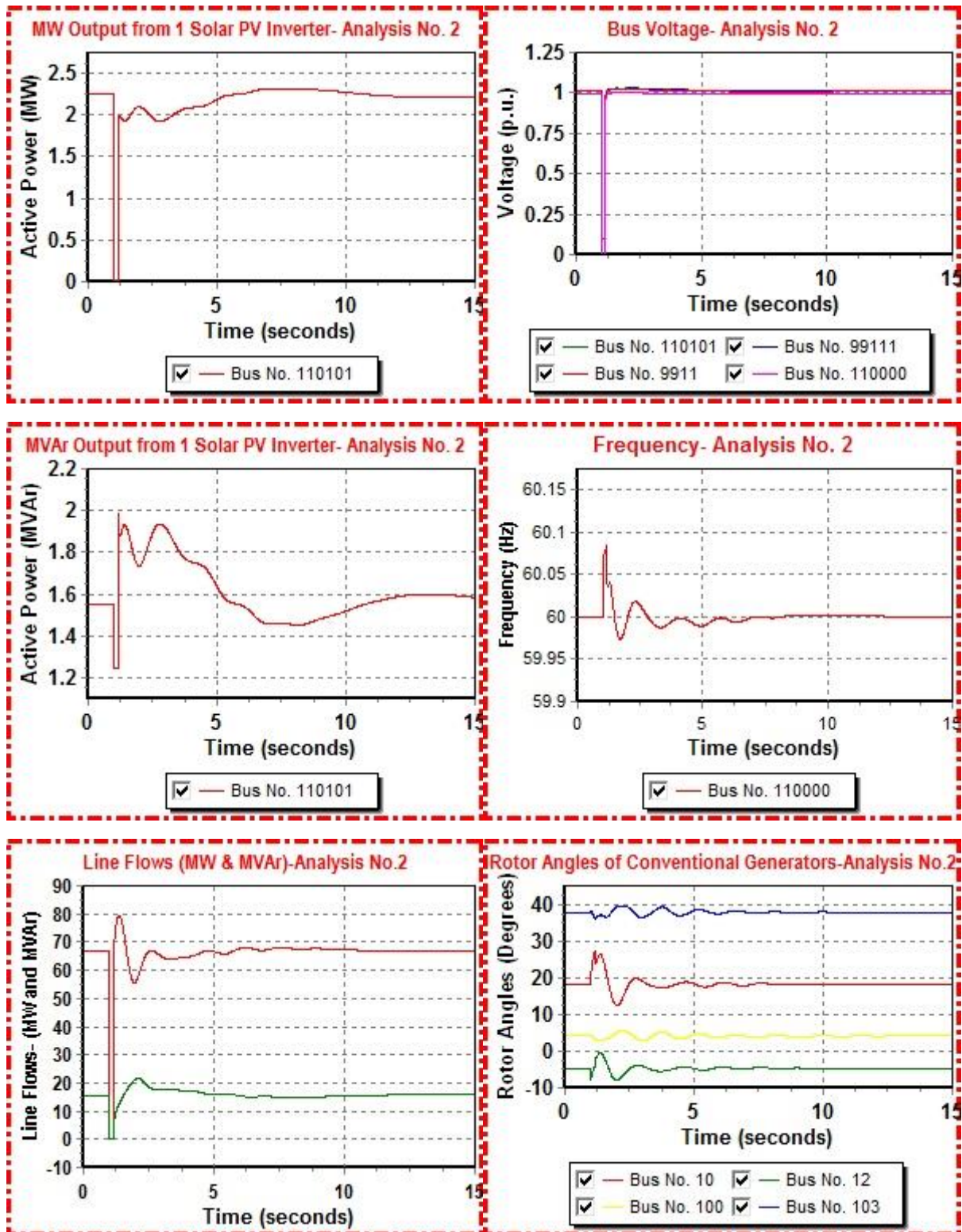


Figure 2.3. Plots for Analysis No.2

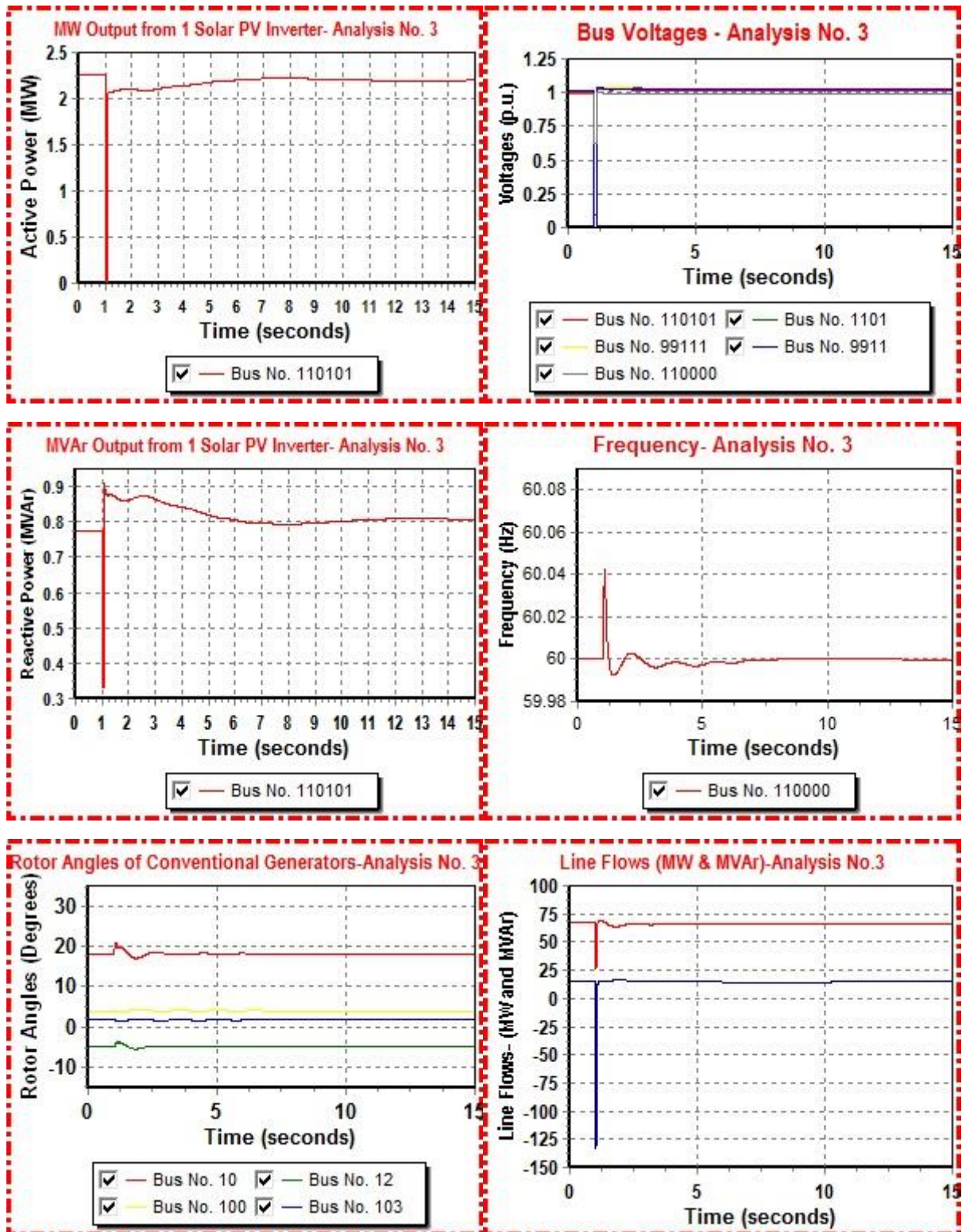


Figure 2.4. Plots for Analysis No.3

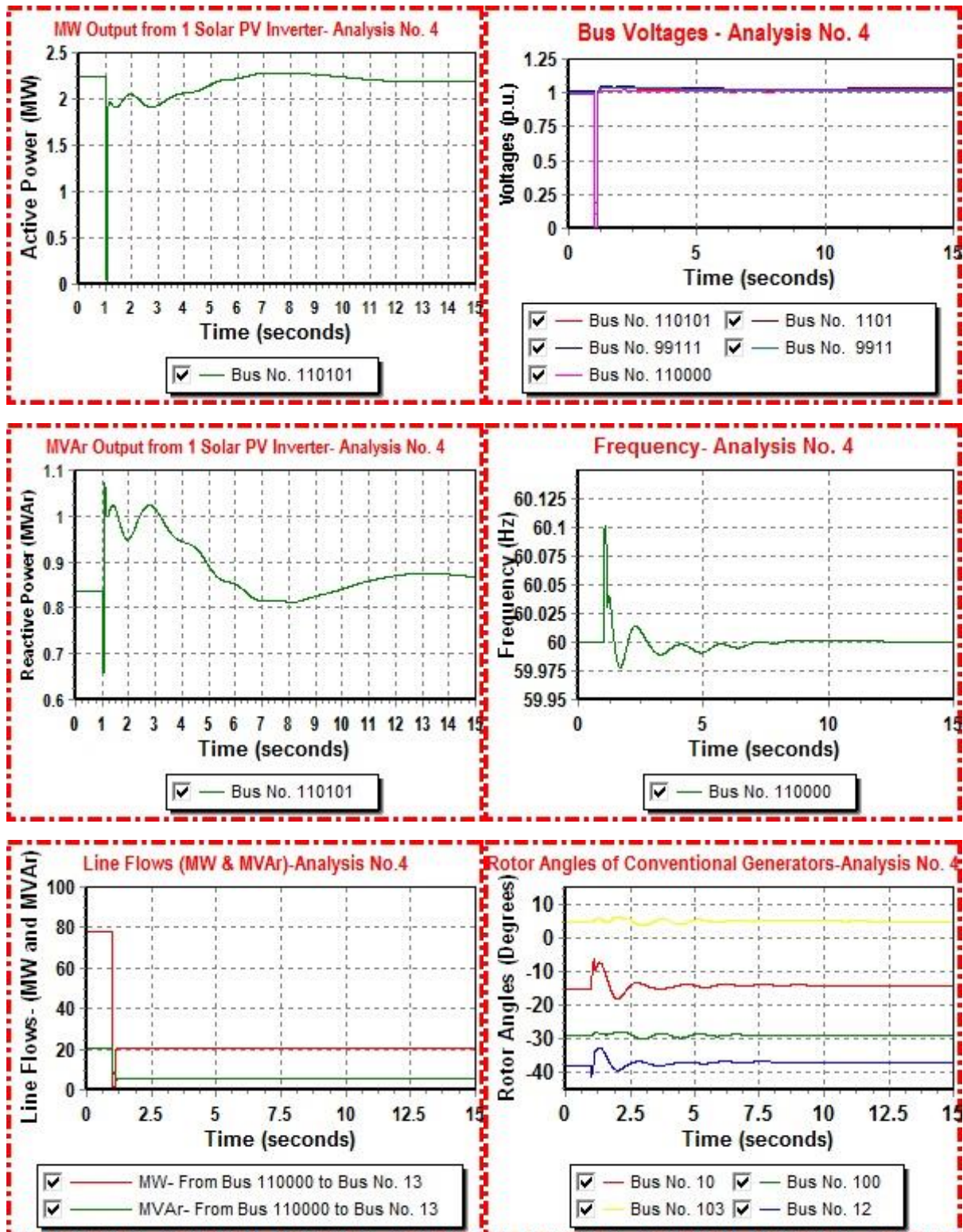


Figure 2.5. Plots for Analysis No.4

2.3.4.1 Observations and Comments on Stability Analysis

Some of the observations from above analysis (Analysis 1-4) are:

- The voltages recover smoothly and quickly to their pre-disturbance values (though in some cases, they become slightly higher which is not a problem)
- The system frequency shows nominal excursions of frequency that damps down.
- The MW and MVar output of the solar PV inverter return to normal after the fault clearance.
- The MW and MVar output on the adjacent transmission network return to normal after the fault clearance.
- The relative rotor angles of some of the other conventional generators of the system show that they remain in synchronism with the system generators and stay stable. The angular swings are also nominal and damped out with time.

The plots make it clear that the system is stable after integrating the 54 MW GAMESA Solar PV power plant. However, the active and reactive power outputs from the PV inverters along with the frequency is taking much time to return to normal state. This point needs to be further investigated. Moreover, the MW, MVar and voltage response from the PV inverter is not as smooth as mentioned in [3] and needs further improvement. The rotor angles are plotted only for conventional generators (to check angular stability of the system) and not required for solar power plants. It is important to mention here that the channels for plotting PV inverter quantities (Pelec, Qelec, Eterm, Pmech, etc.) are not functional in the provided model and this problem needs to be resolved.

2.3.4.2 Verification Using IEEE-14 Bus System

The results from above stability analysis is further verified by integrating 54 MW GAMESA Solar PV power plant into a simpler electrical grid. For this purpose, IEEE 14 bus system is used for the analysis. The solar power plant is connected with Bus No. 13 of the network. Similar to previous case, the dispatch from the generators have been adjusted in the base case and dynamic data for the conventional generators has been assumed as well. The IEEE-14 bus system has been shown in Figure 2.6.

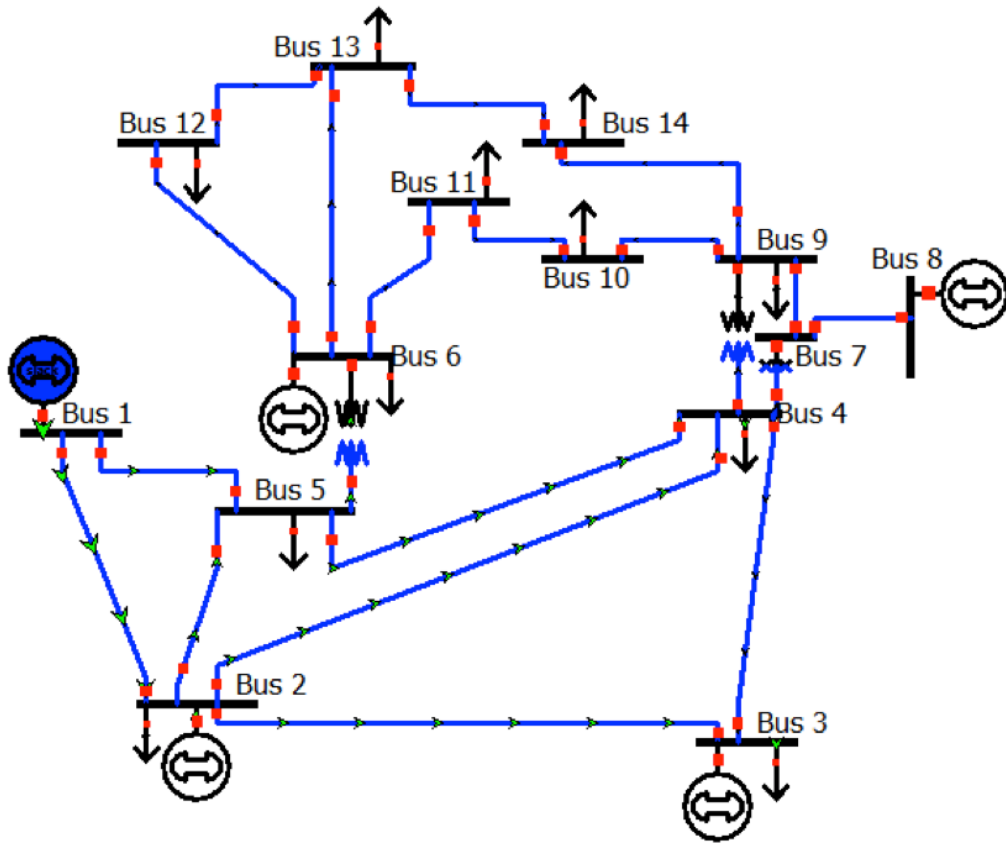


Figure 2.6. IEEE-14 bus system [6]

Here as well, transient stability analysis is carried out to check the response from 1 PV inverter of the solar power plant. Three phase fault having normal clearing time of 5 cycles has been applied at bus No. 9 and the response from a PV inverter has been observed. The plots for Active Power Output (MW), Reactive Power Output (MVA_r), Voltage response (p.u.) and frequency response (Hz) are shown in the below figures.

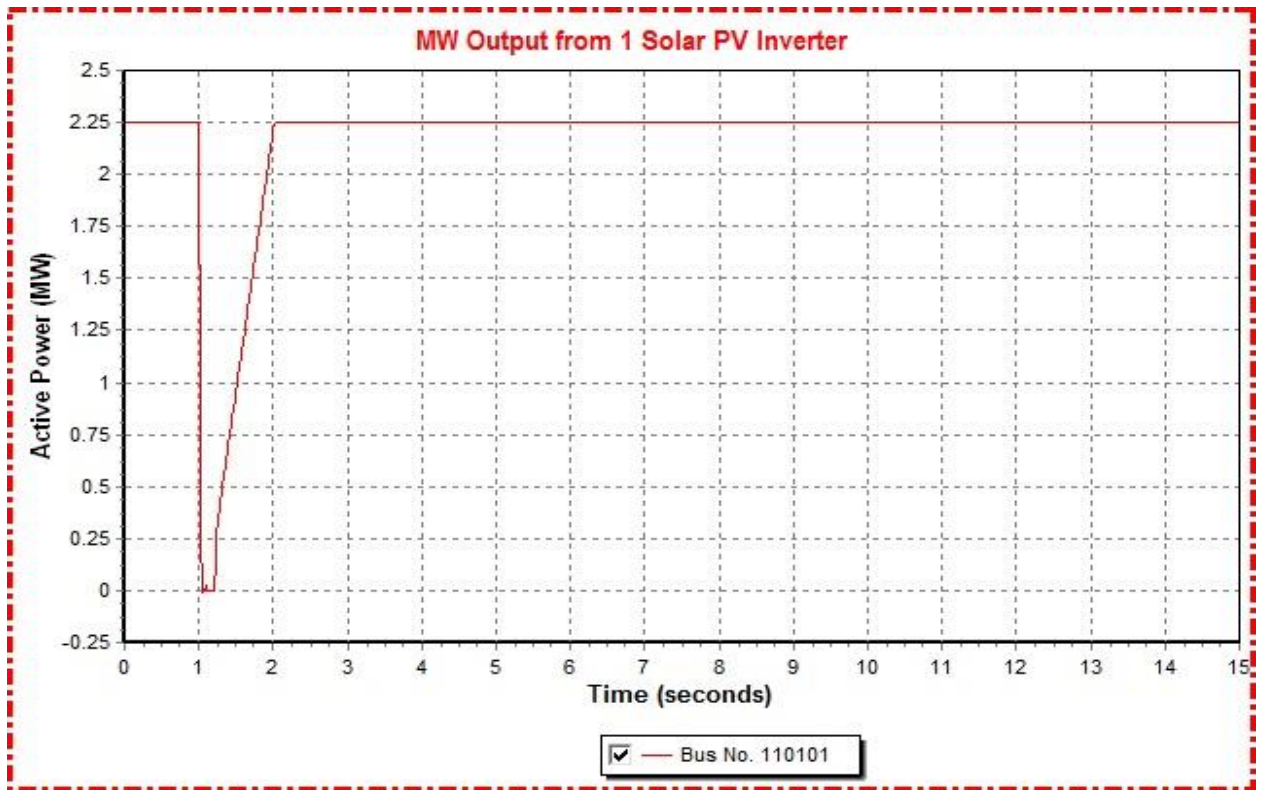


Figure 2.7. Active Power Plot for Stability Analysis with IEEE-14 bus system

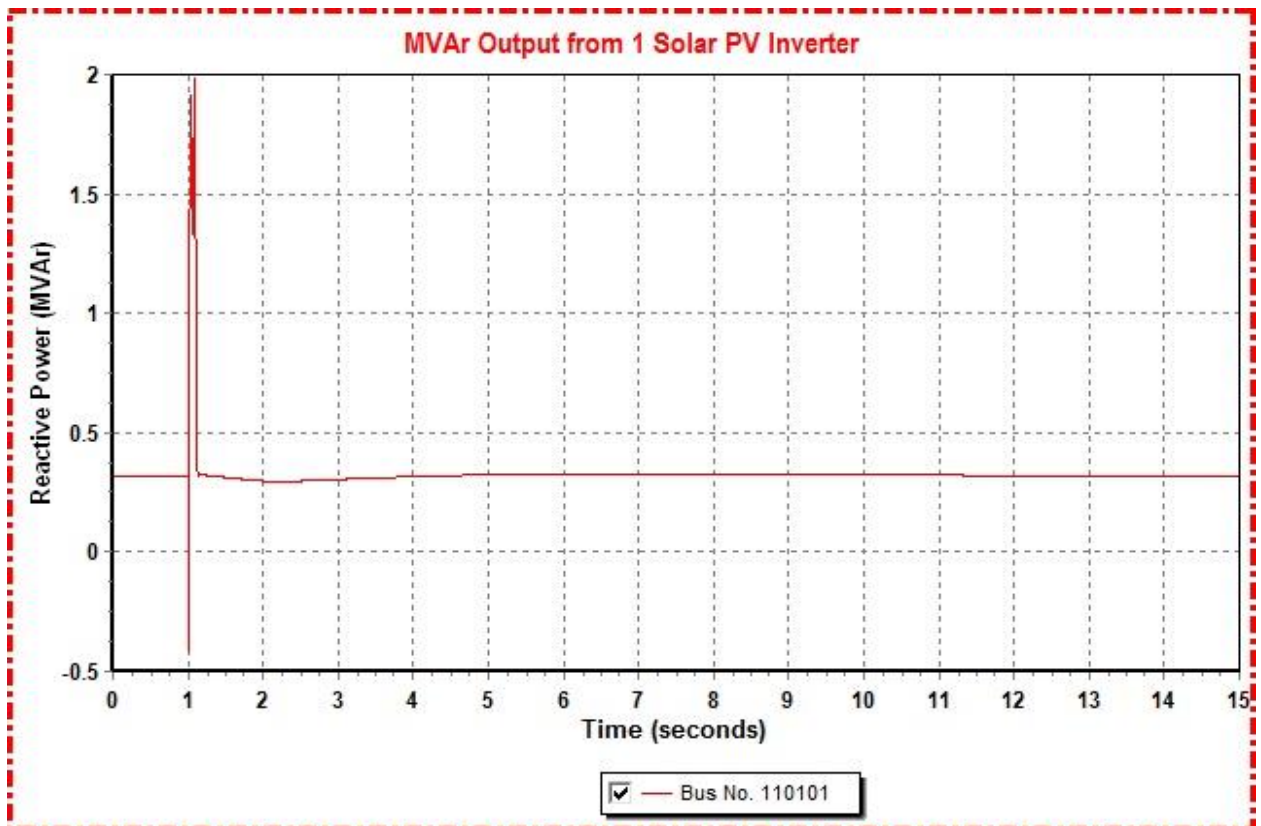


Figure 2.8. Reactive Power Plot for Stability Analysis with IEEE-14 bus system

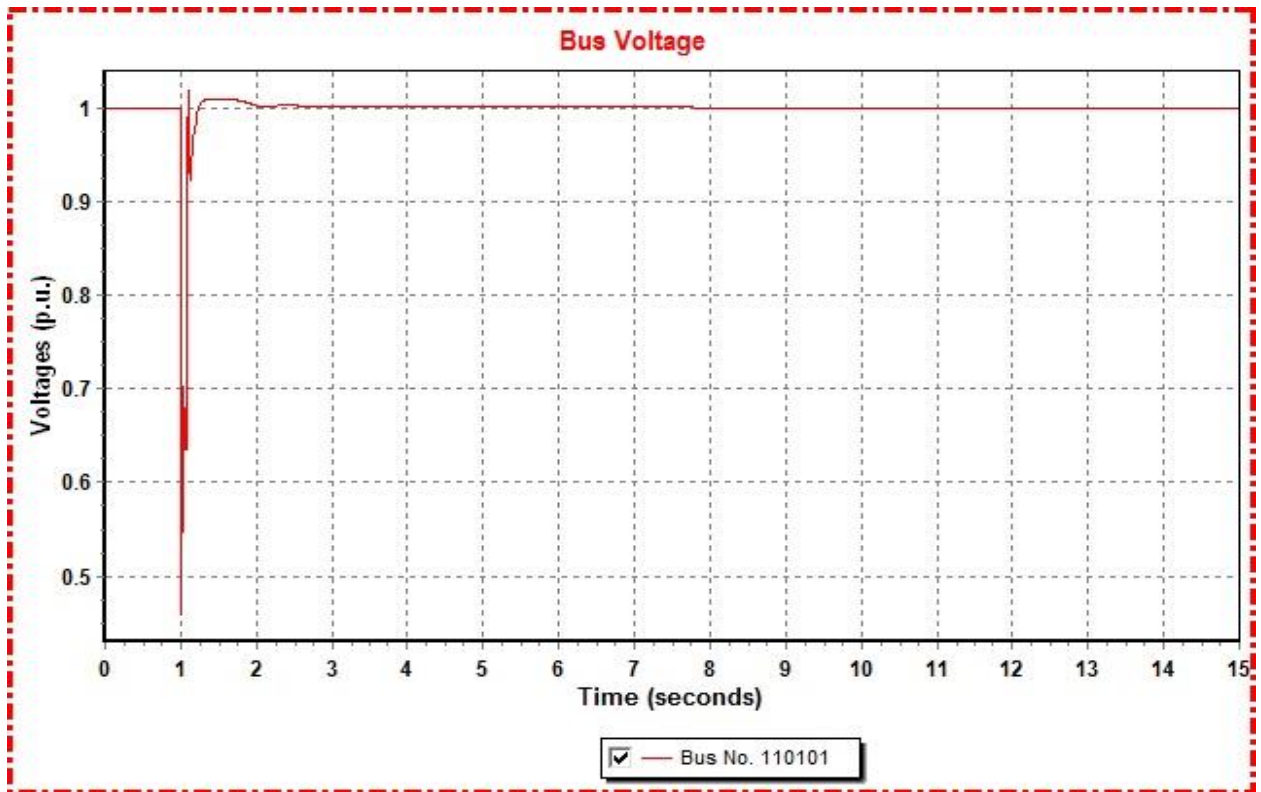


Figure 2.9. Bus Voltage Plot for Stability Analysis with IEEE-14 bus system

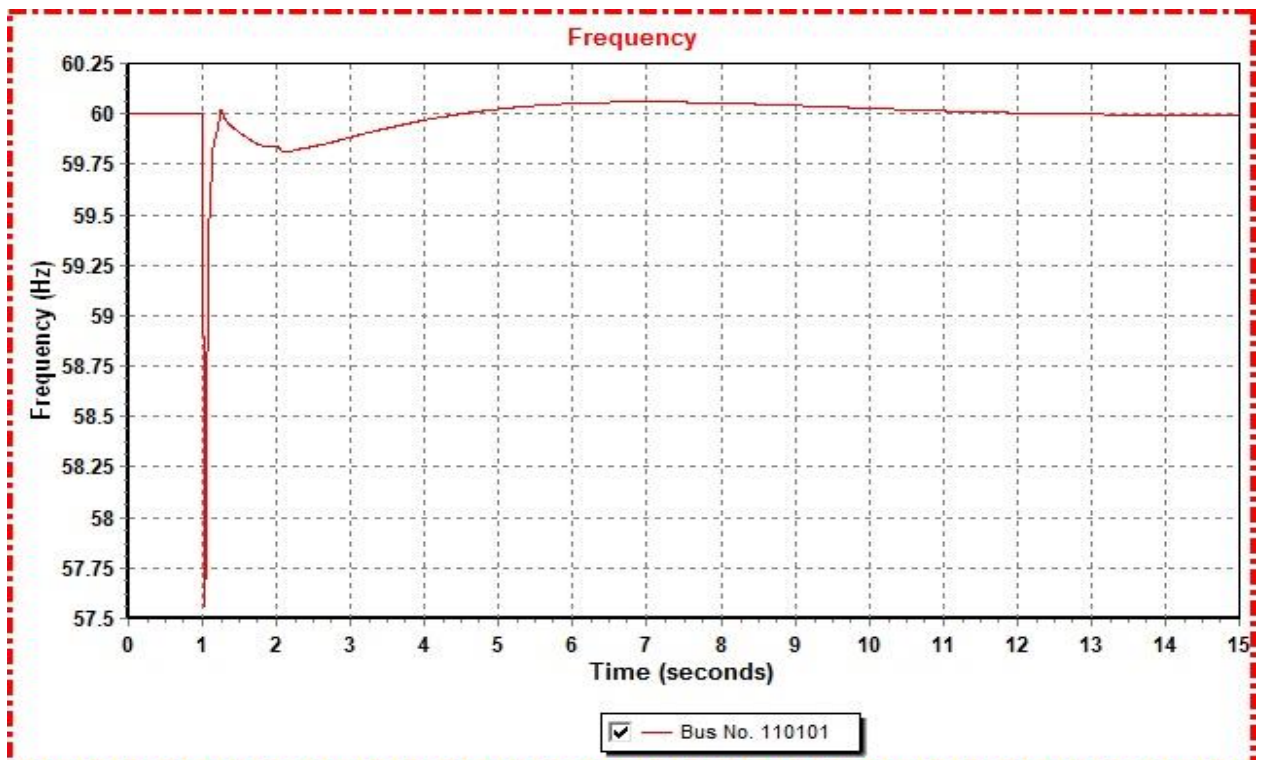


Figure 2.10. Frequency Plot for Stability Analysis with IEEE-14 bus system

As evident from the above graphs, the response from the solar PV inverter is better as compared to the scenario when tested with the network of 118 buses. However, it is better to further smooth the response of reactive power output and voltage in the provided model.

Chapter 3

Grid Code Compliance of Gamesa Solar PV Power Plant Model

3.1 INTRODUCTION

The grid code compliance for the provided solar PV inverter model is checked for most of the clauses of Mexican Grid Code. The two major compliances checked are HVRT/LVRT and active power and frequency regulation.

3.2 LVRT/HVRT STUDIES

As provided in [1], voltage-time characteristics including voltage-dip trip, over-voltage trip and under-voltage trip of Gamesa PV Inverter models are plotted along with LVRT/HVRT requirements mentioned in [2] and [4]. The graphs are shown in Figure 3.1 and 3.2 plotted for 10 seconds and 1 second respectively. It appears from Figure 3.2 that Gamesa PV Inverter model is compliant with HVRT requirement and is not compliant with LVRT requirement of Mexican grid code. It is due to the reason because LVRT requirement of Mexican grid code needs that the PV Inverter should stay connected with the grid for zero-voltage fault of 400 msec (0.4 sec) and as per Gamesa Voltage Dip curve, it can endure zero-voltage fault only for 100 msec (0.1 sec).

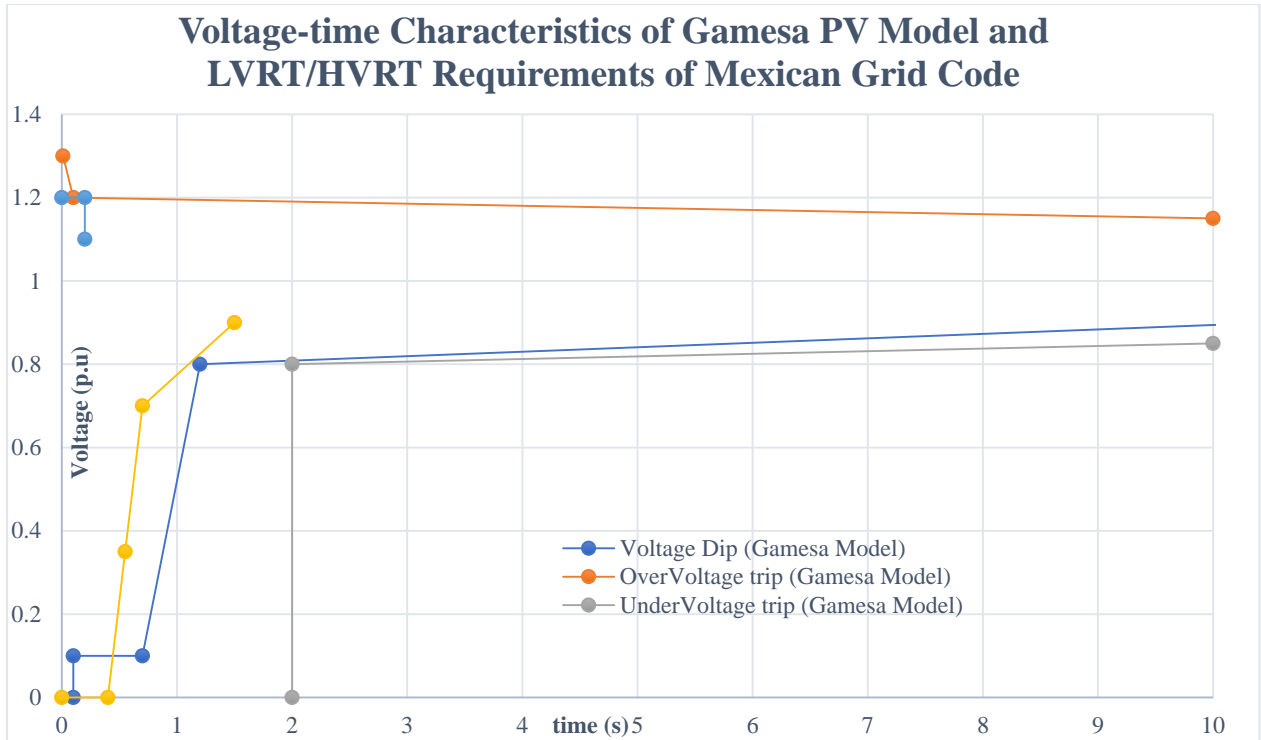


Figure 3.1. Plot for Grid Code Compliance for LVRT/HVRT – Plotted for 10 seconds

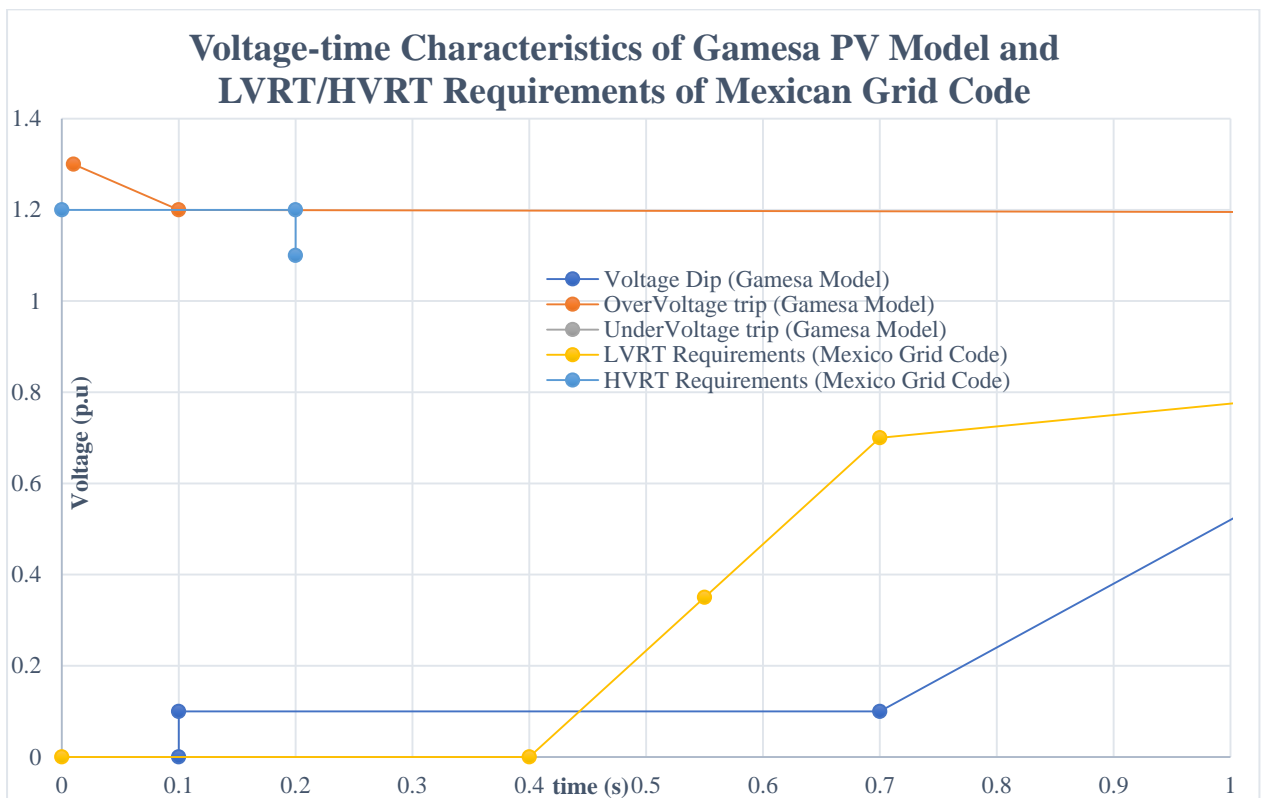


Figure 3.2. Plot for Grid Code Compliance for LVRT/HVRT – Plotted for 1 second

To check/verify this non-compliance, LVRT/HVRT studies of Gamesa PV Inverter have been carried out in PSS/E which are discussed below.

Three type of faults have been applied in PSS/E to check LVRT compliance of Gamesa PV Inverter.

1. Zero-voltage fault for 400 msec (0.40 sec)
2. 0.45 p.u. voltage fault for 600 msec (0.60 sec)
3. 0.70 p.u. voltage fault for 700 msec (0.70 sec)

3.2.1 ZERO-VOLTAGE FAULT FOR 400 MSEC (0.40 SEC)

A dynamic simulation has been started and run for a normal condition till 1 second. Then to apply zero-voltage fault, three phase bus fault is applied at the output terminal of Gamesa PV Inverter (Bus # 110101) at 1 second and run for 400 msec. At 1.4 second, the fault is cleared and the simulation is run till 5 seconds. The plot of this simulation is shown below in Figure 3.3.

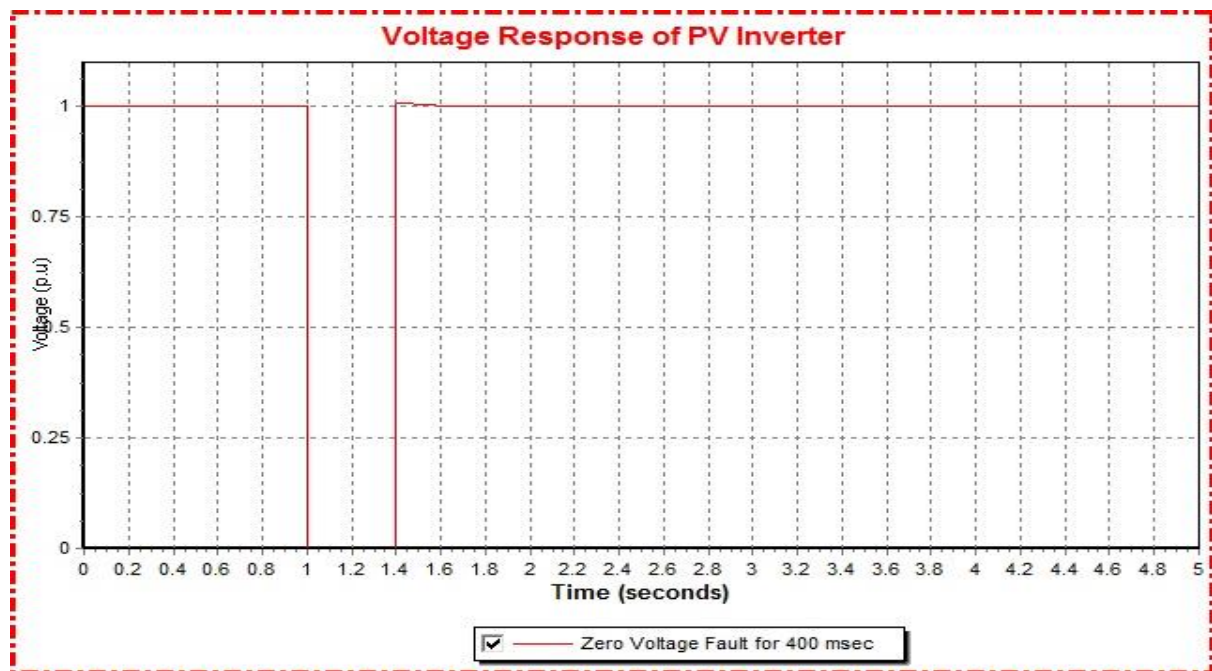


Figure 3.3. Zero-voltage fault for 400 msec (0.4 sec)

3.2.2 0.45 P.U. VOLTAGE FAULT FOR 600 MSEC (0.60 SEC)

To apply 0.45 p.u. voltage fault, three phase bus fault is applied at bus # 13 (a bus in the proximity of output terminal of Gamesa PV Inverter) at 1 second and run for 600 msec. At 1.6 second, the fault is cleared and the simulation is run till 5 seconds. The plot of this simulation is shown below in Figure 3.4.

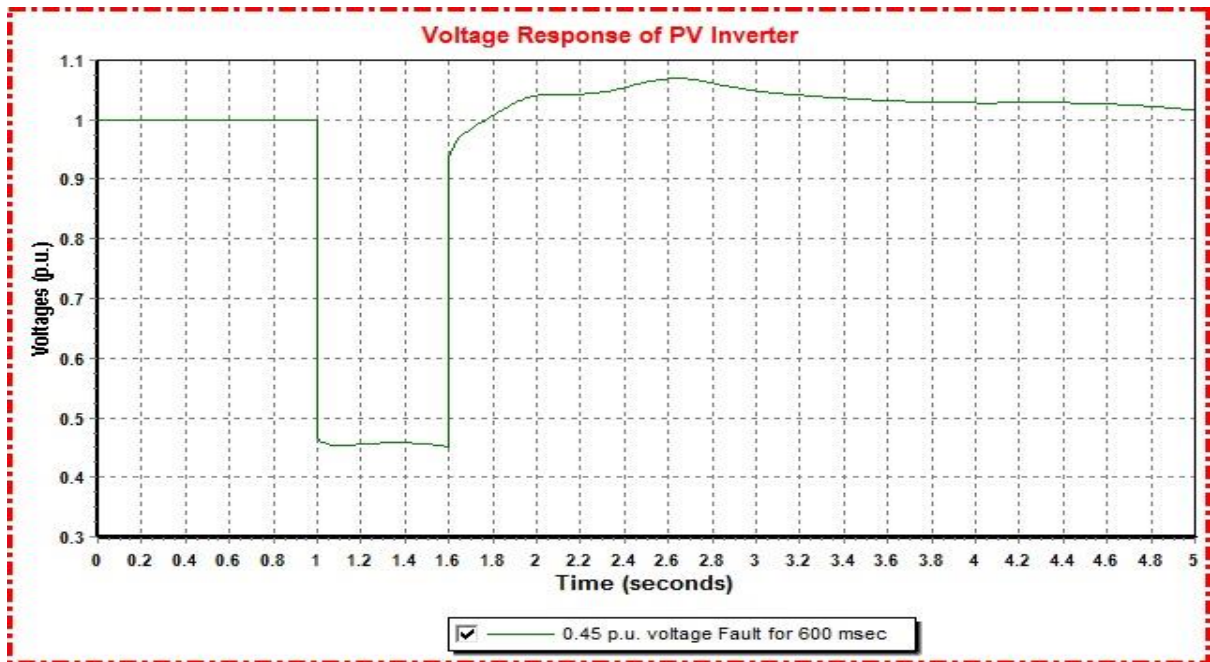


Figure 3.4. 0.45 p.u. voltage fault for 600 msec (0.6 sec)

Meanwhile, the voltage output from bus # 13 is shown in Figure 3.5 for this fault.

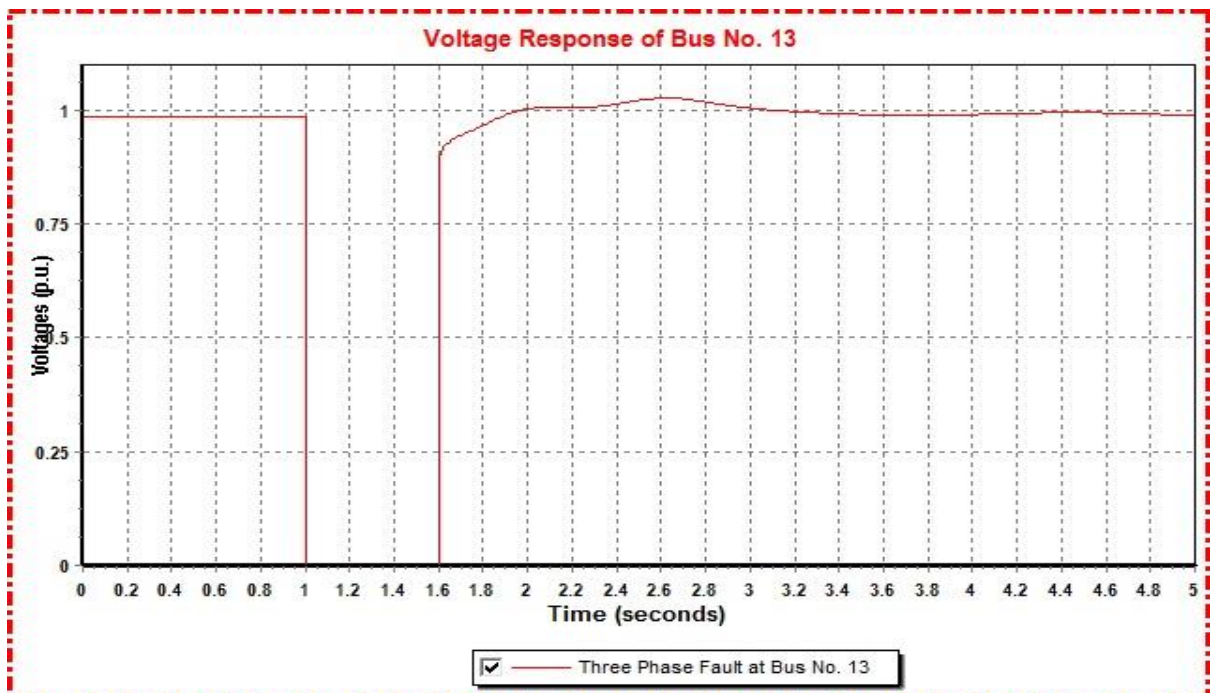


Figure 3.5. Voltage response from Bus # 13

3.2.3 0.7 P.U. VOLTAGE FAULT FOR 700 MSEC (0.70 SEC)

To apply 0.7 p.u. voltage fault, three phase bus fault is applied at bus # 33 (a bus far from the output terminal of Gamesa PV Inverter) at 1 second and run for 700 msec. At 1.7 second, the fault is cleared and the simulation is run till 5 seconds.

It is important to mention here that the voltage at output terminal of Gamesa PV Inverter (Bus # 110101) is not exactly 0.7 p.u. but slightly lower than that, which is perfectly alright as it causes more stress than 0.7 p.u. The graph of this simulation is shown below in Figure 3.6.

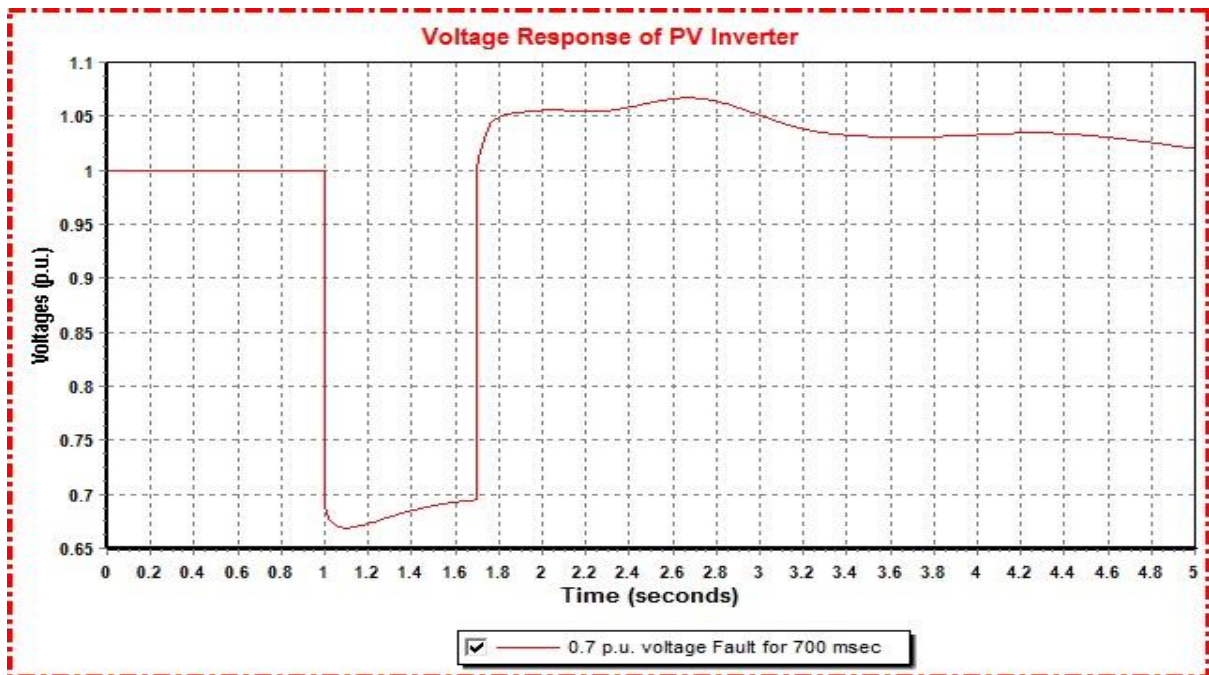


Figure 3.6. 0.7 p.u. voltage fault for 700 msec (0.7 sec)

Meanwhile, the voltage output from bus # 33 is shown in Figure 3.7 for this fault.

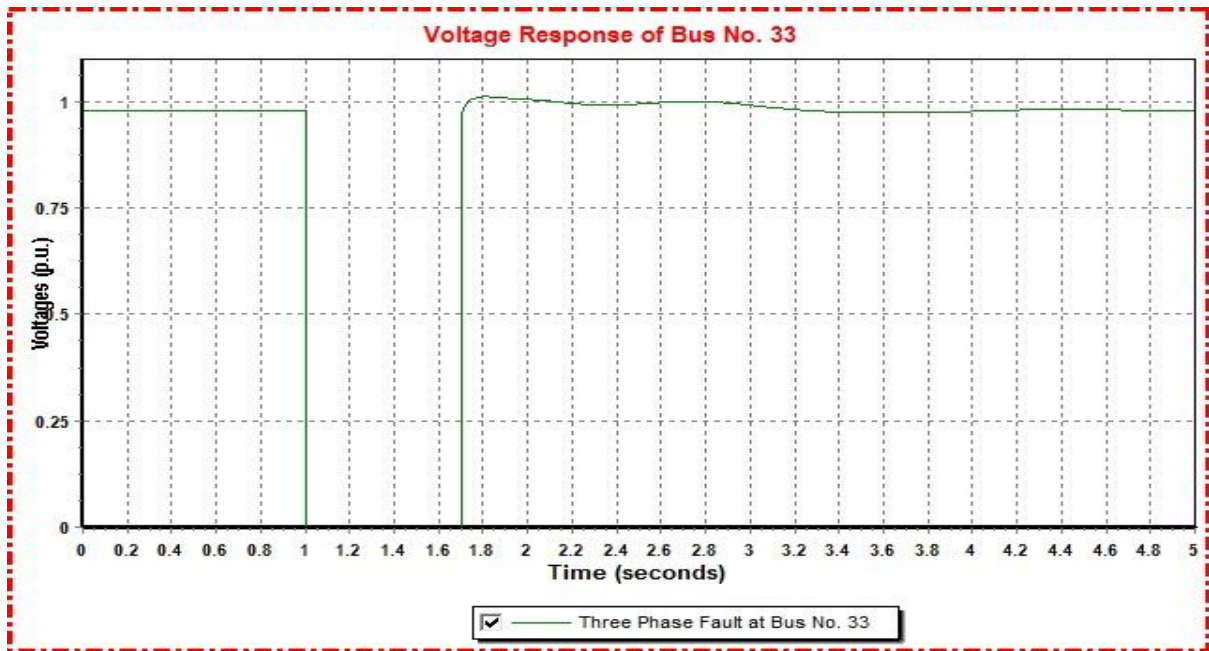


Figure 3.7. Voltage response from Bus # 33

From the above plots, it can be observed that the PV inverter model is compliant with the Mexican Grid code. However, some modifications are required to be done in [1].

3.3 FREQUENCY RESPONSE AND ACTIVE POWER REGULATION

Summarizing the main clauses mentioned in Mexican Grid Code [2] regarding Frequency Response and Active Power Regulation, these are as follows:

- The Solar PV power plant should not provide any active power regulation (change in the output) if system frequency changes by 30 mHz (dead band).
- If system frequency goes up or down, the solar PV power plant should provide active power regulation in the range of 3 – 10%.

To perform the verification simulation in PSS/E, the base case is slightly modified according to the requirements. Since, sudden frequency drop is required to be simulated, the dispatch from the generator at Bus No. 12 is adjusted to supply only the active power with negligible supply of reactive power. Moreover, a new bus '120000' is added with zero impedance line from Bus No. 12 having the active power load equal to dispatch of the generator at Bus No. 12.

To perform the simulation, it has been run for a normal condition till 4 seconds. Then to drop the frequency of the system, the generator at Bus No. 12 is switched out from the network. The system is run for additional 1.5 seconds to check the active power regulation characteristics of 54 MW GAMESA Solar PV power plant. Then to recover the frequency, the load at Bus No. 120000 is disconnected and the simulation is run till the steady state achievement for the system.

Three scenarios are tested to verify the performance of the Solar PV Inverter:

- **Case A:** The Solar PV Inverter has a dispatch of 1.5 MW (66%) and a sudden loss of 100 MW generator is occurred causing frequency drop of 40 mHz.
- **Case B:** The Solar PV Inverter has a dispatch of 2.25 MW (100%) and a sudden loss of 100 MW generator is occurred causing frequency drop of 40 mHz.
- **Case C:** The Solar PV Inverter has a dispatch of 1.5 MW (66%) and a sudden loss of 50 MW generator is occurred causing frequency drop of 20 mHz.

For these simulations, the graphs of MW output from 1 Solar PV Inverter and frequency are shown below in Figure 3.8, 3.9, 3.10 (both normal and zoomed in graphs).

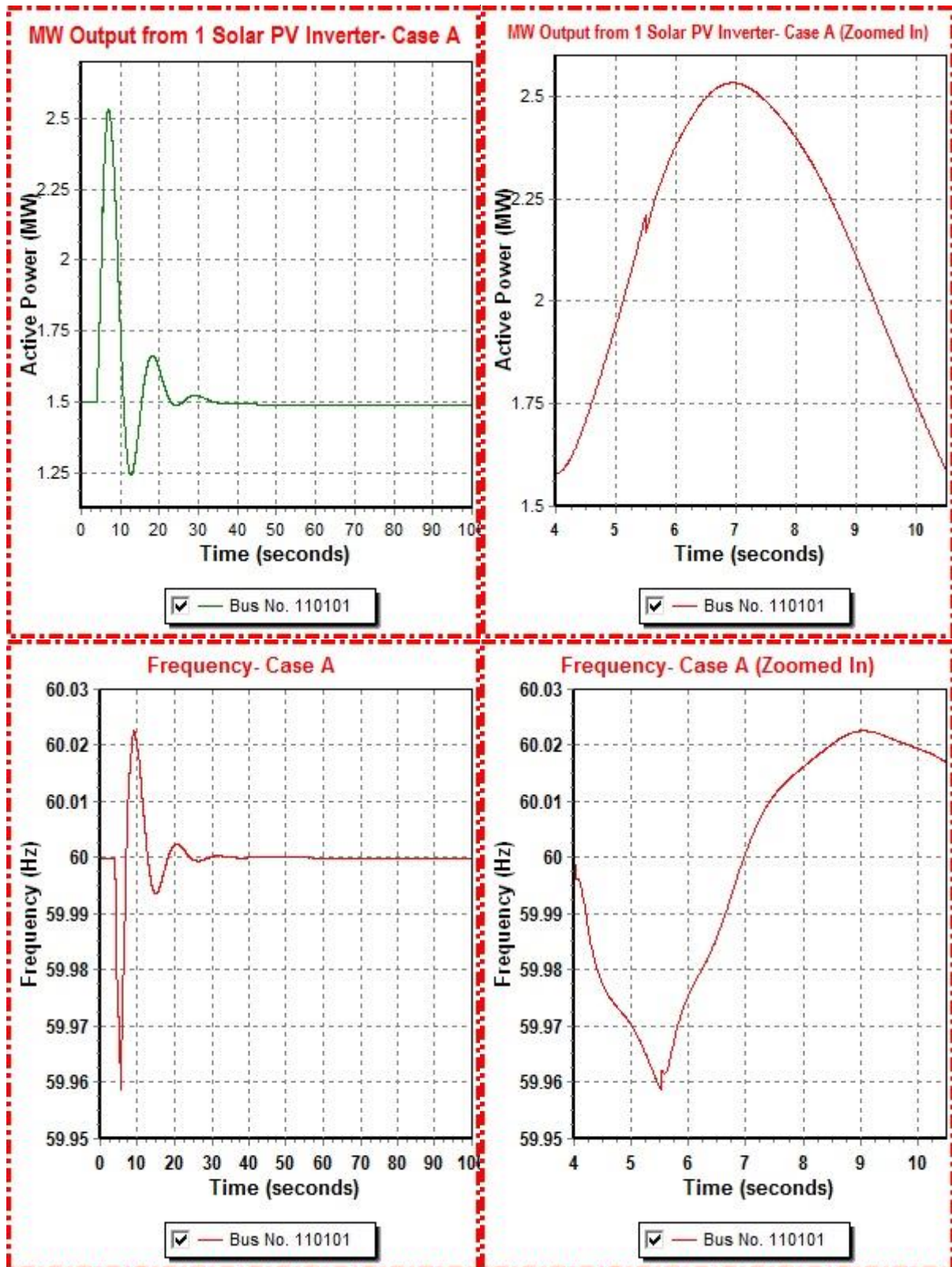


Figure 3.8. Plots for Case A

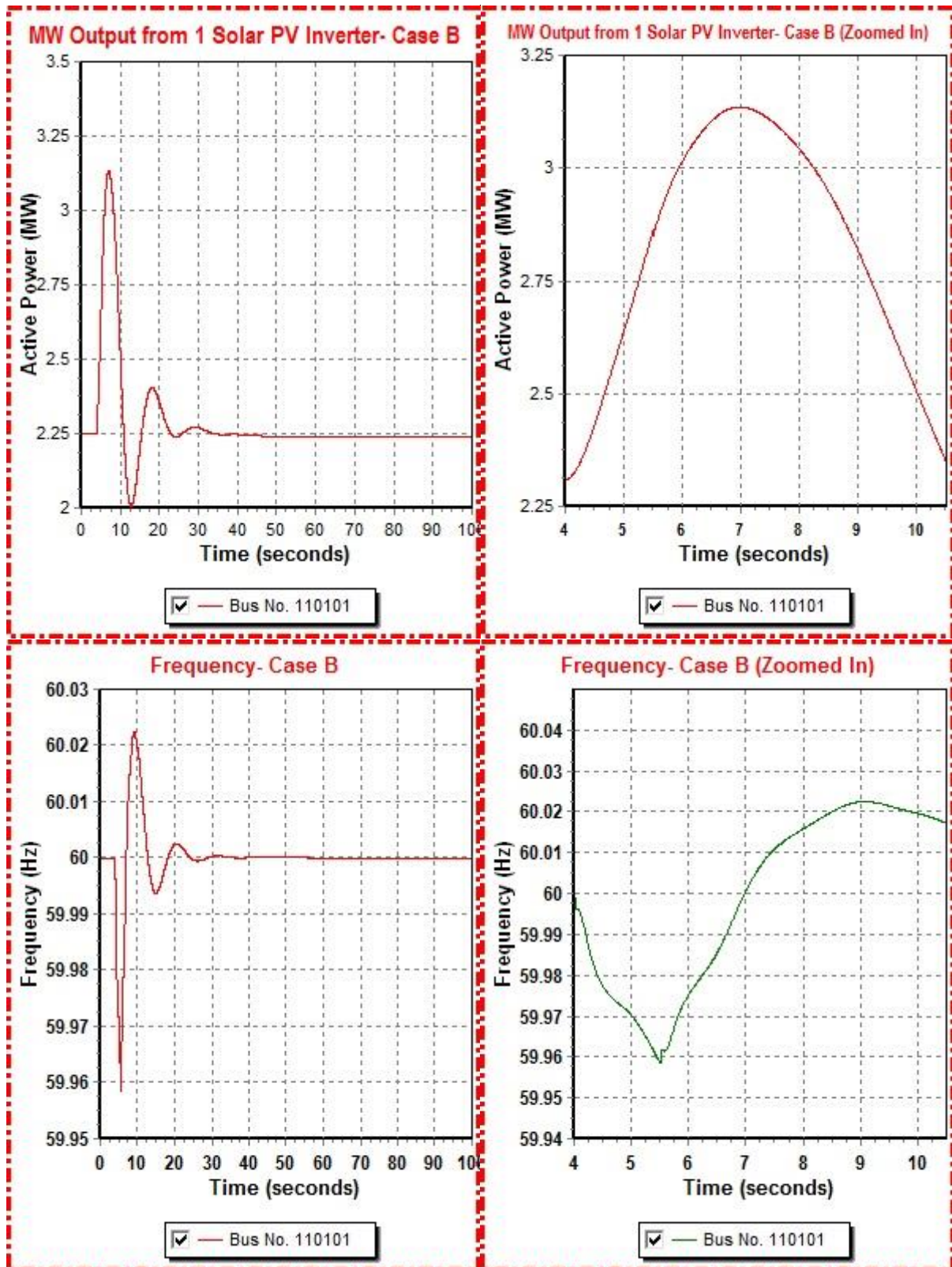


Figure 3.9. Plots for Case B

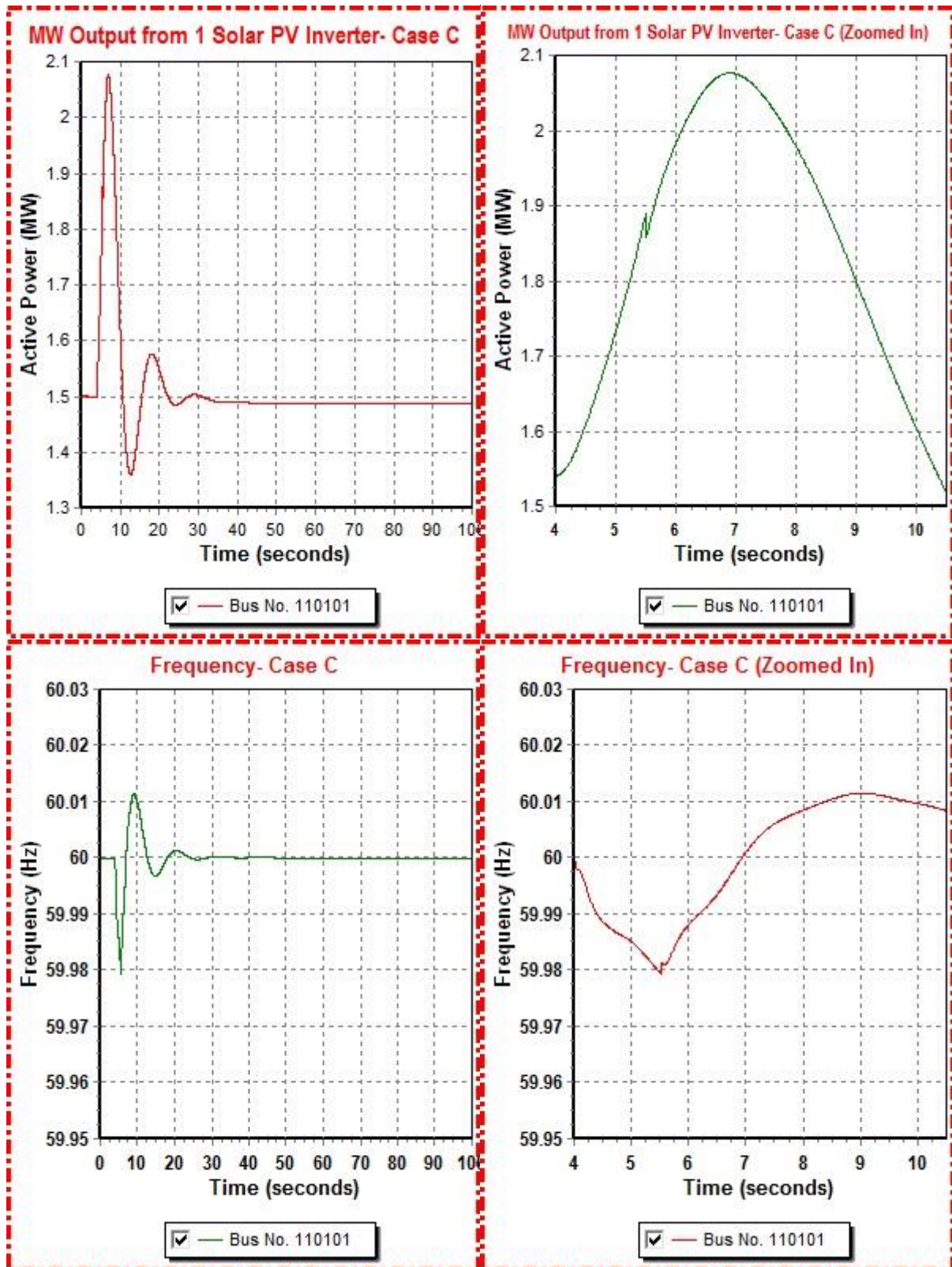


Figure 3.10. Plots for Case C

From the above plots, it can be observed that the Solar PV inverter is following the frequency control characteristics but not in the required range of Mexican grid code. Moreover, the PV inverter is responding even in the dead band of the frequency. These issues need to be further investigated.

Chapter 4

Methodologies for Solar PV Plant Output Patterns and Ramp-Down Analysis

4.1 INTRODUCTION

This chapter focusses on the main concepts regarding different methodologies to find the power output patterns from solar PV power plant based on a single point irradiance data. These techniques include single section, N-section and WVM methods which are explained in detail in the chapter. Moreover, a comparison has been performed for these three methods as well.

After determining the output profiles, in order to cater the clouding effect, power ramping analysis is performed. In addition to this, PV Plant design and dimension calculations are carried out as well.

4.2 PV PLANT DIMENSIONING

Here, an approximate design and size of the solar PV plant is calculated based on the data inputs and assumptions stated in the following section 4.2.1.

4.2.1 DATA INPUTS

The data inputs for design calculation of the solar PV power plant are as follows:

The PV module JKM 320PP-72-V is assumed to be used at the solar PV power plant. It has the following basic specifications at STC [9]:

- Maximum Power (P_{max}) = 320 Wp
- NOCT = 45°C
- Maximum Power Voltage (V_{mp}) = 37.4 V
- Maximum Power Current (I_{mp}) = 8.56 A
- Open-circuit Voltage (V_{oc}) = 46.4 V
- Short-circuit Current (I_{sc}) = 9.05 A
- Maximum system voltage = 1500 Vdc

- Temperature coefficient of $V_{oc} = -0.3 \text{ \%}/^{\circ}\text{C}$

Since 1500 V is the maximum system voltage for JKM 320PP-72-V, therefore GAMESA E-2.25 MVA inverter is considered.

The data inputs for size calculation of the solar PV power plant are as follows:

- Land area required for installing solar PV power plant per MW: Approximately 4 acres [7].
- Rectangular-shaped land area of the solar PV power plant has been assumed having width to length ratio of 1:4
- Installed Capacity of the solar PV power plant: 122.8 MWp
- 1 Acre = 4046.86 m²

4.2.2 DESIGN CALCULATIONS

For 122.8 MWp, the number of PV modules required is $(122.8 \times 10^6)/320=383750$.

The required number of PV modules in series in each string would be $1500/46.4=32.33 \approx 32$ but the final number of panels considering the V_{oc} temperature coefficient is 30.

The power from one string is $30 \times 320 = 9600 \text{ Wp}$.

And the total number of strings in the power plant are $(122.8 \times 10^6)/9600=12791.67 \approx 12792$.

4.2.3 PV PLANT DIMENSIONS CALCULATIONS

For 122.8 MWp capacity of the solar PV power plant, land area required = $122.8 \times 4 = 491.2$ acres.

Land Area required in m² = $491.2 \times 4046.86 = 1987817.632 \text{ m}^2$.

Now, to find the width (w) and length (l) of the plant, $w \times l = 1987817.632$.

Since $l = 4w$, therefore, $4w^2 = 1987817.632$ and $w = 704.95 \text{ m}$.

This gives length of the plant, $l = 704.95 \times 4 = 2819.8 \text{ m}$.

These length and width dimensions of the solar PV power plant can be rounded off to 700 m and 2800 m respectively to simplify the calculations. So the approximate plant dimensions would be 700x2800 m.

4.3 CATEGORIZATION OF SOLAR DAYS

In order to characterize the solar plant site, the first step is to categorize it in terms of number of days for a specific variability in the solar irradiance. To cater this variability, a quantitative metric DARR (Daily Aggregate Ramp Rate) is determined for each day of the available data and its distribution is determined as shown in figure 4.1. The DARR can be calculated using the formula [2]

$$DARR_{min} = \sum_{t=1}^{1440} \frac{|I_t - I_{t-1}|}{C} \tag{4.1}$$

Where I_t and I_{t-1} is the irradiance at time ‘t’ and ‘t-1’ respectively, while C is irradiance for 1 sun (1000 W/m^2).

As per [16], the days are classified into five categories, Category.1 being the very stable day and Category.5 a highly variable one in terms of solar irradiance fluctuations. The criteria for categorization is:

- Category 1: $DARR_{min} < 3$
- Category 2: $3 \leq DARR_{min} < 13$
- Category 3: $13 \leq DARR_{min} < 23$
- Category 4: $23 \leq DARR_{min} < 33$
- Category 5: $33 \leq DARR_{min}$

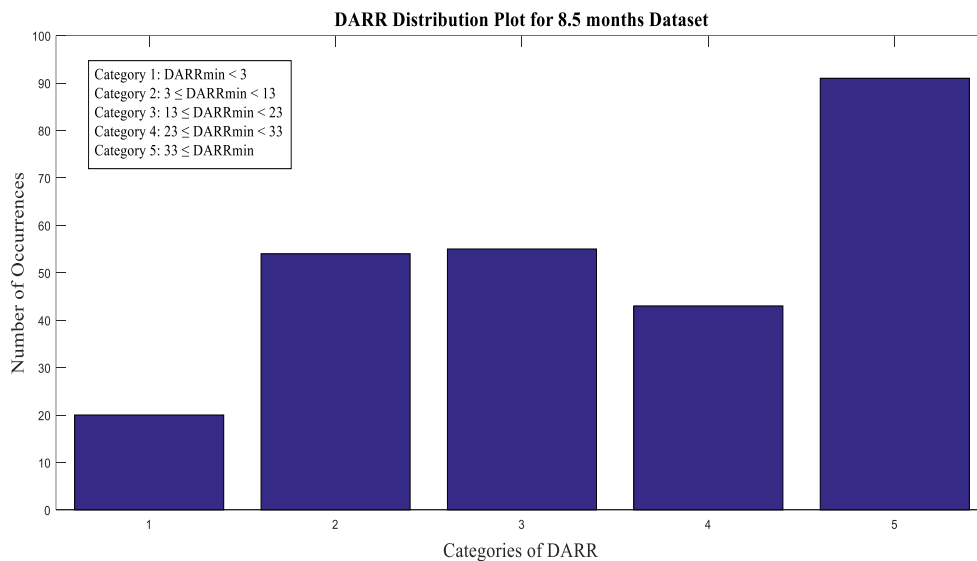


Figure 4.1. Distribution Plot for DARR Categories

It is evident from figure 4.1 that a big portion of the days are in the category 4 and 5, i.e., having highly variable solar irradiance profile, therefore, it is important to determine the power output profile of the entire PV plant accurately and then perform the ramp-down analysis based on that output profile.

Just for a comparison, irradiance profile for Cat.1 and Cat.5 Solar Day is shown in figure 4.2. The difference between the two types of solar days is quite evident along with the effectiveness of DARR metric.

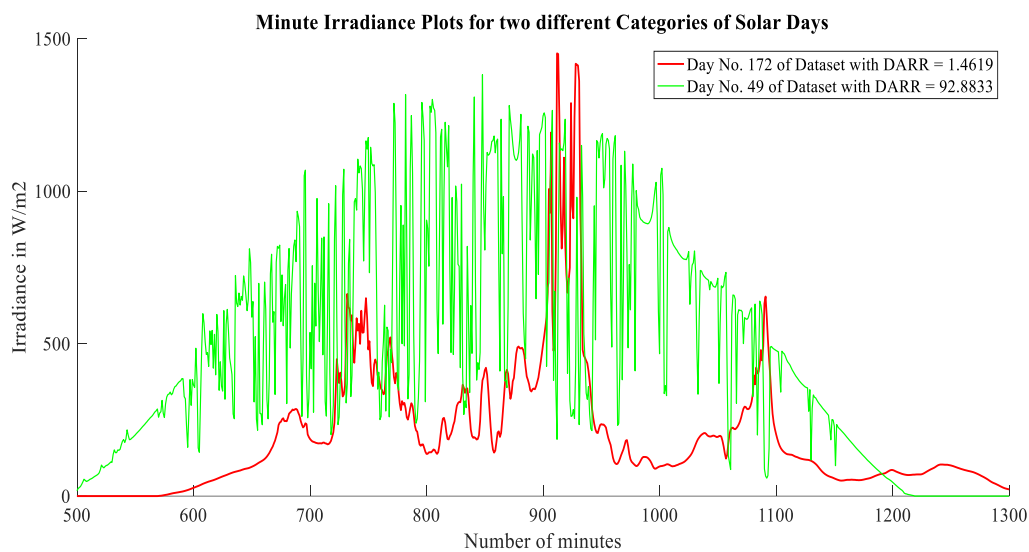


Figure 4.2. Comparison of Irradiance for Cat.1 and Cat.5 Solar Days

4.4 POWER PRODUCTION CALCULATIONS

The input data and power equations used to calculate the power output from solar PV power plant are presented in this section.

The recorded solar irradiance data at the site is used to calculate the approximate power output pattern from the 122.8 MWp solar PV power plant using MATLAB. The solar PV output power profile is plotted for daily, hourly and minutely basis according to the provided irradiance data. However, minute resolution data is analysed in detail for power production ramp-down analysis of the solar PV power plant.

4.4.1 DATA INPUTS

4.4.1.1 Solar Irradiation and Temperature

Temperature 'T' and solar irradiance 'G' values are obtained from the recorded irradiance data (provided excel sheets) while other parameters are constants as mentioned below [9]:

4.4.1.2 PV Panel Parameters

- Maximum power of the PV module at STC $P_{mp,ref} = 320$
- Reference irradiance at STC $G_{ref} = 1000$
- Reference ambient temperature at STC $T_{ref} = 25$
- Temperature coefficient of the PV module $\gamma = -0.003$
- Required number of PV modules $N = 383750$ (as calculated in section 4.2.2)

4.4.1.3 Efficiencies

The efficiencies assumed for the PV power production calculation are:

- Inverter Efficiency $\eta_{inv} = 98.5\%$ (generic value for sole purpose of this analysis)
- Transformer Efficiency $\eta_{tr} = 98\%$
- Cables Efficiency $\eta_{cables} = 99\%$

4.4.2 EQUATIONS

The power output from the inverters of PV power plant is calculated using the following equation mentioned in [10]:

$$P_{inv} = \frac{G}{G_{ref}} * P_{mp,ref} * [1 + \gamma(T - T_{ref})] * N * \eta_{inv} \quad (4.2)$$

To calculate cell temperature T_c , the following formula is used:

$$T = T_a + \frac{NOCT-20}{800} * E \quad (4.3)$$

Where:

- T_a is the ambient temperature from the excel datasheet
- NOCT is the nominal operating cell temperature
- E is the irradiance from the excel datasheet

And the output power at the MV side of the grid would be calculated taking into account the transformer and cables efficiency, given by:

$$P_{mv} = P_{inv} * \eta_{tr} * \eta_{cables} \quad (4.4)$$

Combining Eq.4.2 and Eq.4.4 will give the output power profile of the solar PV power plant which are implemented in MATLAB.

It has been assumed that the power output on the AC side of the inverter can only reach up to maximum of 100 MW and the remaining available output is clipped off.

4.5 METHODOLOGIES FOR POWER OUTPUT PROFILE DETERMINATION

Three different approaches are applied to determine the solar PV power output profiles, which are:

1. Single-section Method (Considering the plant as one section)
2. N-section Method (Considering the plant divided into N sections)
3. WVM (Wavelet Variability Model) Method

These methodologies are explained in the succeeding sections.

4.5.1 SINGLE-SECTION & N-SECTION METHODS

Single-section method is the simplest method of all of them in which solar plant is considered as one section and the corresponding output is calculated without applying any additional technique for accumulating clouding effect. However, for N-section method, irradiance input is considered with time delays incorporated for the calculation of solar plant output, to have different irradiance data for each section at one instant of time. This method is further explained below.

4.5.1.1 Cloud Movement Modelling for the PV Plant in N-section method

The cloud movement for the solar PV power plant is modelled based on the fact that the provided solar irradiance data already include the cloud movement. Since the provided data is measured at one sensor point, and logically it should be different for various sections of the complete solar plant, therefore, a time shift of 1 minute (1 sample) is introduced in the observed data for various sections of the plant. In other words, the first section will have irradiance at 't', the second section at 't+1', the third section at 't+2', up to 't+N'. The solar PV power plant is divided into N sections (assumed equal to 4 here), so it can be said that the clouds would move over the plant in 4 minutes.

Each section is generating $1/N$ ($1/4$) of the total power output of the plant proportional to the irradiance data. The final power output of the plant would be the sum of the power outputs from the N sections. A simple figure demonstrating the cloud movement over the 4 sections of the PV power plant is shown in figure 4.3. At $t = 1$, the cloud will entirely cover section 1 and similarly moving in the same direction, it will entirely cover section 4 and $t = 4$.

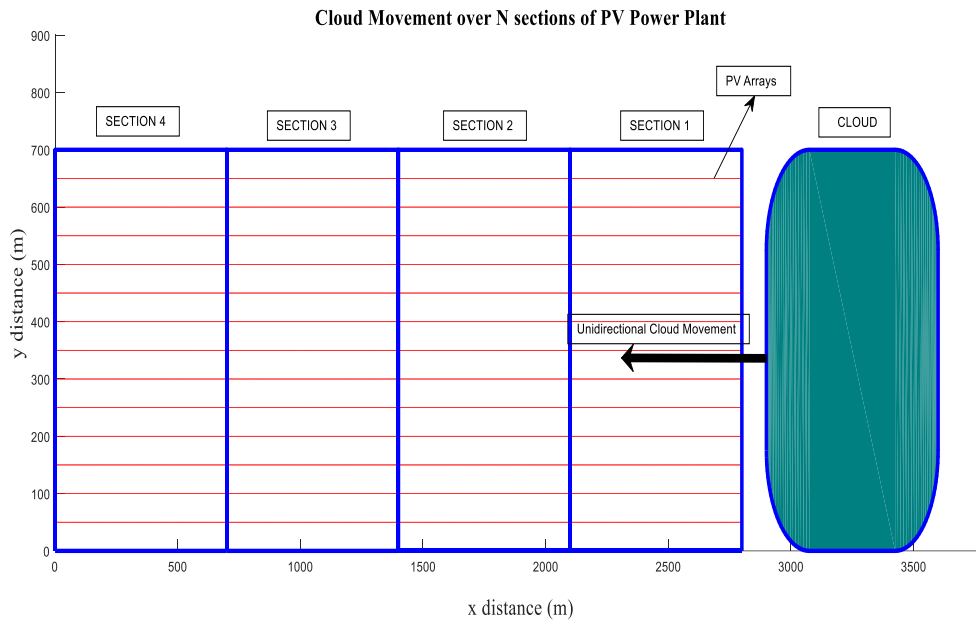


Figure 4.3. Simplified Cloud Movement Modelling (Position at $t = 0$)

The above explanation can be seen in other perspective as well. As mentioned above, solar plant has dimensions equal to 700×2800 m, which gives the dimension of each section equal to 700×700 m. Reference [8], cloud speeds can vary in the range of 1 to 25 m/s and cloud sizes in the range of 100×100 m to 3000×3000 m. Here, cloud speeds of 11.5 m/s (almost median value) is considered which is equal to 41.4 km/h. Moreover, only unidirectional movement (along the length of the solar plant) of the clouds is assumed. Therefore, the time required by the clouds having speed of 11.5 m/s to cross each section would be 60.86 s (approximately 1 minute).

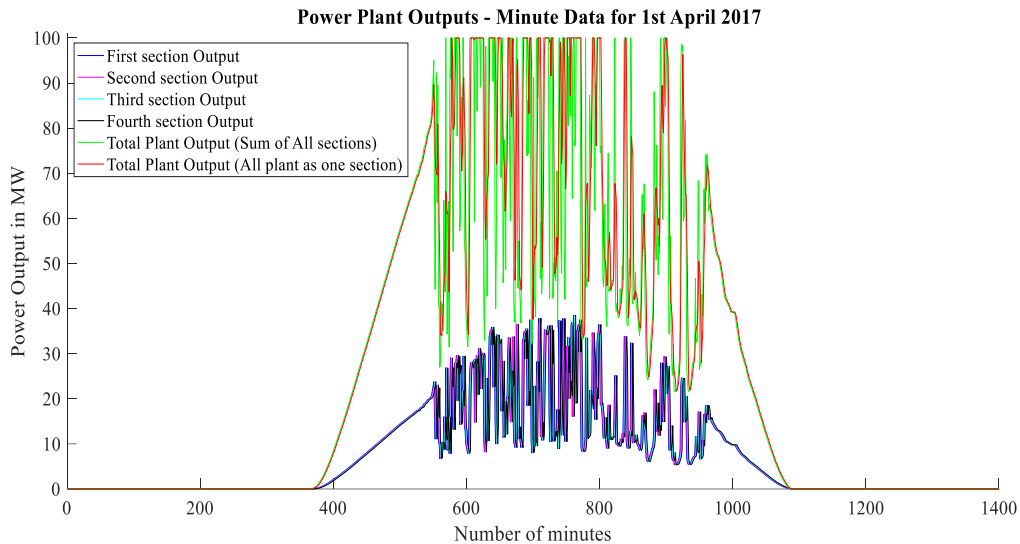


Figure 4.4. Solar PV power plant output for minutely irradiance data – sections’ output and total output (zoomed-in)

The plant output from each section and the total cumulative output using N-sections method is shown in figure 4.4, it is compared with single-section plant output as well. As clear from the figure 4.4, there is more variability in output pattern for single-section than N-section. It is because the variability in solar irradiance get somehow diversified using N-section method.

4.5.2 WVM METHOD

4.5.2.1 Introduction

This section describes WVM methodology and also explains the procedure to use WVM MATLAB toolbox (developed by Sandia National Laboratories, USA) for performing PV ramp-down analysis based on a single point irradiation data. One of the major characteristic of WVM methodology is that it smooth out the measured one-point irradiance pattern according to the area of the PV power plant. It modifies the 1-point measured time-series irradiance data into ready-to-use irradiance data for actual power output calculation based on various inputs. The measured solar irradiance data is smoothed by WVM method as shown in figure 4.5.

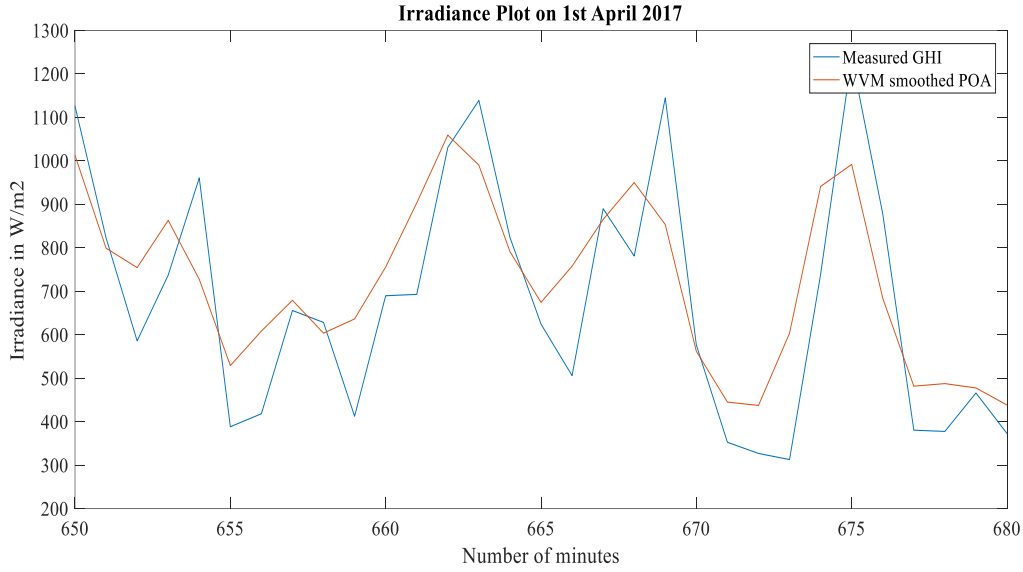


Figure 4.5. Measured and WVM-smoothed irradiance data

4.5.2.2 WVM Methodology

The explanation along with application to the available data on each step while applying WVM is described in this section [11, 12, 13]. The main steps involved are:

- GHI Normalization
- Wavelet Decomposition
- Distances Computation
- Correlations
- Variability Reduction
- Inverse Wavelet Transform

4.5.2.2.1 GHI Normalization

The input solar irradiance time-series data ‘GHI (t)’ from the sensor is normalized to make it a stationary signal (statistical parameters do not change with time) using

$$GHI_{norm}(t) = \frac{GHI(t)}{GHI_{clr}(t)} \quad (4.5)$$

where ‘GHI_{clr}(t)’ is the clear-sky model determined using Ineichen model. In Ineichen/Perez model, various parameters are input like location details of the sensor and the time at which the measurements are recorded, so that using some empirical equations, this model calculate

the GHI for clear sky (without any clouds). ‘GHI_{norm}(t)’ is the clear sky index and its value is equal to 1 during clear condition because during it, both GHI and GHI_{clr} will have the same value.

4.5.2.2.2 Wavelet Decomposition

The wavelet transform of the clear sky index (CSI) is calculated for each wavelet timescale, which is the defined duration of fluctuation. The formula to calculate wavelet transform is

$$w_{\bar{t}}(t) = \int_{t_{start}}^{t_{end}} GHI_{norm}(t') \frac{1}{\sqrt{\bar{t}}} \psi\left(\frac{t'-t}{\bar{t}}\right) dt' \quad (4.6)$$

where \bar{t} is the wavelet timescale and ‘t’ is variable of integration. Here the wavelet used to decompose CSI is a simple square wave which has an amplitude equal to 1 and -1 for $1/4 < T < 3/4$ and $(0 < T < 1/4$ or $3/4 < T < 1)$ respectively, whereas has zero value elsewhere. Since the calculations are performed in discrete domain, therefore wavelet modes are computed for \bar{t} ranging from 2 sec ($j = 1$) to 4096 sec ($j = 12$). For $j > 12$, the smoothing is not much significant. Moreover by limiting up to $j = 12$, an important property is achieved, i.e., the summation of all wavelet modes should be equal to the original input signal. Wavelets modes (from 7th to 12th) and CSI for dataset of August 2016 is shown in figure 4.6. The first six modes are insignificant having very lower values and ignored. It is quite evident from figure 4.6 that CSI is the sum of the wavelet modes.

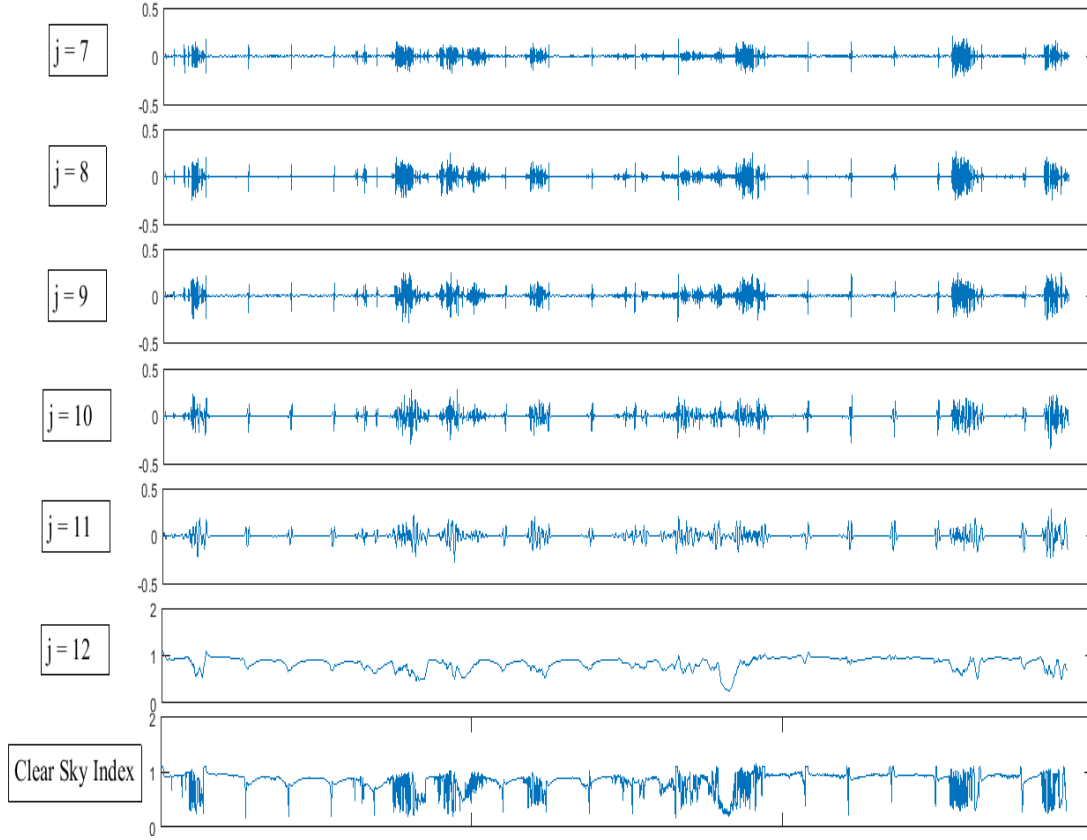


Figure 4.6. Wavelet Modes and Clear Sky Index Time-series for dataset of August 2016

4.5.2.2.3 Distances Computation

The power plant is discretized into individual hypothetical sites, practically a PV panel in the power plant. The distances $d_{m,n}$ between between all pairs of sites ('m' and 'n') are calculated for the PV plant. First, the length and width of the square shaped (assumed) power plant is calculated using

$$length = width = \sqrt{\frac{MW\ Capacity\ of\ PV\ Plant * 10e6}{PV\ Plant\ Density}} \quad (4.7)$$

For 100 MW plant with PV density of 61.77 W/m², length comes out to be 1272 m. Therefore, the total number of hypothetical sites would be 1272² = 1617984 and the number of entries for distances among them, $d_{m,n}$ will be $\sqrt{(1272^2)^2 + (1272^2)^2} = 2288174$. The maximum value of distance can be found using Pythagoras formula, $\sqrt{1272^2 + 1272^2} = 1798.89$ m. The zoomed-in distance (dmn) plot is shown below.

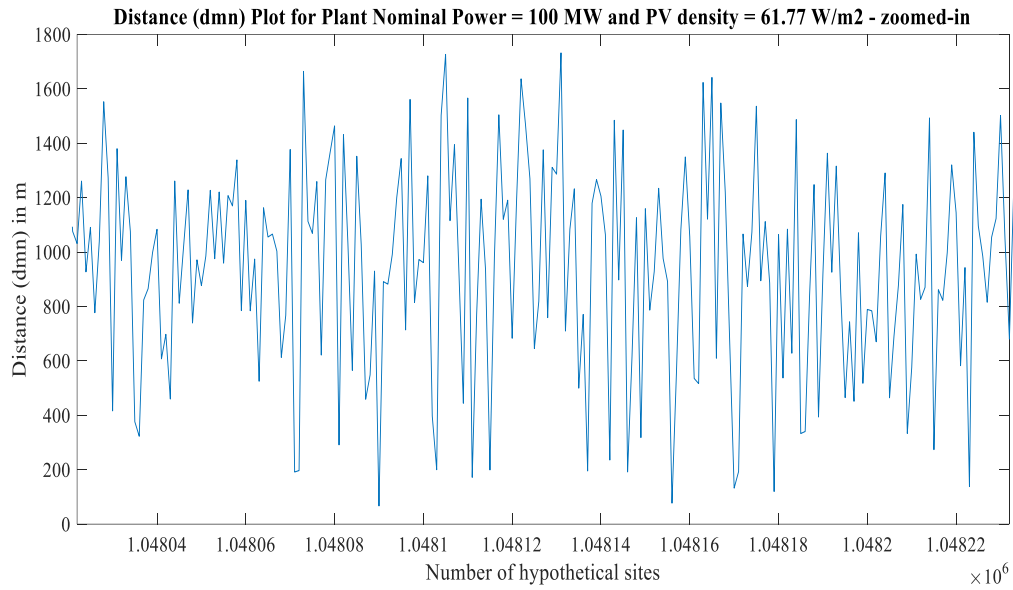


Figure 4.7. Distance (dmn) Plot – zoomed-in

4.5.2.2.4 Correlations

The correlations between the sites are determined on each timescale.

As per [15], there always exists a decaying exponential relation between wavelet correlation and the distance between PV panels. The results of practical study carried out in [15] are shown in figure 4.8. Low, medium and high are the categorization of the days for low, medium and high level of power fluctuations. Here λ are the wavelet modes.

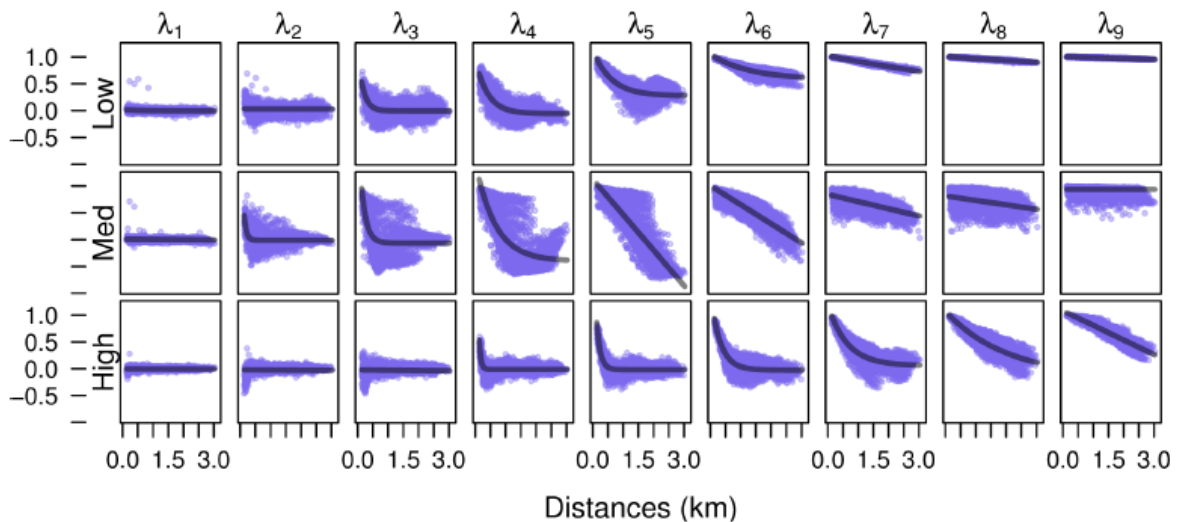


Figure 4.8. Wavelet correlation versus the distance between inverters (exponential decay model) [15]

The formula to find the correlation function is given by [14]

$$\rho(d_{m,n}, \bar{t}) = \exp\left(-\frac{1}{A} \frac{d_{m,n}}{\bar{t}}\right) \quad (4.8)$$

where ρ is the correlation between the hypothetical sites and A is the correlation scaling factor. The exact value of A can be found by back-solving the above equation but there must be an availability of data (distances, timescales and correlations) for at least 4-6 sites. A closed form methodology is proposed in [17], in which using meteorological and geographic variables, the values of A is determined without the requirement of multiple irradiance sensors. The value of A depends on the cloud speed, for simplicity purpose it can be assumed equal to half the cloud speed.

4.5.2.2.5 Variability Reduction

Variability Reduction (VR) can be defined as:

$$VR(\bar{t}) = \frac{\text{Variability}_{\text{point sensor}}}{\text{Variability}_{\text{PV plant}}} \quad (4.9)$$

Here the variability is measured in the solar irradiance profile. It is important to mention that $VR \geq 1$ because the variability of the aggregate PV system will always be less than or equal to variability at the point sensor. The greater geographic smoothing renders larger values of VR. Similarly, since short-timescale fluctuations get more damped by geographic smoothing, therefore, as the timescales of the wavelet increases, VR value is expected to decrease. For longer timescales, VR value approaches to 1.

Mathematically, VR of a timescale can be defined as the ratio of the variance of the point sensor to the variance of the complete PV plant at each timescale. VR is calculated on each timescale using equation below.

$$VR(\bar{t}) = \frac{N^2}{\sum_{m=1}^N \sum_{n=1}^N \rho(d_{m,n}, \bar{t})} \quad (4.10)$$

Where N is the total number of hypothetical sites.

If the characteristic pattern from the sites is completely independent, then VR will be equal to N, while for completely dependent sites, VR will be equal to 1.

Table 4.1. Variability Reduction for the modes of Wavelets

S. No.	wavelet modes (j)	Summation of Correlations	VR
1	7	$(1358500)^2$	2.3995
2	8	$(1680900)^2$	1.5673
3	9	$(1878000)^2$	1.2556
4	10	$(1987200)^2$	1.1214
5	11	$(2044700)^2$	1.0591
6	12	$(2074300)^2$	1.0292

As per table, VR value approaches to 1 for wavelet modes of 11 and 12 (longer timescales), and not due to strong correlation of solar irradiance profiles.

4.5.2.2.6 Inverse Wavelet Transform:

Here the simulated wavelet modes (inverse wavelet transform) of the power plant are calculated using the formula:

$$w_{\bar{t}}^{sim}(t) = \frac{w_{\bar{t}}(t)}{\sqrt{VR(\bar{t})}} \quad (4.11)$$

The simulated wavelet modes of are scaled in magnitude by the square root of VR. Finally the simulated wavelet modes (inverse wavelet transform) are summed to determine the spatially-averaged GHI over the power plant. This is an equivalent GHI which can be used to calculate the power output pattern from the entire power plant using one-point measured irradiance data.

4.5.2.3 Procedure to Use WVM Toolbox

- (i) Download WVM and PV_lib toolbox from Sandia National Labs website. These toolboxes have already been developed by Sandia National Laboratories, USA [18], [19].
- (ii) Copy these files to one folder:

From WVM Toolbox:

- pvl_WVM.m

From WVM Toolbox (supporting Programs):

- moving.m
- pdist_vector.m
- pvl_WVM_compute_VR.m

- pvl_WVM_compute_clear_sky_index.m
- pvl_WVM_compute_distances.m
- pvl_WVM_compute_wavelet.m
- pvl_getaoi_NaN.m
- pvl_haydavies1980_NaN.m

From PV_Lib Toolbox:

- pvl_absoluteairmass.m
 - pvl_alt2pres.m
 - pvl_clearsky_ineichen.m
 - pvl_date2doy.m
 - pvl_ephemeris.m
 - pvl_extraradiation.m
 - pvl_grounddiffuse.m
 - pvl_leapyear.m
 - pvl_makelocationstruct.m
 - pvl_maketimestruct.m
 - pvl_relativeairmass.m
- (iii) Copy 'Required Data' Folder from PV_Lib Toolbox and delete all files excluding LinkeTurbidities.mat.
- (iv) Copy the excel file containing the data of irradiance, temperature and timestamps [20].
- (v) Finally, copy the file Task_gamesa.m in the same folder and run it. It will plot the results. This program is developed while doing this thesis.

In this MATLAB code, the program is implemented in three steps. First the time vector at which the irradiance and temperature data is recorded is converted to serial date number format [22]. Then the irradiance and temperature data are read from the excel file and the required inputs for WVM method are provided in the code. These inputs can be varied depending upon the studied scenario. Finally, using the formula mentioned in [21], power ramps are determined and respective results are plotted.

4.5.2.4 Inputs Used in the Program

The used inputs in the program are mentioned below:

4.5.2.4.1 Sensor Inputs: [20]

- Sensor latitude = -15.23914
- Sensor longitude = 28.08105
- Sensor altitude (in meters) = 1276
- Tilt for GHI sensor = 2°
- Azimuth for GHI sensor = 34°
- Sensor UTC offset = 2

4.5.2.4.2 Solar Plant Inputs:

- Tilt for solar modules (approximately equal to latitude tilt) = 15°
- Azimuth for solar modules (assume it to be same as of the sensor) = 34°
- Assumed shape of PV plant = square
- MW capacity of PV plant = 100
- PV density = 61.77 W/m² (1MW per 4 acres)

4.5.2.4.3 Cloud Input:

- Assumed cloud speed = 11.5 m/s

4.5.2.4.4 Irradiance and Temperature Inputs:

- The irradiance and corresponding temperature data has been read in the MATLAB code from the provided excel sheets.

4.5.2.4.5 Timestamps:

- In addition to irradiance and corresponding temperature data, an additional input of the time (time at which the irradiance and corresponding temperature data is measured) is also required. For timestamps (datetime) inputs, the toolbox requires them to be in serial date number format. This is accomplished in the start of the MATLAB code [22].

4.5.2.5 WVM Toolbox Explanation

As mentioned above, only 21 files (20 .m files and 1 .mat file) are required from the toolboxes to calculate equivalent irradiance for the solar output yield. A brief working of each function in the toolbox is described below:

function pdist_vector:

This function is used to avoid the need for square-form function available in Statistics Toolbox.

function moving:

It calculates the moving averages of order n. Clear sky index is inputted to this function for smoothing.

function pvl_WVM:

It calculates the spatially-smoothed irradiance using the wavelet variability model.

function pvl_WVM_compute_VR:

It computes variability reduction (VR), which depends on the distances between sites (dist), the clouds speed (CS) and the timescales.

function pvl_WVM_compute_clear_sky_index:

It uses Hay/Davies method to calculate clear sky index based on Clear sky GHI, DNI, DHI, which are found using Ineichen/Perez model.

function pvl_WVM_compute_distances:

It calculates the distances are calculated between all pairs of sites of the PV plant based on Latitude and Longitude input along with shape/type of the plant.

function pvl_WVM_compute_wavelet:

It computes the wavelets from clear sky index based on timescales.

function pvl_absoluteairmass:

It calculates absolute (pressure corrected) airmass from relative airmass and pressure. The formula used is:

$$\text{absolute airmass} = (\text{relative airmass}) * \text{pressure} / 101325$$

function pvl_alt2pres:

It determines the atmospheric pressure on the site based on the altitude input. This calculation is performed based on some assumptions which are:

- Base pressure = 101325 Pa
- Temperature at zero altitude = 288.15 K
- Gravitational acceleration = 9.80665 m/s²
- Lapse rate = -6.5e-3 K/m

- Gas constant for air = 287.053 J/(kg*K)
- Relative Humidity = 0%

function pvl_clearsky_ineichen:

It determines clear sky GHI, DNI, and DHI from Ineichen/Perez model. It uses $DHI = GHI - DNI * \cos(\text{zenith})$. This implementation of the Ineichen model requires a number of other PV_LIB functions as well.

function pvl_date2doj:

It calculates the day of the year using the day, month and year of the Gregorian calendar.

function pvl_ephemeris:

This function calculates the position of the sun based on the provided time, location, and optionally temperature and pressure.

function pvl_extraradiation:

It determines the quantity of extra-terrestrial solar radiation in watts per square meter on the surface normal to the sun based on the day of the year.

function pvl_getaoi:

It determines angle of incidence from surface tilt/azimuth and apparent sun zenith/azimuth.

function pvl_grounddiffuse:

It estimates diffuse irradiance (the portion of irradiance on a tilted surface due to ground reflections) based on irradiance, albedo and surface tilt.

function pvl_haydavies1980_NaN:

It calculates diffuse irradiance from the sky on a tilted surface (ground reflected irradiance is not included) based on various inputs using Hay & Davies' 1980 model.

function pvl_leapyear:

It determines if a given year is a leap year or not based on 400 year cycles.

function pvl_makelocationstruct:

It creates a location struct to define a site location.

function pvl_maketimestruct:

It generates a time structure given a MATLAB datenum (vector of MATLAB serial date numbers) and UTC offset code.

function pvl_relativeairmass:

It calculates the sea-level airmass based on sun zenith angle.

4.5.2.6 Input Flow Diagram

The diagram below (figure 4.9) explains how some basic inputs are used to find the inputs for other various functions in the toolbox and finally to calculate the WVM smoothed irradiance.

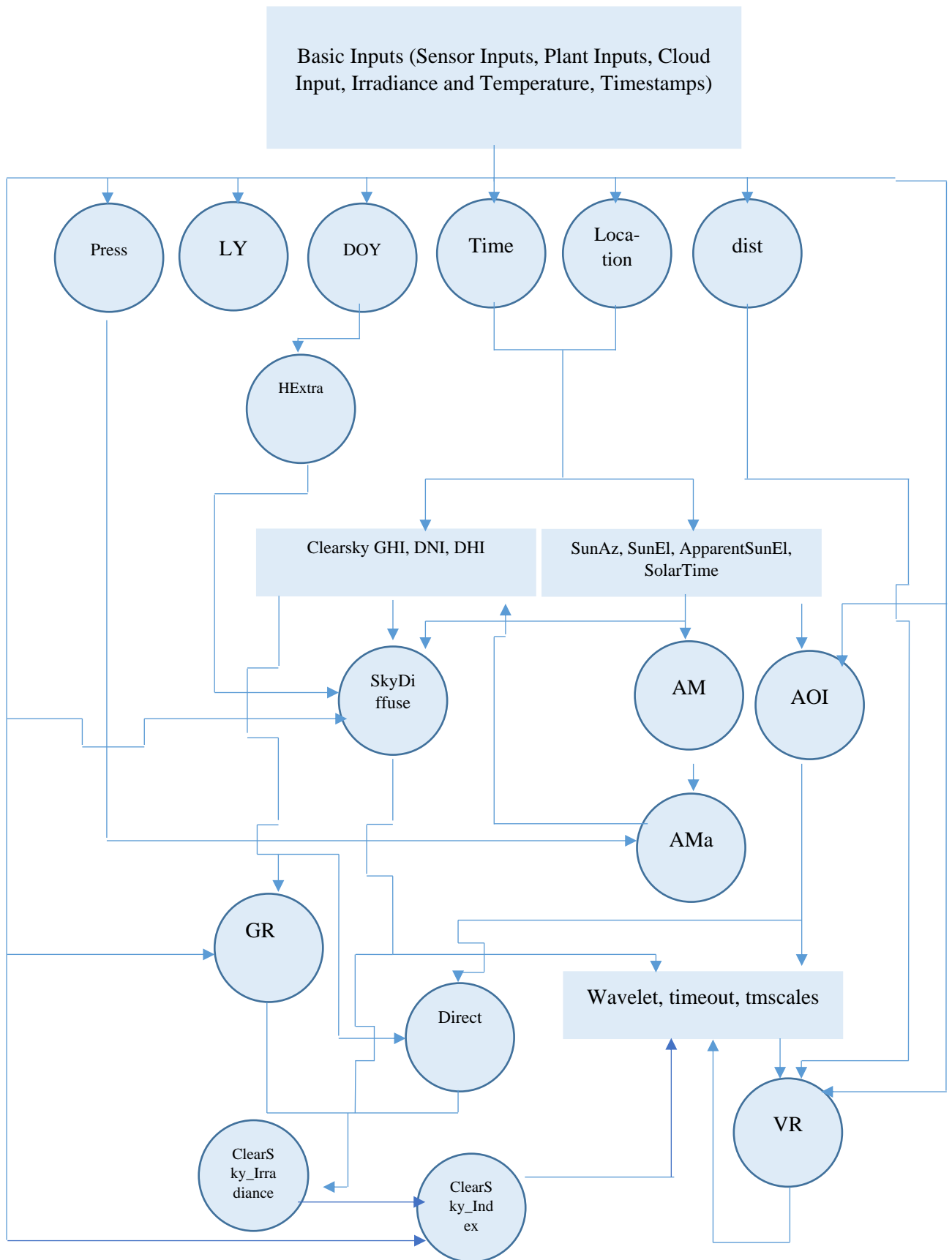


Figure 4.9. Input Flow Diagram

Abbreviations used in figure. 4.9 are:

AOI:	Angle Of Incidence
GHI:	Global Horizontal Irradiance
DNI:	Direct Normal Irradiance
DHI:	Diffuse Horizontal Irradiance
CS:	Cloud Speed
VR:	Variability Reduction
Direct:	Direct Normal Irradiance
GR:	Ground Diffuse
AM:	Air Mass
AMa:	Air Mass absolute
LY:	Leap Year
Press:	Pressure
DOY:	Day of Year
Dist:	Distance
Tmscales:	Time Scales
HExtra:	Extra-terrestrial Radiation
UTC:	Coordinated Universal Time
SunAz:	Sun Azimuth
SunEl:	Elevation of Sun
ApparentSunEl:	Apparent Elevation of Sun

It is important to mention here that the above mentioned model uses too many statistical and empirical formulas for the calculation of different quantities. To get a better understanding of the model, the user is advised to analyse each function of the toolbox thoroughly. Further modelling details of WVM method is described in [24].

4.5.3 COMPARISON OF THREE METHODS FOR POWER PATTERNS

A comparison of above-discussed methods has been presented for analysing solar PV outputs. To compare the results, three different cases are plotted using MATLAB code as shown in the figure 4.10 below.

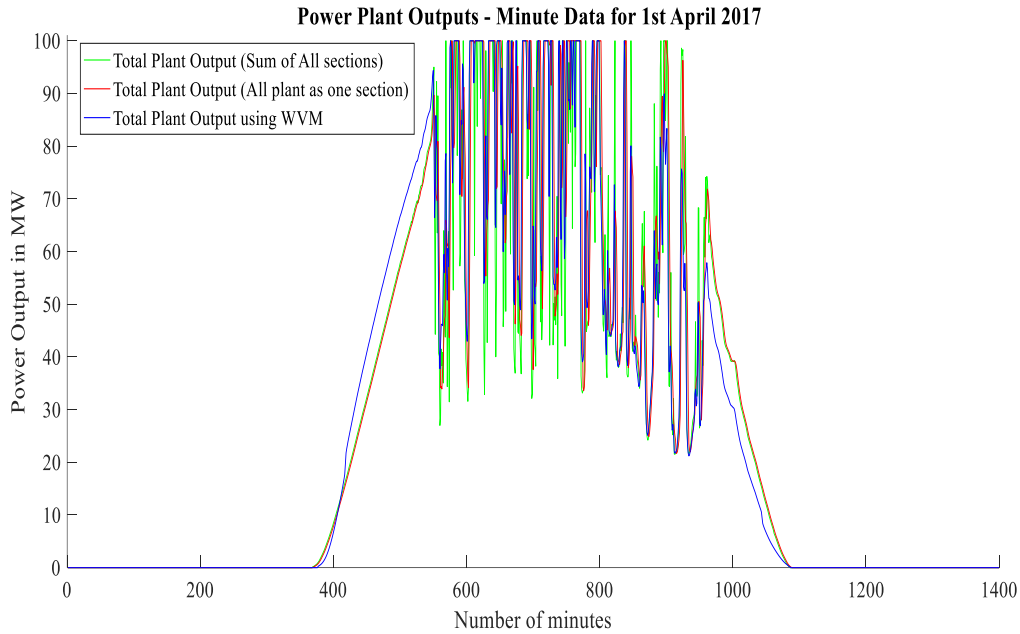


Figure 4.10. Comparison of power output from Solar PV plant for 3 methods (zoomed-in)

The power output pattern for N-section method and WVM method is very similar to each other, however, the output profile for single-section method varies from them, especially during the power ramp-downs.

4.6 POWER RAMP-DOWN ANALYSIS

Finally, the ramps (both ramp-ups and ramp-downs) are calculated by subtracting the power output at 't+1' from power output at 't', which is the rate of change of power output per minute.

Since the power ramp-down in solar PV power plants is a new topic and lot of research is ongoing in this field, therefore, before proceeding further, a brief literature review is presented for it below.

4.6.1 PV PLANT POWER RAMP-DOWN LITERATURE REVIEW

A brief literature review for PV plant ramp down analysis is discussed in this section. In [12], a forecasting method called as wavelet variability model (WVM) is explained to simulate the solar photovoltaic (PV) power plant output. It is based on irradiance time-series data from single sensor point using correlations of physical space and time. The variability reduction is proposed to occur when applying upscaling from the one point sensor to the complete PV plant. The model is validated against actual measurements of a residential distributed PV power plant

of capacity of 2 MW and also of utility-scale power plant of capacity of 48 MW, the detailed discussion of validation is presented in [13].

In [25], the ramp rates from solar PV power plant are discussed in detail. Various aspects like variability of ramps according to specific site and storage requirements are analysed after the imposition of ramp limitations by some utilities (e.g. 10% of capacity per minute limit by Puerto Rico Electric Power Authority PREPA). Here again, WVM is used to obtain power output profiles from irradiance time-series data.

In [26], the issue of PV ramping is analysed for small standalone grid of Hawaii using solar data of four locations on the island collected by NREL. The power output ramps from individual sites and the effect of accumulating the PV production from all the locations is analysed to find the possible worst-case scenario of PV ramping.

In [27], an analysis of variability in solar power output for two installations due to weather changes is presented. It has been found that increase in MW capacity of the plants and increasing distance between them results in lower variability in power outputs.

4.6.2 POWER RAMP-DOWNS SENSITIVITY ANALYSIS FOR N-SECTIONS METHOD

Additional analysis has been performed by varying the number of sections and percentage increase in number of panels. To clearly observe the impact on ramps by varying these two parameters, 4 scenarios are considered.

- Scenario 1: Number of sections = 5, Percentage increase in number of panels = 5%
- Scenario 2: Number of sections = 5, Percentage increase in number of panels = 30%
- Scenario 3: Number of sections = 20, Percentage increase in number of panels = 5%
- Scenario 4: Number of sections = 20, Percentage increase in number of panels = 30%

The ramps plots on first day of April 2017 considering above scenarios are shown below:

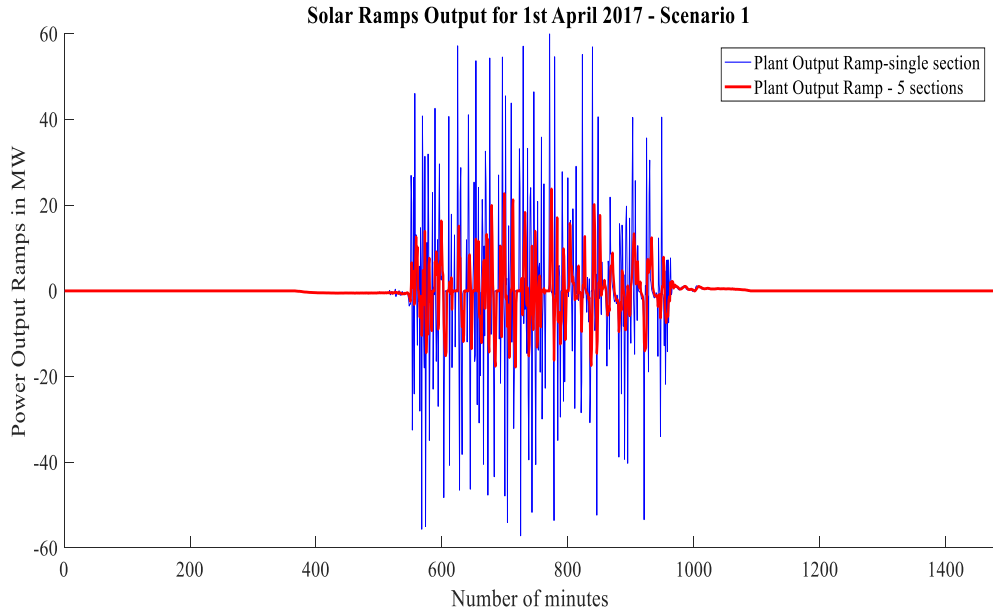


Figure 4.11. Scenario 1 Solar Ramp outputs

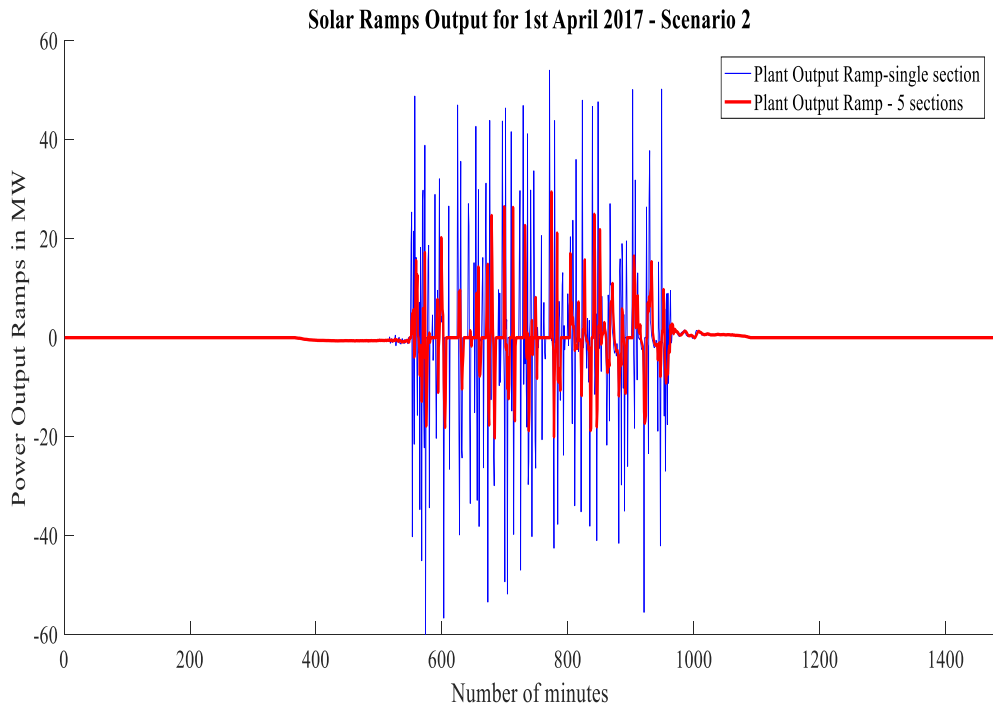


Figure 4.12. Scenario 2 Solar Ramp outputs

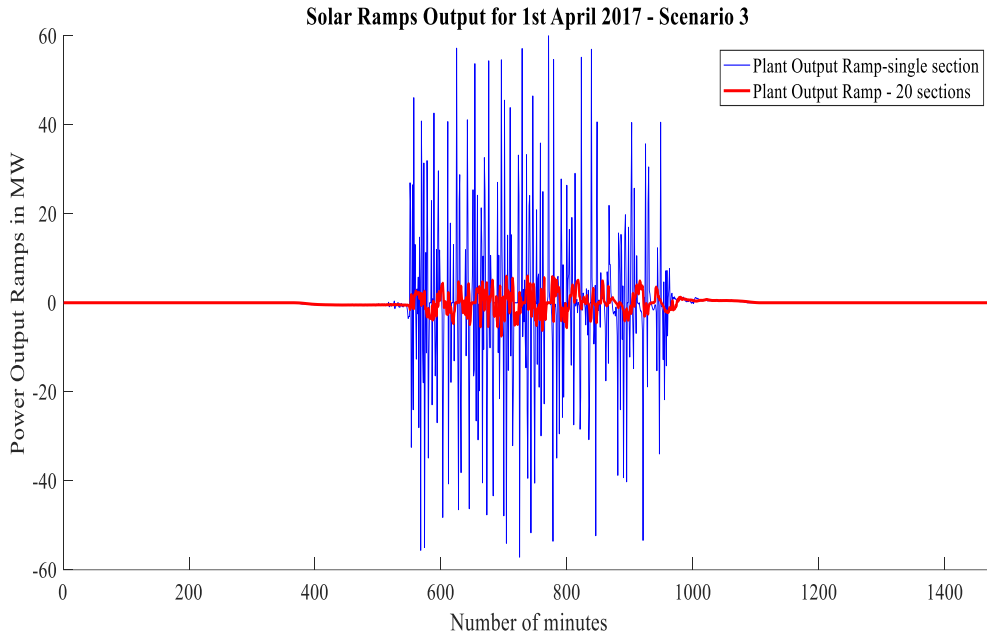


Figure 4.13. Scenario 3 Solar Ramp outputs

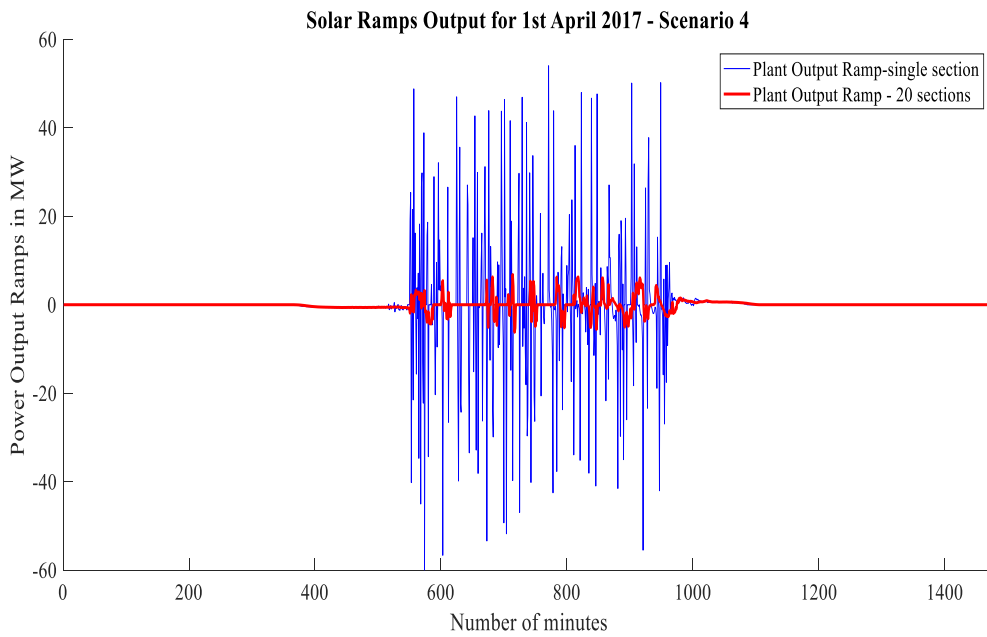


Figure 4.14. Scenario 4 Solar Ramp outputs

As clearly evident from the above figures, the magnitude of the ramps decrease significantly by increasing the number of sections and increase slightly by increasing the percentage number of panels.

4.6.3 COMPARISON OF THREE METHODS FOR POWER RAMPS

To compare the power ramping results, the ramps patterns are plotted using MATLAB code as shown in the figures (presented below as Fig. 4.15 and 4.16).

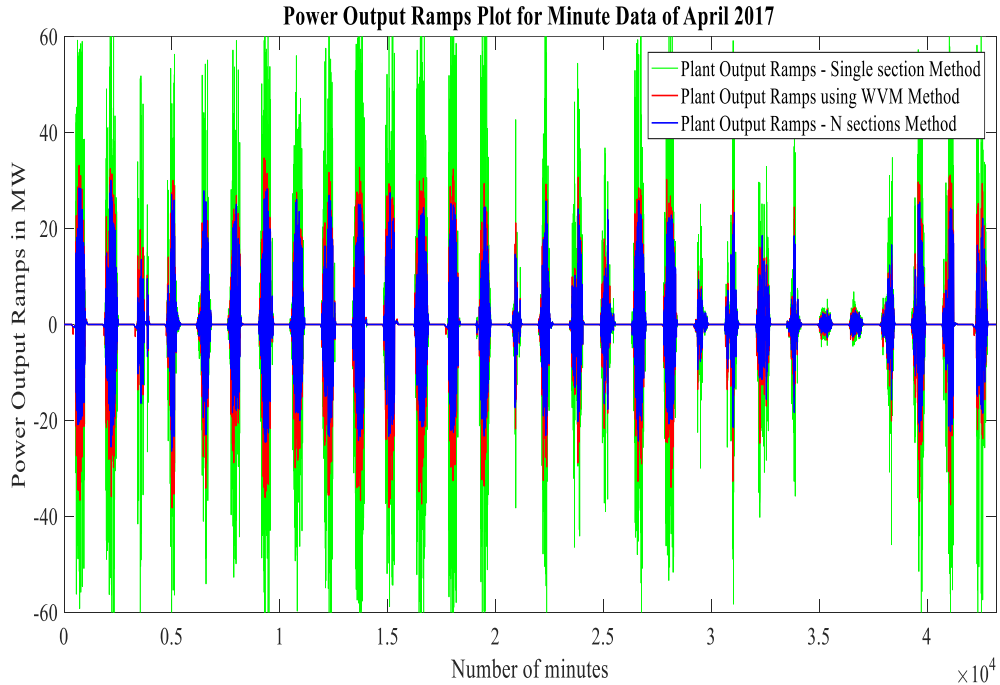


Figure 4.15. Comparison of power ramps from Solar PV plant for 3 methods

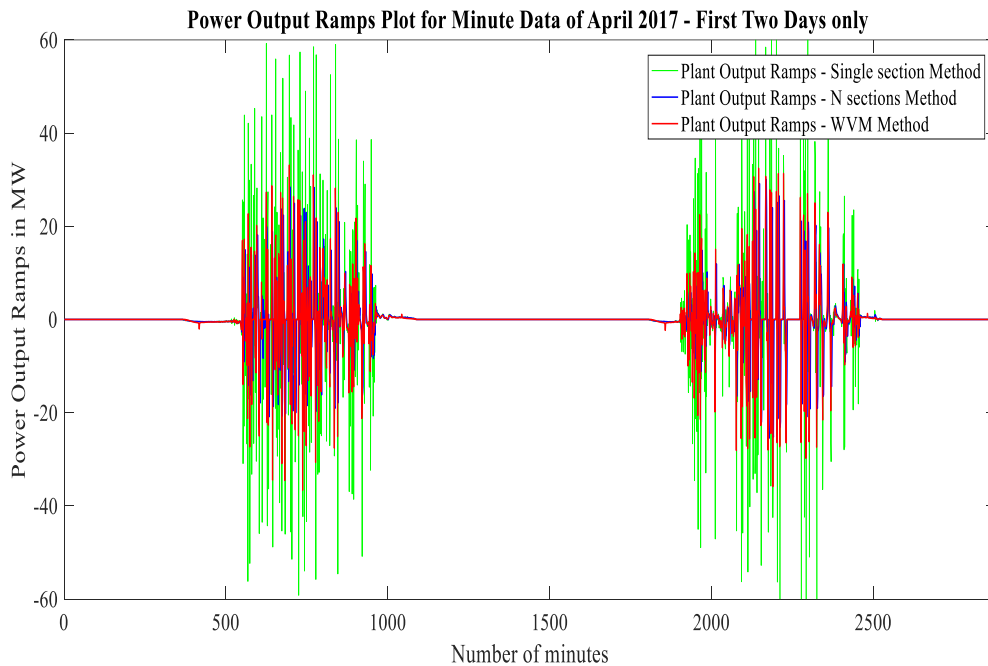


Figure 4.16. Comparison of power ramps from Solar PV plant for 3 methods (zoomed-in)

Here the positive value of the ramps are ramp-downs while the negative values are ramp-ups in MW/min. As clear from the figure 4.16., the magnitude of the power ramps decrease significantly for WVM and N-Section method compared with single-section method. The magnitude of maximum ramp-downs determined for the whole dataset of 8.5 months come out to be 35.67, 31.88 and 75.19 MW/min for WVM, N-section and single-section methods respectively.

The results are further analysed using distribution plots and CDF (Cumulative probability distribution function) plots as shown in figure 4.17 and 4.18 respectively.

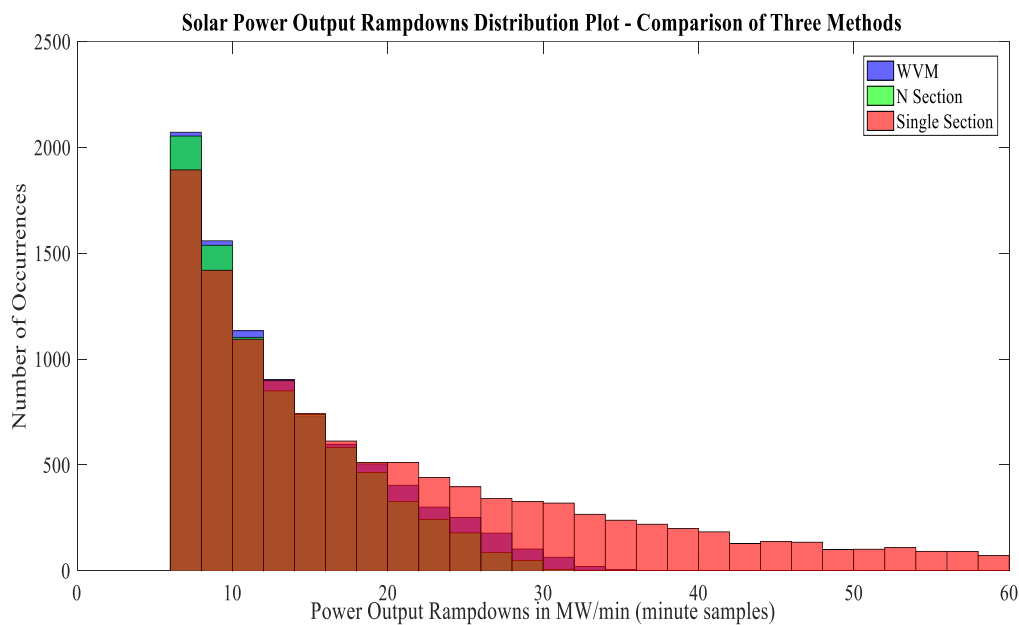


Figure 4.17. Distribution Plot for power ramps for three methods

It is evident from the figure 4.17 that the range of the power ramps magnitude is narrower for WVM and N-section methods, however, there is a significant number of larger magnitude ramps for single-section method. Since the normal limitation on power ramps are 10% (here 10 MW/min), based on the results from WVM and N-section method, the problematic range of ramp-downs is 10-30 MW/min, however for single-section, it is from 10-60 MW/min, which can lead to an over-investment for the design of the preventive solution for the problem.

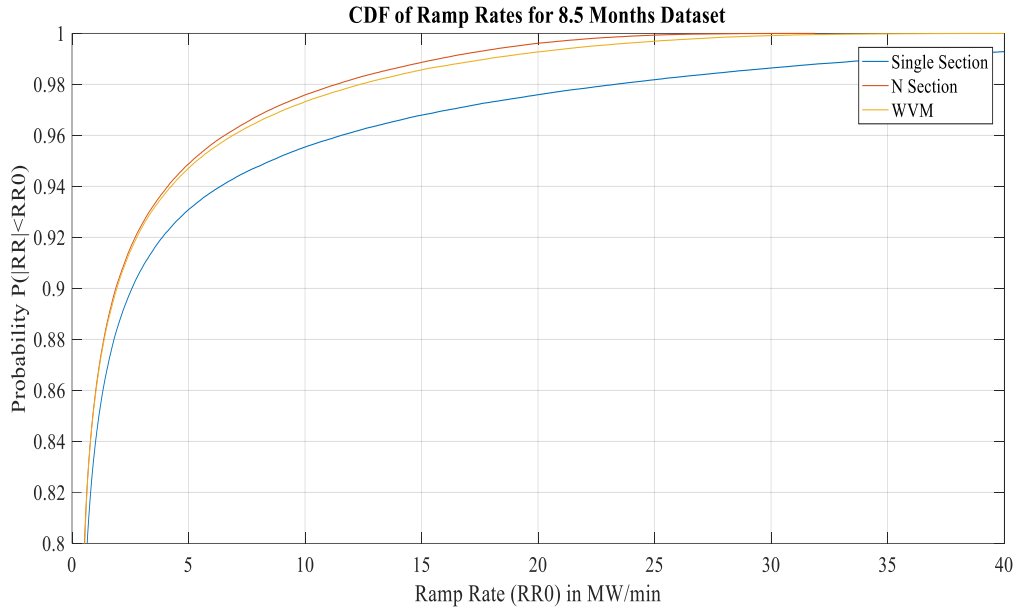


Figure 4.18. CDF Plot for Power Ramp Rates for three methods

According to figure 4.18, 10 MW/min ramp violation limit is exceeded for 2.3%, 2.5% and 4.5% of the time for N-section, WVM and single-section method respectively. Although the results from WVM and N-section method are quite close, WVM can be selected as the most reliable methodology among the three because the results from WVM method lies between the two ranges of results from N-section and single-section method. Moreover, it also has a recognition in the present ongoing research on the solar PV power ramping problem.

4.6.4 CONCLUSIONS

From the above analysis, the ramps magnitude for a 100 MW solar PV plant are approximately up to 30 MW, which is 30% of the installed capacity. Furthermore, a reasonable decrease in ramps magnitude can be seen when dividing the plant into 4 sections (cloud movement is considered as irradiation movement) as oppose to the case when considering the same irradiation over the entire plant. This also suggests that distributing the power plant over into smaller sections that are not stacked together shall minimize the ramp-down to certain level. Moreover, the results for N-section and WVM method are almost the same.

Chapter 5

Sizing and Economic Viability of DC-DC BESS

5.1 INTRODUCTION

In this chapter, an analysis is presented for the feasibility of additional DC-DC BESS which is used to reduce the number of power ramp rate violations by capturing the clipped energy above the nominal rating of the solar power plant. Unlike the strategy discussed in other similar analysis [29], in which the BESS is assumed to get charged without any constraints, here only the clipped energy is utilized for this purpose without any external source of charging the BESS. The nominal AC rating of the solar power plant is 100 MW and all the equipment including AC/DC converter is installed as per the nominal rating of the plant. However, by observing the power output profile (as in figure. 5.1) from the solar PV plant, it can be clearly observed that the output is going above 100 MW and if no additional arrangement is used, this clipped energy is going to be wasted.

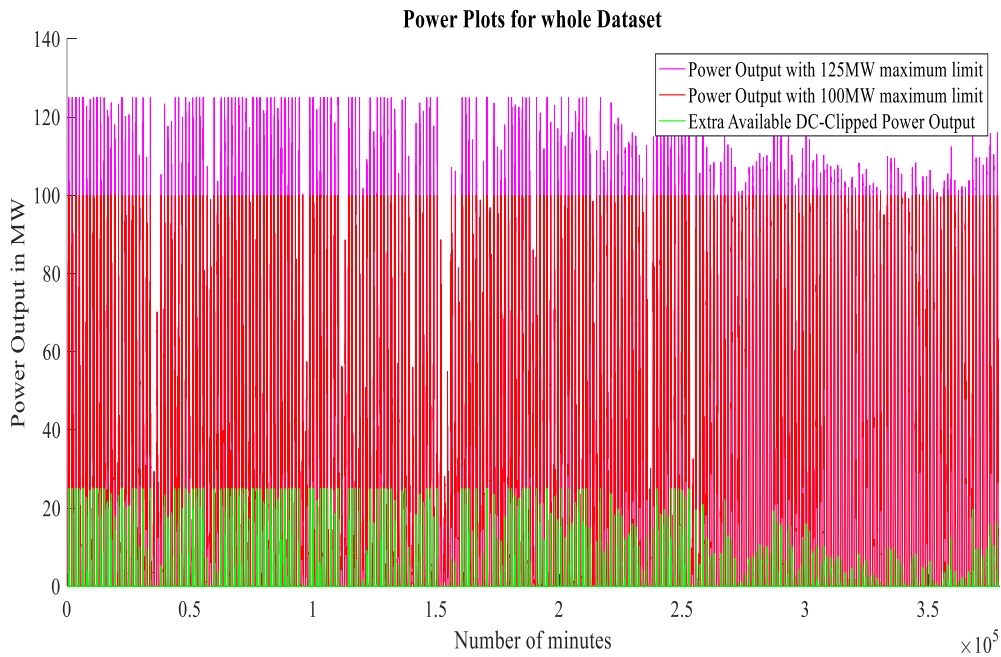


Figure 5.1. PV plant power outputs

In order to utilize this extra available energy effectively, an additional DC/DC system (including mainly DC/DC converter and batteries) is proposed to reduce the number of power ramp rate violations its economic viability has been evaluated.

The DC to AC power ratio is varied from 1.01 to 1.60 and the value of available clipped energy is found, the results are plotted in in figure 5.2.

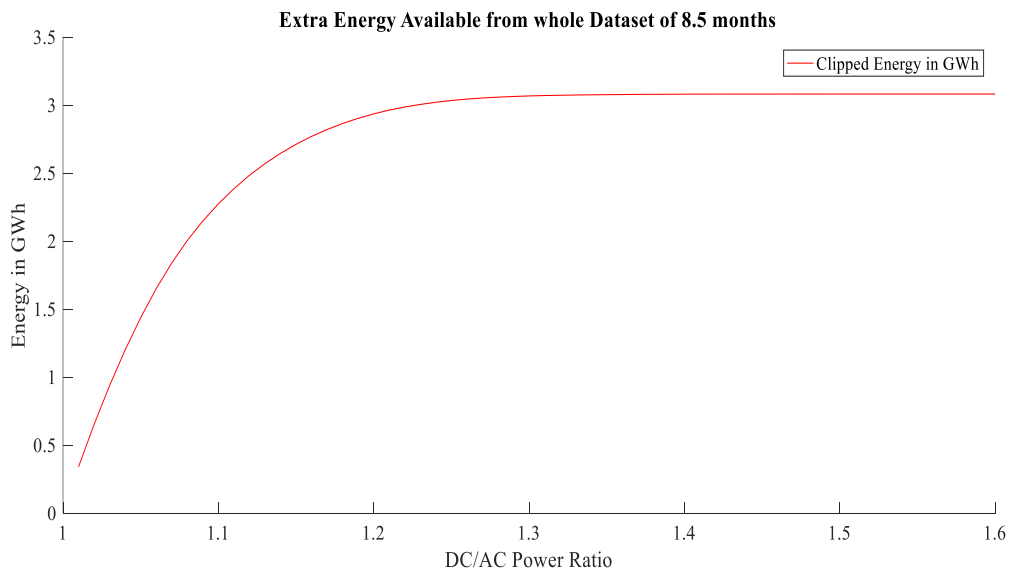


Figure 5.2. Extra Available DC Clipped Energy

It is quite evident that the amount of available extra energy get saturated after the DC to AC power ratio of 1.25. It is an indication to consider the maximum size of DC-BESS system to be 25 MW. However, further analysis in this regard will be presented in the following sections. For DC to AC power ratio of 1.25, the extra available energy from clipped DC power is 3.0333 GWh, while the total directly extractable energy from 100 MW plant is 154.92 GWh.

5.2 LITERATURE REVIEW OF BESS FOR SOLAR PV INSTALLATIONS

In [30], probabilistic methodology is discussed to find the power capacity specification for a hybrid energy storage system HESS (composed of a super-capacitor and battery energy storage system (BESS)). In [31], a method is presented for examining the use of energy storage for ramping control caused by clouding for seven utility scale PV plants in USA and Canada. The observed ramp rates are summarized for plants of different capacity, i.e., for 5, 21, 48, 80 and

250 MWac plants, the maximum ramp rates found are 0.7, 0.58, 0.53, 0.43 and 0.35 times the plant's nominal capacity respectively. Moreover ESU (Energy Storage Units) with high power-to-energy ratio are proposed to mitigate output ramps in solar PV plants. In [32], a utility-scale BESS is suggested for PV power plant with a multilevel inverter having medium frequency transformer link. The power flow is regulated using a 3-level bidirectional boost-buck DC-DC converter which is interfaced between battery and the PV system DC bus. It has been shown that 80% irradiance fluctuations are mitigated by using BESS of 10% active power rating. The simulation has been performed for design example of 125 kW BESS.

In [33], an improvement in grid integration of PV system is discussed using a centralized plant controller for storage system and with an experimental example of 1.2 MW PV plant in Tudela (Navarre, Spain). While a new optimized strategy has been proposed in [34] for PV plants with energy storage. In [35], a novel strategy of deloading (PV plant running with some reserve margin) has been proposed for PV plants without energy storage to avoid the frequency drops in case of clouding. It has been tested for PV plant in northern Chile with various scenarios of power network and deloads. In [36], the utility benefits (peak power support, power generation, reduced line losses, etc.) and the cost of battery storage (lifetime and size) are discussed for energy storage management system.

In [37], a hybrid energy storage system (HESS) having a supercapacitor bank and battery is proposed for smoothing the fluctuations in the output power of the PV plant. In [38], some important control characteristics for battery energy storage (like peak shaving, PV output smoothing, etc.) are discussed for improving the grid integration of large solar PV plants under various load and network conditions. An optimal method is presented in [39] for smoothing active power output and has been compared with moving average method of ramp rate control. The simulation has been performed for data from real time ac micro-grid. In [40], statistical models are developed to estimate the power dispatch performance and HESS capacities for solar PV power plant through extensive simulation data. It has been observed that power capacity of HESS has larger impact on deciding the indices for dispatch performance as compared to energy capacity.

In [41], the applications of a hybrid system (composed of BESS and PV generator) are discussed in generation, transmission and distribution and customer services. In [42], a novel strategy called as dynamic ramp-rate control algorithm has been proposed for utility-scale PV plants (having energy storage systems). This algorithm provides a simple SOC control and 30

% less cycling degradation than conventional ramp-rate control. It has been tested for recorded power outputs from Amareleja PV plant (45.6 MWp, Portugal). In [43], different techniques for smoothing solar power output (simple moving average based smoothing, single and half window based smoothing with energy compensation, single and half window based moving average) are compared. The simulations are performed for a typical moving cloud day output of a solar power-plant with nominal rating of 5 MWp.

5.3 TOPOLOGY OF DC BESS

The topology of the system (DC-DC BESS) is shown below:

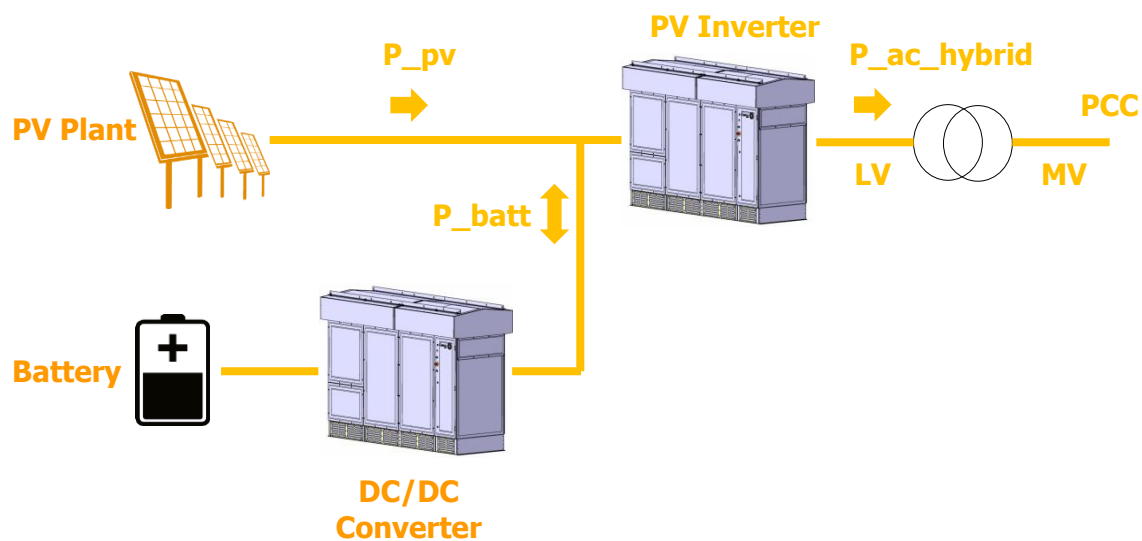


Figure 5.3. Topology of DC Coupling for Solar PV plant [28]

Reference figure 5.3, the dispatch of PV power output has been carried out using standard AC/DC inverter having its rating equal to the nominal rating (100 MW) of the solar PV power plant. It is important to mention that the equivalent additional energy from DC-DC BESS has to be calculated by catering the efficiencies of DC/DC converter and battery for twice, once for storing the energy in the battery and the other for dispatching the stored energy.

5.4 ASSUMPTIONS

The assumptions considered for the analysis are:

- The cost for a complete DC-DC system, including the DC-DC converter and the battery is considered as \$600/kW, \$1050/kW and \$1950/kW for 1, 2 and 3 hours battery system

respectively.[28] For 30 minutes system, the cost is assumed to be 65% of the cost for 1 hour system, i.e., \$390/kW.

- The maximum output level from the solar PV plant is 125 MW (as discussed in section 5.1).
- The extra revenue which can be received (depends upon the location of the plant) on the basis of energy supply during peak-load hours is not considered.
- Efficiency of batteries for unidirectional flow of energy is taken as 0.98.
- Efficiency of DC/DC converter for unidirectional flow of energy is taken as 0.967.
- The complex financial calculations (including cash flows, interest rate, debt service etc.) are not carried out due to unavailability of the required data.
- The power ramp-down greater than 10% of the nominal plant capacity to be considered as Ramp Rate Violation (RRV). [29]

5.5 METHODOLOGY

The basic algorithm of the implemented MATLAB code is explained step by step below:

1. Initialize the variables used in the code.
2. Calculate the power output profile (data points) for available data of 8.5 months imposing a maximum limit of 100 MW (nominal output), which is called as direct power output.
3. Calculate the power output profiles (data points) for available data of 8.5 months imposing a maximum limit in the range of 101 to 125 MW.
4. Find the difference in the power output profiles found in step 2 and 3, which gives the extra/clipped power profile for available data of 8.5 months.
5. Implementing State of Charge (SOC) constraint for the BESS taking into the following main points:
 - i. The maximum power at point of common coupling (PCC) at one instant of time should be 100 MW.
 - ii. Four options are considered for the possible rating of the battery-energy supply time, which are half an hour, 1 hour, 2 hours and 3 hours.
 - iii. The maximum stored energy at one instant of time (normally in minute resolution here) should be equal to “MW capacity*battery-energy supply time in minutes”, e.g. for the rating of 25 MW for 1 hour, maximum stored energy

would be 1500 MW-min. It is better to do that because all the available data is in minute resolution. MW-min is a unit of energy and can be converted to MWh by dividing it by 60.

- iv. Since the BESS has a fixed MW capacity, the maximum power supply at one instant of time should be equal to the specified power capacity (ranging from 1 to 25 MW).
 - v. Whenever the power output is greater than 100 MW, the energy is used to charge the batteries.
 - vi. Two methodologies are applied in implementing the discharging of the BESS to support the power output at PCC. In the first approach, the energy support has been provided from the battery storage system depending upon the difference between nominal power plant rating and direct power output (power output without any BESS support). However, in the second approach, BESS energy support depends on the difference between 90% of the nominal plant rating and the direct power output. In both approaches, the purpose is to make the power output at PCC equal to 100 MW, given that at that instant of time the batteries have some stored energy in it. These are discussed in detail in the next section.
 - vii. The remaining stored energy in the battery system is updated after every minute according to import or export of power from it.
6. Perform simple energy calculations finding out energy in GWh for with and without additional DC coupling arrangements, extra captured energy which can be supplied to grid, extra captured energy which has to be wasted due to limitations of maximum nominal power, etc. The equivalent additional energy from DC-DC BESS has to be calculated by catering the efficiencies of DC/DC converter and battery for twice, once for storing the energy in the battery and the other for dispatching the stored energy. These energy calculations are implemented into the following points:
- i. The additional captured energy can be found by calculating the energy from the clipped power output. The energy from power is calculated using 'trapz' function of MATLAB which gives the numerical integration of the variable using trapezoidal method.
 - ii. The additional captured energy which is utilized at the PCC is found by subtracting the energy from power output profile (having maximum limit of 100

MW) from the energy from power output at PCC. Only this energy is sold to the utility and the revenue is received as per the specified tariff.

iii. The additional captured energy which has to be wasted is found by subtracting the energy from power output at PCC from the energy from clipped power (extra MWs) storage in the battery. Even this energy can be stored in the batteries but due to limitation from (i), it cannot be supplied to the grid and must be wasted.

7. Improvement in the power ramping down problem is recorded.

8. Display and plot the results.

Based on the above methodology, direct power output, PCC power output and battery supply power output in MWs are plotted for the whole dataset of 8.5 months as shown in figure 5.4. The outputs are plotted in a zoomed window to have a clear idea of the working.

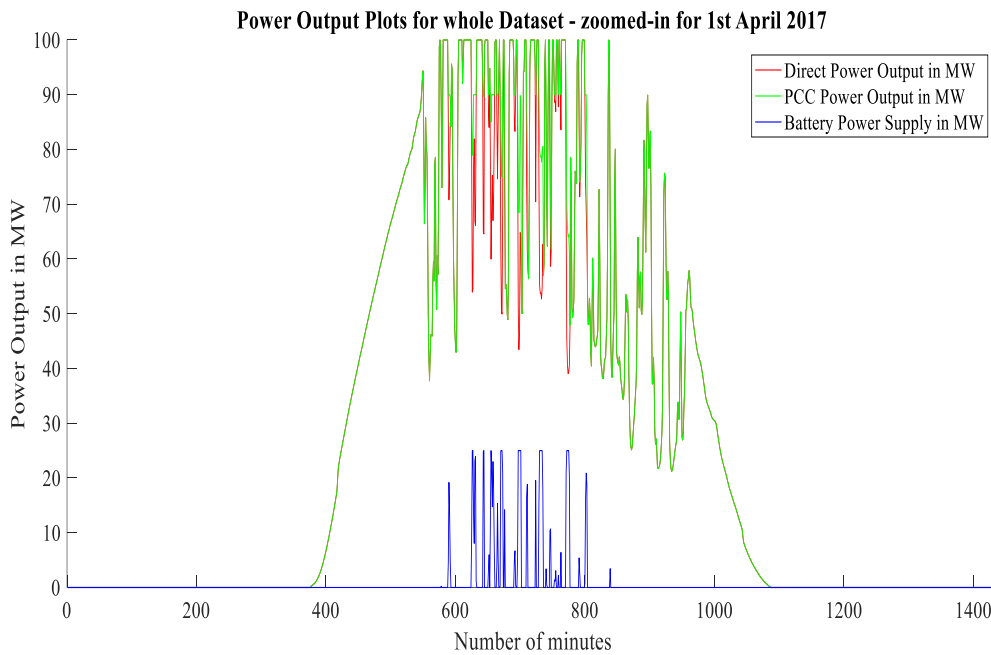


Figure 5.4. Power Output Plots

It can be easily observed that the PCC output is more smooth (having less power variations) as compared to the direct power output. Moreover, the ramping down variations in direct output are supported by the battery power supply given that BESS has some storage to do it. Since these are plotted for the case of DC-BESS capacity of 25 MW, it is evident that the maximum rating of it 25 MW.

Reference figure 5.4, it can be observed that the BESS get completely discharged in two-third of the solar day in supporting the PCC power output profile to reduce the power ramp-downs.

For the last one-third part of the solar day, there is no available support from BESS and the power output profile get suffered from most of the ramp-downs in that part. For future work, this problem can be minimized implementing dual DC-BESS scheme, in which the first DC-BESS will have the high power-to-energy ratio and the second should be with lower power-to-energy ratio, in order to support the first two-thirds and the last one-third part of the solar day respectively. It is because the second one is required to store the available captured energy for longer duration of time each day.

5.6 COMPARISON OF THE TWO APPROACHES

As discussed in section 5.5, two approaches are applied for implementing SOC algorithm. The difference between them is the condition when to support the PCC output, either depending upon 100% power plant rating or 90% of it. The factor of 90% is used because any power ramp greater than 10% is considered as ramp-rate violation. It is very interesting to observe that after applying this factor, there is a remarkable improvement both in ramp-down violation count and the avoided RRV violation energy (MW-sec).

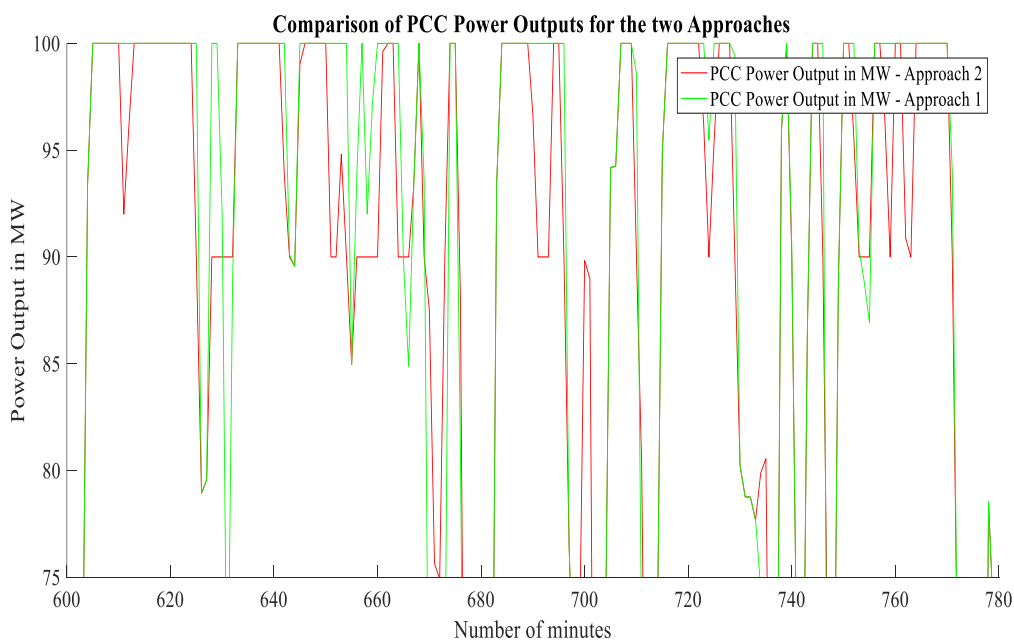


Figure 5.5. Comparison of the two approaches (zoomed-in)

The comparison plot of power outputs at PCC for both the approaches is given in figure 5.5. In the first approach, BESS is trying to make the PCC output equal to 100 MW irrespective of the consideration for next ramp-down, however, in the second approach, BESS is supporting PCC power output and the same time keeping some energy for the next ramp. For example, in

approach 2, BESS is smartly storing some energy at $t = 607$ without going for any ramp-rate violation at PCC and in the next ramp-down at $t = 630$, it is avoiding RRV. However, for approach 1, BESS is keeping 100 MW at PCC during $t = 607$ and suffered from RRV at $t = 630$ due to unavailability of enough stored energy. The comparison in ramp-down down improvement for these two approaches has been shown in Table 5.1.

Table 5.1. Factors Calculated for BESS Approaches

Factors	Approach 1	Approach 2
Ramp-down violation Count (number of times)	4377	3701
Avoided RRV Violation Energy (MW-sec)	800878	1230370
Maximum ramp value (MW)	49.649	46.485
Captured Utilized Energy (GWh)	2.6552	2.6436

The above comparison results are for 25 MW 1 hour system. There is much improvement in number of ramp-down violations and avoided RRV violation energy for approach 2. There is a slight improvement in maximum ramp value, however, the captured utilized energy almost remains same for both the approaches.

5.7 SIZING THE DC-BESS

Approach 2 is used to size the DC-DC BESS for the solar PV plant. In the analysis, the criteria followed to find the power and energy rating of the DC-DC BESS are the ramp-down violations count and the avoided RRV violation energy (MW-sec). The size with least number of ramp-down violations and the maximum avoided RRV violation energy would be the best option. The results for power ramp and energy calculations are presented in Table 5.2.

Reference Table 5.2, MW capacity of DC-BESS is varied from 1 to 25 MW and the corresponding occurrences of ramp-down violations and the values of avoided RRV violation energy are observed. As evident from the table 5.2, by increasing the power rating of BESS, there is significant improvement in ramp-down violations, however, energy rating has a very less impact on them. Therefore, the maximum power rating for the minimum duration has been selected, i.e., 25 MW system for 30 minutes.

Table 5.2. Results of Analysis – Power Ramp Calculations

MW Rating of DC- BESS	30 minutes System		1 Hour System		2 Hour System		3 Hour System	
	RRV count	Avoided RRV Energy	RRV count	Avoided RRV Energy	RRV count	Avoided RRV Energy	RRV count	Avoided RRV Energy
1	5103	86166	5100	89340	5100	89317	5099	89972
2	4983	185169	4972	194078	4973	193846	4972	194513
3	4879	276545	4871	285186	4871	285434	4870	286169
4	4772	369681	4765	378480	4767	377079	4765	378316
5	4710	439555	4696	453373	4696	453529	4696	453529
6	4621	518420	4606	535760	4606	535283	4607	534557
7	4525	596993	4517	612046	4516	612006	4517	611342
8	4471	655040	4452	679191	4452	678193	4451	678721
9	4403	714047	4377	741211	4375	744448	4375	744166
10	4340	770092	4313	800164	4314	799390	4313	799640
11	4291	817570	4265	849171	4265	851296	4266	851202
12	4223	873296	4196	905905	4198	906884	4198	907423
13	4191	902136	4156	940884	4161	939701	4161	939804
14	4156	932841	4134	963129	4133	960184	4134	959327
15	4112	970749	4086	1004074	4083	1004899	4082	1005506
16	4058	1001928	4033	1035563	4028	1041919	4028	1041975
17	4002	1046104	3985	1072465	3983	1075461	3984	1074586
18	3944	1083299	3923	1111776	3920	1114692	3920	1114673
19	3904	1112995	3884	1140773	3882	1144604	3882	1143505
20	3865	1131325	3850	1152511	3843	1157729	3843	1157650
21	3829	1152887	3810	1176894	3808	1180837	3809	1180011
22	3781	1176655	3751	1207396	3752	1206286	3753	1205650
23	3768	1186089	3750	1206173	3749	1207868	3749	1207989
24	3734	1201812	3715	1224711	3715	1223897	3715	1223897
25	3719	1208461	3701	1230074	3701	1230370	3701	1230370

For the highlighted selected size of the DC-DC BESS, the utilized captured energy comes out to be 2.2809 GWh.

5.8 BATTERY DEGRADATION CONSIDERATIONS

Here an important factor of battery degradation is compared for 30 minute, 1 hour, 2 hour and 3 hour battery storage systems. A factor of energy throughput is used to determine an approximate life time of the BESS. Energy throughput is the amount of energy that can be supplied from the battery for the complete duration of its life. For example, assuming 4000 full discharges, Energy throughput of 25 MW 30 minute BESS = 4000 cycles x 100% of the capacity = 4000 x (25x0.5) MWh = 50,000 MWh. [44]

Then the energy discharged during the operation of the battery for 8.5 months data is found using ‘trapz’ function in MATLAB and the percentage discharge is calculated per year for the 100% capacity of the BESS. Finally the battery life for each case is found. The results are summarized in the table 5.3 below.

Table 5.3. Factors Calculated for Battery System

Factors	30 minutes	1 hour	2 hour	3 hour
Battery discharging Energy (MWh)	2539.83	2943.66	3033.33	3033.33
Energy Throughput (MWh)	50000	100000	200000	300000
Percent Discharge (%)	5.08	2.94	1.52	1.01
Percent Discharge per year (%)	7.17	4.16	2.14	1.43
Battery Life (years)	13.94	24.06	46.70	70.06

Now consider the plot of State of Charge (SOC) of the battery storage system of 25 MW for a 30minutes and 1 hour in a zoomed window as shown in figure 5.6 below:

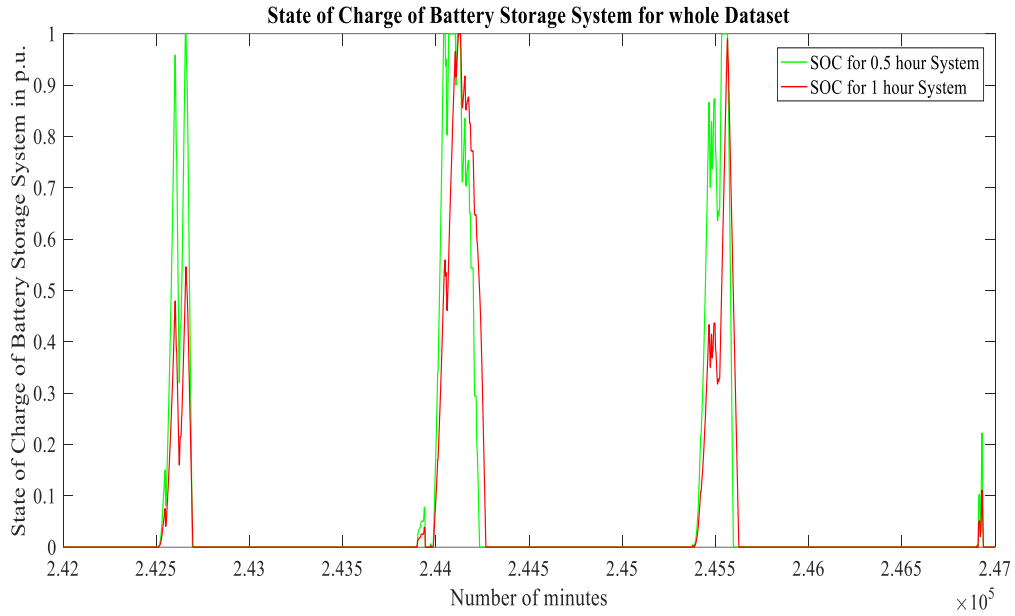


Figure 5.6. State of Charge of Battery System

As evident from the above table 5.3 and figure 5.6, the battery is best utilized for 30 minutes system. Therefore, the choice of 30 minutes BESS is further reinforced by this perspective.

5.9 DISTRIBUTION PLOTS

The above sizing conclusions are further supported by ramp-downs, power outputs and energy-per-day distribution plots for the available data of 8.5 months.

Reference figure 5.7, majority of the occurrences of ramp-downs are up to 20 MW and decreasing up to 35 MW. Since the primary objective of the analysis is to minimize the number of ramp-rate violations, therefore, the design should opt for the maximum available rating of the DC-BESS, i.e., 25 MW.

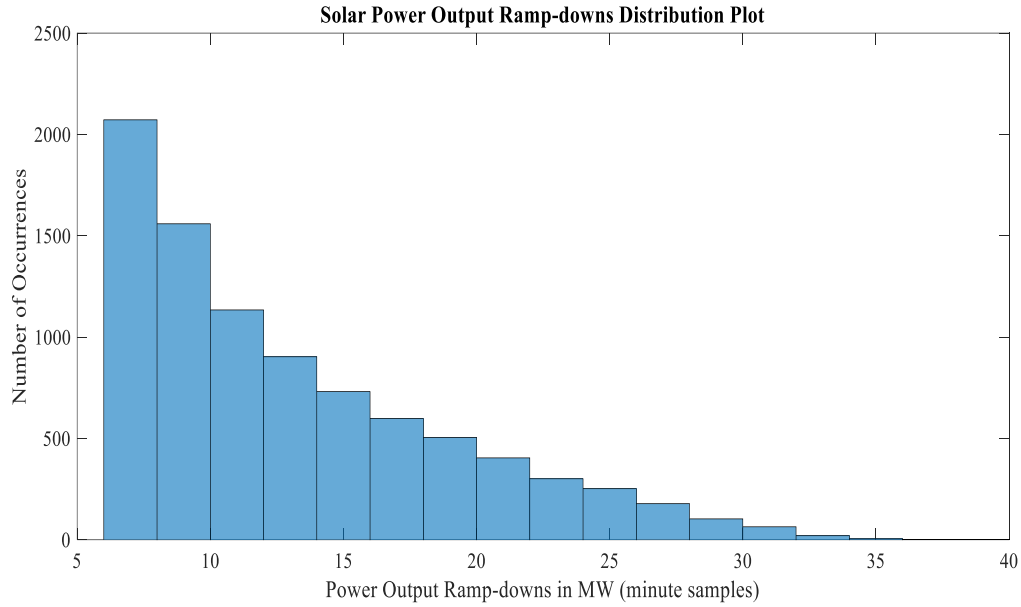


Figure 5.7. Ramp-downs Distribution Plot

Reference figure 5.8, the similar logic is applied as of above and the power capacity of DC-BESS equal to 25 MW comes out to be a reasonable choice.

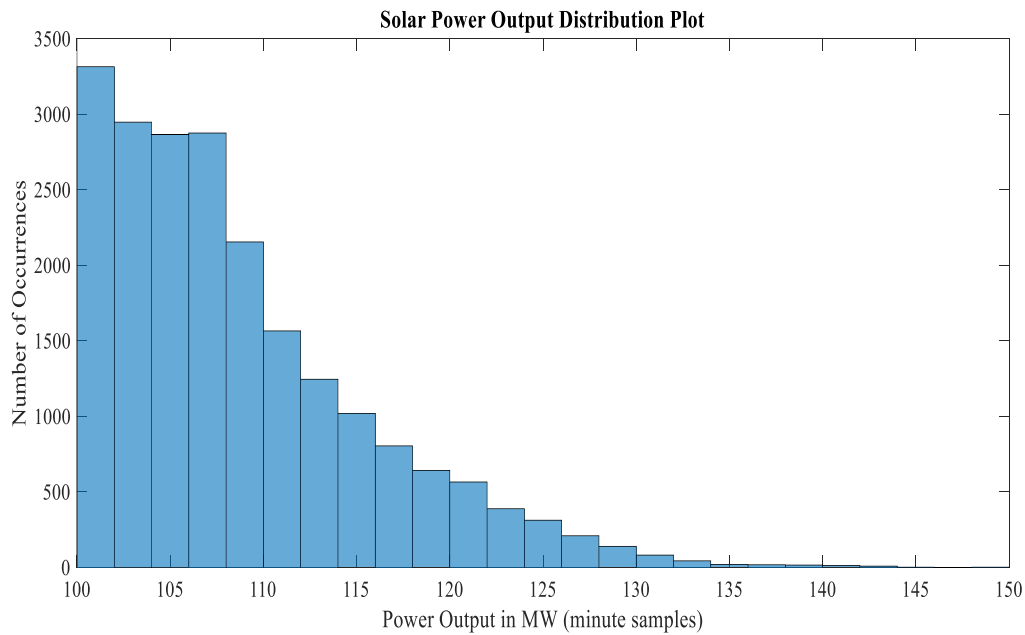


Figure 5.8. Power Distribution Plot

Since the RRVs are in minute resolution and the primary goal is to reduce RRVs and not the long-duration storage of energy, therefore, small energy BESS would be a good option. Reference figure 5.9, majority of the occurrences are up to 15-20 MWh, therefore, in order to both capture and utilize most of the energy, 30 minutes system would be sufficient.

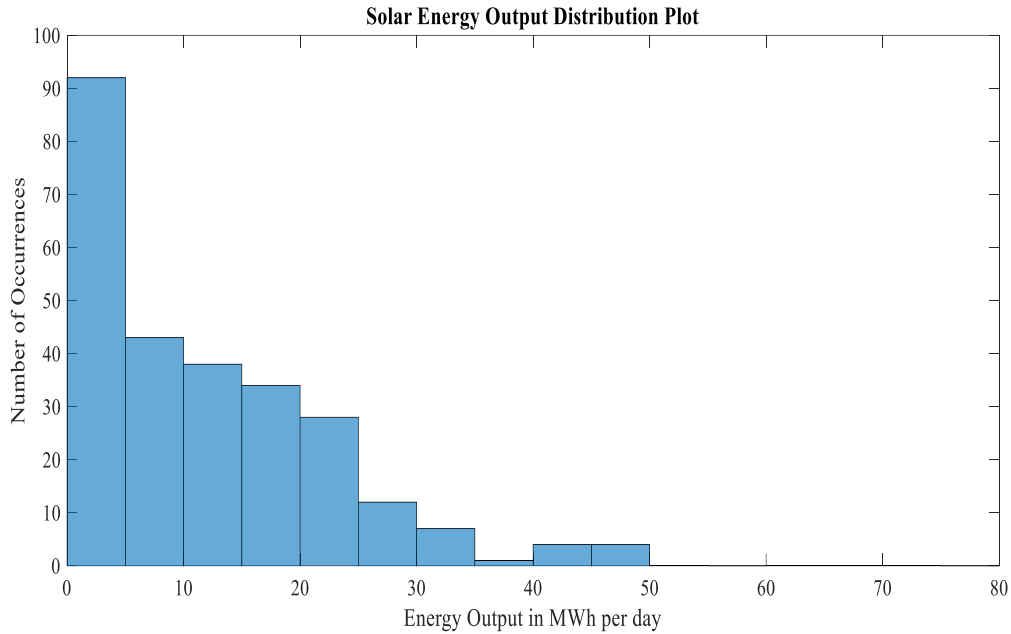


Figure 5.9. Energy-per-day Distribution Plot

5.10 ECONOMIC ANALYSIS

In the previous analysis, the size of DC-BESS including power and energy rating has already been found, i.e., 25 MW system for half an hour. In this section, the minimum tariff of the clipped energy is determined using reverse-engineer technique determining what would be the minimum selling price of the energy to guarantee payback period in the range of 5-15 years. Moreover, since there is no fixed price of penalty on RRV violations, a further indicative analysis is carried out determining the impact of RRV penalty rate on minimum selling tariff. Since the analysis is still at feasibility stage, therefore these minimum tariff findings can help in negotiations with the buying utility during PPA (Power Purchase Agreement), decision regarding location of the solar plant and can be used as an input for the company financial calculations of the project.

The penalties due to Ramp Rate Violations (RRV), which are normally imposed by the electric utilities purchasing the energy, is an important consideration to be taken into account to perform this analysis. It is due to the reason that the grid network operator (normally an electric utility) has to control the generation dispatch according to the load demand and power ramps greater than some percentage of the nominal plant rating can cause a disturbance in the operation of the grid system. Therefore, it is now trending in many electric utilities to impose a penalty on ramp rate violations.

As per [29], let's assume the cost of RRV to be approximately 10 cents per second per MW. In the first step, the energies in RRV (in MW-sec) are determined for both with and without DC-BESS scenarios. The difference in these energies multiplied by the cost of RRV penalty will give the saving as avoided cost per year. The values obtained while finding RRV savings for 8.5 months available data are:

- Number of Ramp-downs without DC-BESS = 5198
- Number of Ramp-downs with DC-BESS = 3719
- Integrated Ramp-down Energy without DC-BESS (MW-min) = 87118.342
- Integrated Ramp-down Energy with DC-BESS (MW-min) = 66977.327
- Integrated Ramp-down Energy without DC-BESS (MW-sec) = 5227100.53
- Integrated Ramp-down Energy with DC-BESS (MW-sec) = 4018639.64
- Penalty Cost of RRV without DC-BESS (\$) = 522710
- Penalty Cost of RRV with DC-BESS (\$) = 401863
- **Savings in Penalty Cost of RRV (\$) = 120846**

Based on this avoided cost value for 8.5 months, minimum tariff for selling the energy is calculated for payback period in the range of 5-15 years as tabulated below in Table 5.4.

Table 5.4. Results of Analysis – Minimum Tariff Calculations

Payback Period (Years)	Captured Utilized Energy per year based on real data (kWh)	Required Revenue Per Year Based on Payback Period (\$)	Saving in RRV per year based on real data (\$)	Total Required Revenue Per Year Based on Payback Period considering Saving in RRV (\$)	Minimum Tariff for selling of captured energy considering Saving in RRV (c/kWh)	Minimum Tariff for selling of captured energy without considering Saving in RRV (c/kWh)
5	3220094	1950000	170606	1779394	55.26	60.56
6		1625000		1454394	45.17	50.46
7		1392857		1222251	37.96	43.26
8		1218750		1048144	32.55	37.85
9		1083333		912727	28.34	33.64
10		975000		804394	24.98	30.28
11		886364		715757	22.23	27.53
12		812500		641894	19.93	25.23
13		750000		579394	17.99	23.29
14		696429		525822	16.33	21.63
15		650000		479394	14.89	20.19

Values Used in Above Calculations:

1. Capacity of DC-BESS Installed (MW) = 25
2. Total Installation Cost of 25 MW DC-BESS (\$) = 9750000
3. Saving in RRV based on 8.5 months real data (\$) = 120846

Reference above table, the selling price of 14.89 c/kWh comes out to be a realistic value, however, the payback period of 15 years is a bit longer. Moreover, it can be observed that there is a significant effect of RRV penalty cost in determining the economics of the project and cannot be neglected.

Now, since the cost of penalty on RRV violations equal to 10 c/MW-sec is just an assumed value, therefore, the improvement in the selling price of energy is analyzed based on the variation in the penalty cost, as shown in figure 5.10. This indicates that if the penalty rate becomes 20 c/MW-sec, the minimum selling price can reduce as much as 9.59 c/kWh, which is quite a reasonable value.

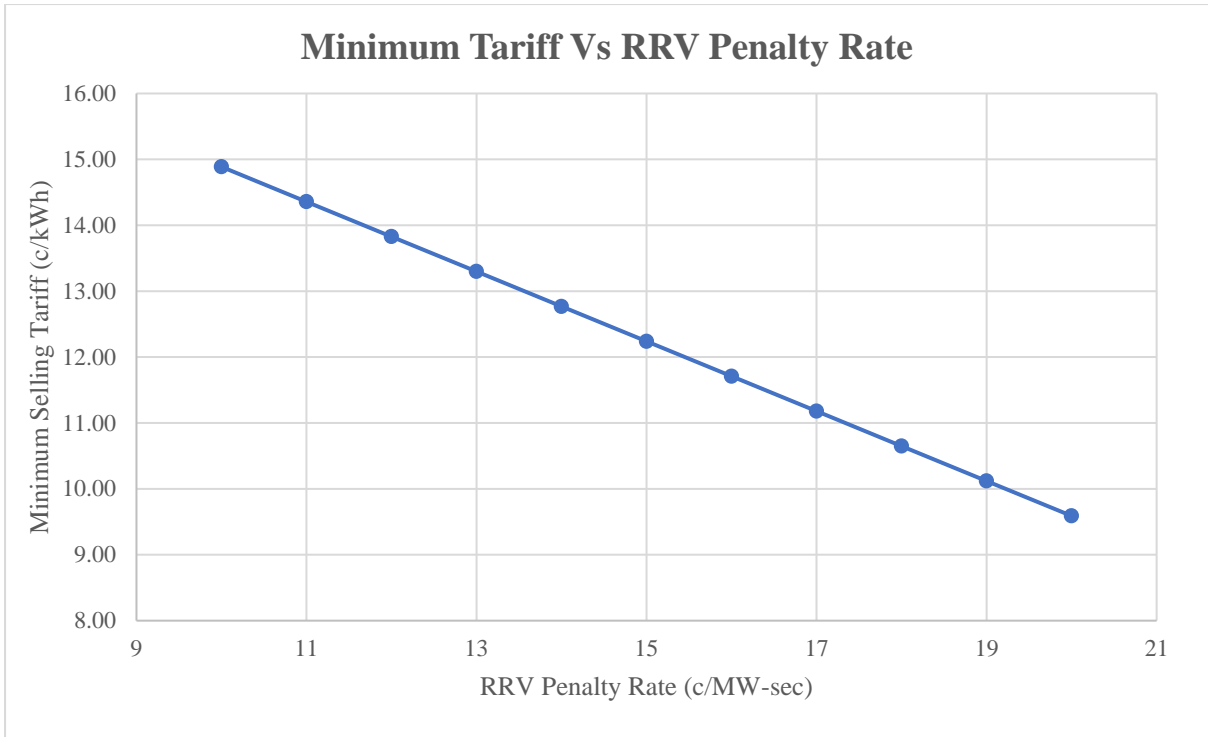


Figure 5.10. Minimum Tariff Vs RRV Penalty Rate

This value will further improve if the possibility of higher selling price during peak-load hours is considered in the analysis. Moreover, since the installation cost of DC-BESS is expected to decrease in future along with an increase in the penalty costs of RRV, DC-BESS would be much economically viable in coming recent years.

Chapter 6

Conclusion

6.1 CONCLUSIONS

The performance of Gamesa PV model regarding grid integration in a large power network (IEEE-118 bus system) is found satisfactory. The results for load flow and short-circuit analysis are perfect, however, for transient stability analysis, due to huge inertia of the connected network, the frequency is taking larger time to recover after the fault. This problem of fault recovery is resolved when simulated in IEEE-14 bus system. Therefore, it is safely concluded that the Gamesa PV model has no issue regarding grid integration.

Regarding Mexican grid code compliance, it has been found that Gamesa PV Inverter model is compliant with HVRT requirement and not compliant with LVRT requirement. It is because that as per the LVRT requirement of Mexican grid code, the PV Inverter should stay connected with the grid for zero-voltage sag of 400 msec, however, as per Gamesa voltage dip curve, it can endure zero-voltage sag only for 100 msec. This point needs to be addressed by Gamesa Electric technical team.

Regarding the frequency support functionality, the Mexican Grid Code requires that the Solar PV power plant should not provide any active power regulation (change in the output) if system frequency changes by 30 mHz (dead band) and if system frequency goes up or down, the solar PV power plant should provide active power regulation in the range of 3 – 10%. This characteristic is found to be absent from the provided Gamesa PV inverter model. However, after contacting Gamesa technical team, it has been confirmed that this feature is not implemented in each individual PV inverter, rather in the Power Plant Controller (PPC) model. This can be verified in the future work.

In order to determine the solar output profiles based on measured one-point solar irradiance data, three methods are used namely single-section, N-section and WVM. WVM method is found reliable and further calculations are based on its results. The number of ramp-down violations greater than 10% of the plant nominal rating are found to be 5198.

To minimize these ramp-down violations, a DC-DC BESS is proposed and its best size is found to be 25 MW for 30 minutes based on the criteria of percentage ramp-down improvement. After installation of this DC-DC BESS, the number of ramp-down violations reduced to 3719, an improvement by 28.45%. This DC-DC BESS will capture almost 76% of the available clipped energy and 1.48% of the total plant energy. Assuming ROI of 15 years, a realistic selling tariff of 14.89 c/kWh for the captured energy is determined, however, if the RRV penalty rate is considered to be on a higher side equal to 20 c/MW-sec, selling tariff of 9.59 c/kWh is found. This economic viability is expected to improve further in the coming recent years.

6.2 FUTURE WORK

Some of the proposed future tasks are as follows:

- To evaluate the frequency support functionality of Gamesa PV inverter model along with Power Plant Controller (PPC) model.
- To perform the dynamic simulation of solar PV plant along with the DC-DC BESS.
- To extend the analysis for one year measured data.

References

- [1] Technical Documentation – User Manual of Gamesa Electric PV Inverter PSS/E Models.
- [2] Fotovoltaica: Código de red de México.
- [3] Technical Documentation –Gamesa Electric PV Inverter PSS/E Models Validation.
- [4] Disposiciones Generales - Manual Regulatorio De Requerimientos Técnicos Para La Interconexión De Centrales Eléctricas Al Sistema Eléctrico Nacional.
- [5] http://www2.ee.washington.edu/research/pstca/pf118/pg_tca118bus.htm.
- [6] <http://icseg.iti.illinois.edu/files/2013/10/WSCC14.png>.
- [7] <http://www.suncyclopedia.com/en/area-required-for-solar-pv-power-plants/>
- [8] Cloud Speed Impact on Solar Variability Scaling - Application to the Wavelet Variability Model, by Matthew Lave and Jan Kleissl, University of California, San Diego, 9500 Gilman Dr. #0411 La Jolla, CA 92093
- [9] Datasheet of the PV module JKM 320PP-72-V
- [10] Gamesa Internal Note
- [11] Cloud speed impact on solar variability scaling – Application to the wavelet variability model by Jan Kleissl and Matthew Lave)
- [12] A Wavelet-Based Variability Model (WVM) for Solar PV Power Plants, by Matthew Lave, Jan Kleissl, and Joshua S. Stein
- [13] Testing a Wavelet-based Variability Model (WVM) for Solar PV Power Plants, by M. Lave and J. Kleissl, Member, IEEE
- [14] T. Hoff, R. Perez, Modeling PV Fleet Output Variability, Submitted to Solar Energy, (2011).

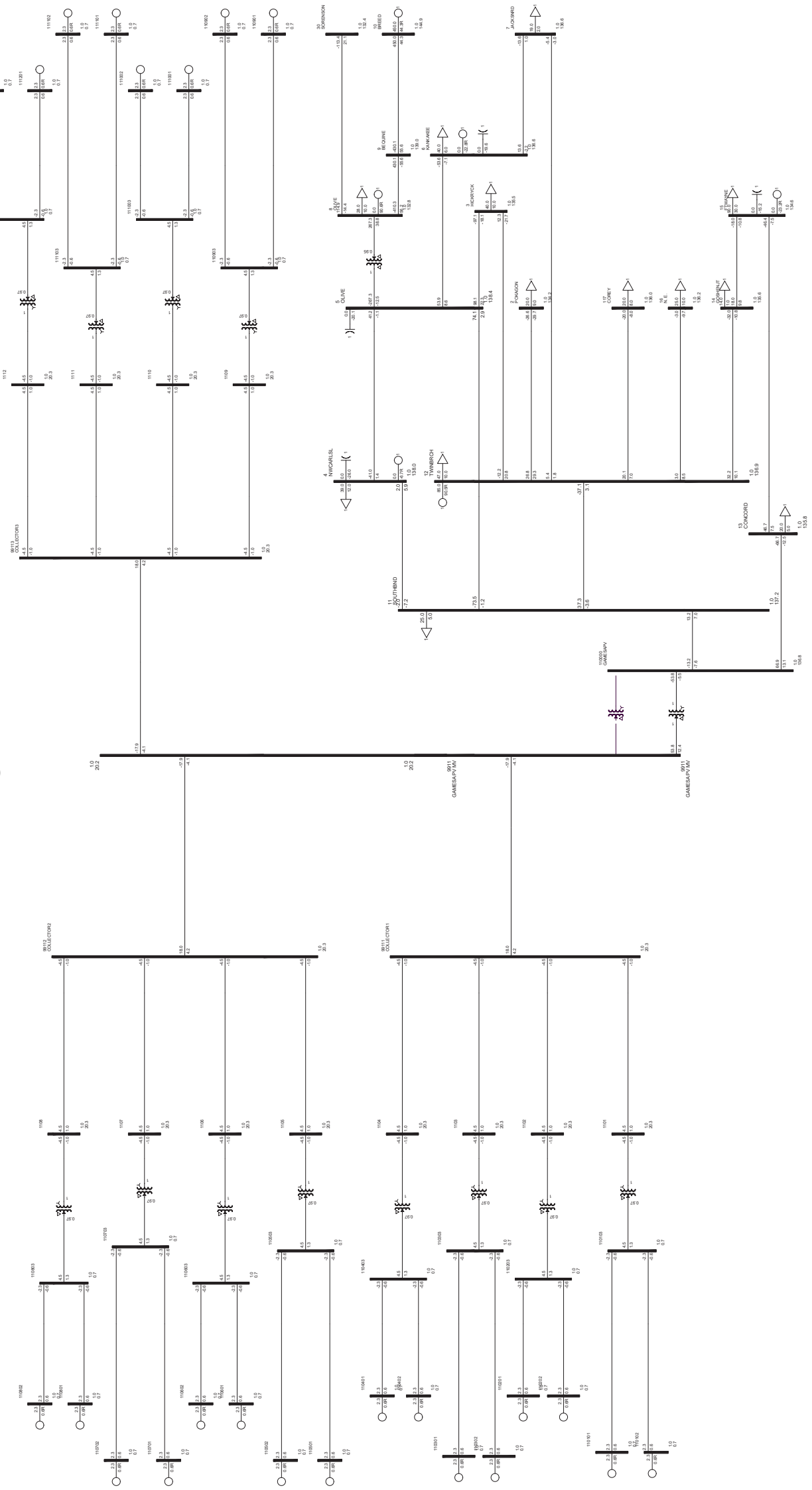
- [15] Electrical power fluctuations in a network of DC/AC inverters in a large PV plant: Relationship between correlation, by Oscar Perpiñán Lamigueiro, Javier Marcos, Eduardo Lorenzo Pigueiras.
- [16] Utility Scale PV Plant Variability and Energy Storage for Ramp Rate Control, by Rob van Haaren, Mahesh Morjaria, and Vasilis Fthenakis.
- [17] Cloud Speed Impact on Solar Variability Scaling - Application to the Wavelet Variability Model, by Matthew Lave, Jan Kleissl
- [18] <https://pvpmc.sandia.gov/>
- [19] <https://pvpmc.sandia.gov/applications/>
- [20] Solar Irradiance Data – Gamesa Internal Note
- [21] Gamesa Internal Note
- [22] <https://es.mathworks.com/matlabcentral/answers/59411-problems-with-importing-date-and-time-from-excel-to-matlab>
- [23] <https://pvpmc.sandia.gov/applications/wavelet-variability-model/wvm-square-plant-example/>
- [24] <https://pvpmc.sandia.gov/modeling-steps/>
- [25] Simulated PV Power Plant Variability: Impact of Utility-imposed Ramp Limitations in Puerto Rico, by Matthew Lave, Jan Kleissl, Abraham Ellis, Felipe Mejia
- [26] PV Ramping in a Distributed Generation Environment: A Study Using Solar Measurements, by Manajit Sengupta, Jamie Keller, National Renewable Energy Laboratory, Golden, CO
- [27] Power Variability Analysis of Megawatt-Scale Solar Photovoltaic Installations, by Mark Mitchell, Michael Campbell, Kathryn Klement, Mohammad Sedighy Hatch, 2800 Speakman Dr., Mississauga, Canada
- [28] Gamesa Internal Notes
- [29] The Economic Value of Forecasts for Optimal Curtailment Strategies to Comply with Ramp Rate Rules, by Daniel Cormode, Antonio Lorenzo, Will Holmgren, Sophia Chen, and Alex Cronin, UNIVERSITY OF ARIZONA, USA

- [30] Capacity Specification for Hybrid Energy Storage System to Accommodate Fast PV Fluctuations, by Xiaoyu Wang, Meng Yue.
- [31] Utility Scale PV Plant Variability and Energy Storage for Ramp Rate Control, by Rob van Haaren, Mahesh Morjaria, and Vasilis Fthenakis.
- [32] A Utility Scale Battery Energy Storage System for Intermittency Mitigation in Multilevel Medium Voltage Photovoltaic System, by Somasundaram Essakiappan, Madhav Manjrekar, Johan Enslin, Jorge Ramos-Ruiz, Prasad Enjeti, Pawan Garg.
- [33] Enhanced Experimental PV Plant Grid-Integration with a MW Lithium-Ion Energy Storage System, by Haizea Gaztañaga, Joseba Landaluze, Ion Etxeberria-Otadui, Asun Padrós, Iñigo Berazaluce, David Cuesta.
- [34] Daily Solar Energy Estimation for Minimizing Energy Storage Requirements in PV Power Plants, by Hector Beltran, Emilio Pérez, Néstor Aparicio, and Pedro Rodríguez.
- [35] Mitigation Control Against Partial Shading Effects in Large-Scale PV Power Plants, by C. Rahmann, V. Vittal, J. Ascui, and J. Haas.
- [36] Integrated Size and Energy Management Design of Battery Storage to Enhance Grid Integration of Large-scale PV Power Plants, by Ye Yang, Qing Ye, Leonard J. Tung, Michael Greenleaf, Hui Li.
- [37] Power Smoothing of Large Solar PV Plant Using Hybrid Energy Storage, by Guishi Wang, Mihai Ciobotaru, and Vassilios G. Agelidis.
- [38] Desirable Control Features of Battery Energy Storage Systems for Commercial Scale Solar PV Plants, by M J E Alam, R Yan, T K Saha
- [39] Ramp Rate consideration of a BESS using Active Power Control for PV generation, by K. Prompinit, S. Khomfoi.
- [40] Dispatch Performance Analysis of PV power plants using various energy storage capacities, by Guishi Wang, Mihai Ciobotaru, and Vassilios G. Agelidis.
- [41] Battery Energy Storage System in Smoothing Control Application of Photovoltaic Power Fluctuations Caused by Clouds Passing, by M. Garcia-Plaza, J. Eloy-Garcia Carrasco, J. Alonso-Martinez, A. Peña Asensio.
- [42] Ramp Rate Control of Photovoltaic Power Plant Output Using Energy Storage Devices, by Vahid Salehi, Brian Radibratovic.

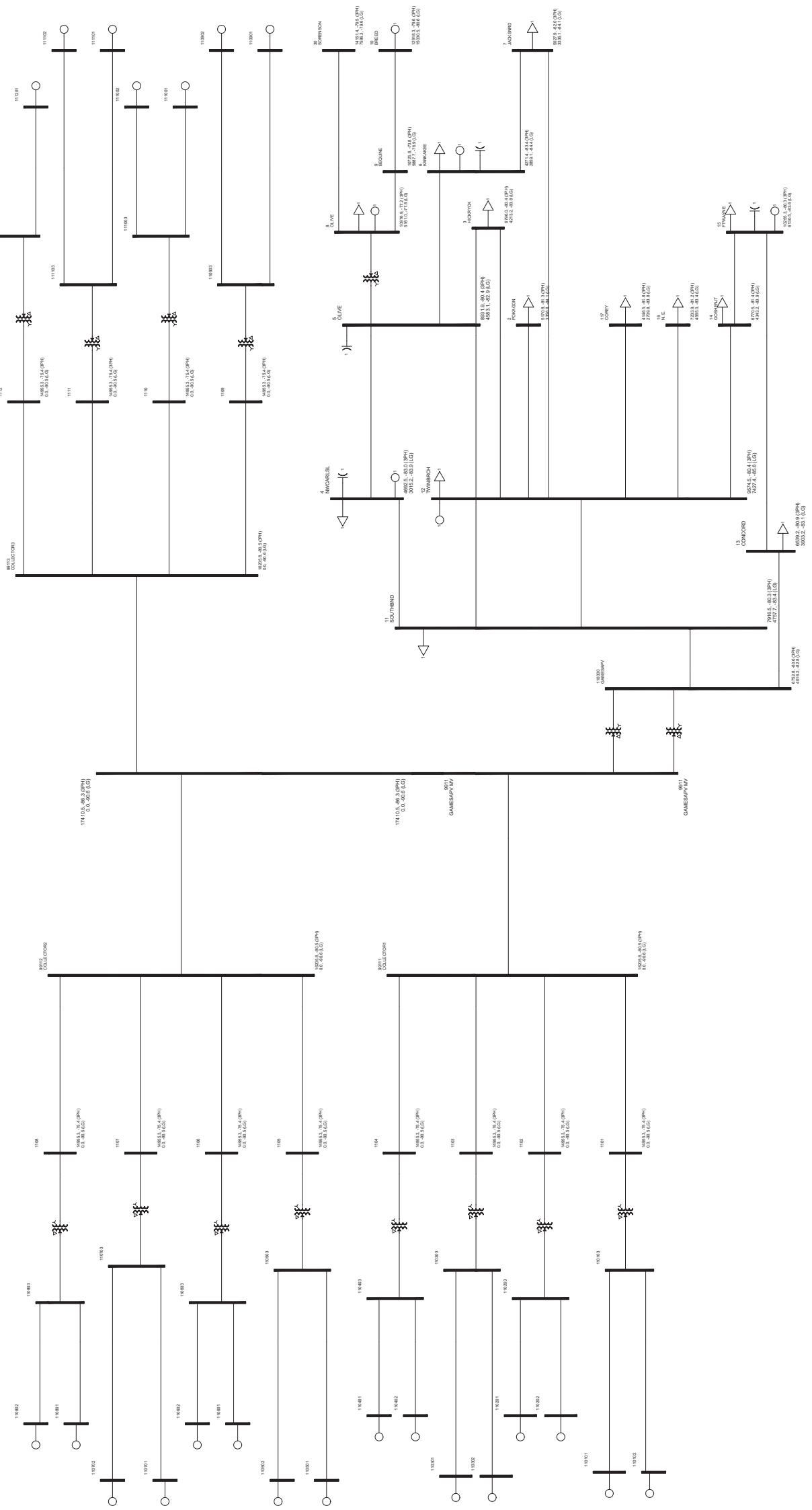
- [43] Solar Photovoltaic Output Smoothing: Using Battery Energy Storage System, by R P Sasmal, Subir Sen, Ankur Chakraborty.
- [44] <http://www.energystoragedirect.com.au/energy-storage/energy-throughput-vs-cycle-life/>

APPENDIX

54 MW GAMESA Solar PV Power Plant and the Electrical Network in its vicinity Transformer From 20kV GAMESAPV MV To 138kV GAMESAPV Switched Out Diagram No.3



54 MW GAMESA Solar PV Power Plant and the Electrical Network in its vicinity With Case - Short Circuit Analysis Diagram No.6



OPTIONS USED:

- SET PRE-FAULT VOLTAGES AND PHASE SHIFT ANGLES TO POWER FLOW SOLUTION
- SET SYNCHRONOUS/ASYNCHRONOUS MACHINE POWER OUTPUTS TO POWER FLOW SOLUTION
- SET GENERATOR POSITIVE SEQUENCE REACTANCES TO SUBTRANSIENT
- TRANSFORMER TAP RATIOS AND PHASE SHIFT ANGLES UNCHANGED
- LINE CHARGING REPRESENTED IN +/-0 SEQUENCES
- LINE/FIXED/SWITCHED SHUNTS AND TRANSFORMER MAGNETIZING ADMITTANCE REPRESENTED IN +/-0 SEQUENCES
- LOAD REPRESENTED IN +/-0 SEQUENCES
- DC LINES AND FACTS DEVICES BLOCKED
- IMPEDANCE CORRECTIONS NOT APPLIED TO TRANSFORMER ZERO SEQUENCE IMPEDANCES

```

<-SCMVA-> <-Sym I''k rms-->
                RE(I)    IM(I)
X----- BUS -----X
                MVA      AMP
   2 [POKAGON   138.00] 3PH  1235.95   783.7  -5111.1
                        LG   802.36   346.7  -3338.9
THEVENIN IMPEDANCE, X/R (OHM)  Z+:3.529+j14.332, 4.06131  Z-:3.529+j14.332, 4.06131  Z0:6.007+j38.282, 6.372

```

```

<-SCMVA-> <-Sym I''k rms-->
                RE(I)    IM(I)
X----- BUS -----X
                MVA      AMP
   3 [HICKRYCK  138.00] 3PH  1624.40  1129.3  -6701.5
                        LG  1007.05   452.4  -4188.8
THEVENIN IMPEDANCE, X/R (OHM)  Z+:2.754+j10.956, 3.97756  Z-:2.754+j10.956, 3.97756  Z0:4.652+j31.801, 6.835

```

```

<-SCMVA-> <-Sym I''k rms-->
                RE(I)    IM(I)
X----- BUS -----X
                MVA      AMP
   4 [NWCARLSL  138.00] 3PH  1121.61   570.0  -4657.7
                        LG   720.70   320.8  -2998.1
THEVENIN IMPEDANCE, X/R (OHM)  Z+:3.200+j16.095, 5.02969  Z-:3.200+j16.095, 5.02969  Z0:7.398+j43.174, 5.835

```

```

<-SCMVA-> <-Sym I''k rms-->
                RE(I)    IM(I)
X----- BUS -----X
                MVA      AMP
   5 [OLIVE     138.00] 3PH  2134.92  1495.1  -8805.9
                        LG  1095.47   569.0  -4547.7
THEVENIN IMPEDANCE, X/R (OHM)  Z+:1.896+j8.511, 4.48905  Z-:1.896+j8.511, 4.48905  Z0:5.108+j33.173, 6.49430

```

```

<-SCMVA-> <-Sym I''k rms-->
                RE(I)    IM(I)
X----- BUS -----X
                MVA      AMP
   6 [KANKAKEE  138.00] 3PH  1020.96   492.2  -4242.9
                        LG   683.38   280.9  -2845.2
THEVENIN IMPEDANCE, X/R (OHM)  Z+:3.553+j17.703, 4.98238  Z-:3.553+j17.703, 4.98238  Z0:7.459+j44.197, 5.925

```

```

<-SCMVA-> <-Sym I''k rms-->
                RE(I)    IM(I)
X----- BUS -----X
                MVA      AMP
   7 [JACKSNRD  138.00] 3PH  1201.79   699.9  -4979.0
                        LG   797.40   341.5  -3318.6
THEVENIN IMPEDANCE, X/R (OHM)  Z+:3.394+j14.941, 4.40169  Z-:3.394+j14.941, 4.40169  Z0:6.041+j38.196, 6.322

```

```

<-SCMVA-> <-Sym I''k rms-->
                RE(I)    IM(I)
X----- BUS -----X
                MVA      AMP
   8 [OLIVE     138.00] 3PH  2623.73  2431.8  -10704.1
                        LG  1233.61  1094.3  -5043.7
THEVENIN IMPEDANCE, X/R (OHM)  Z+:1.578+j7.044, 4.46469  Z-:1.578+j7.044, 4.46469  Z0:6.473+j30.953, 4.78193

```

```

<-SCMVA-> <-Sym I''k rms-->
                RE(I)    IM(I)
X----- BUS -----X
                MVA      AMP
   9 [BEQUINE   138.00] 3PH  2563.71  2986.1  -10301.7
                        LG  1407.29  1334.8  -5734.4
THEVENIN IMPEDANCE, X/R (OHM)  Z+:2.111+j7.250, 3.43383  Z-:2.111+j7.250, 3.43383  Z0:5.184+j25.684, 4.95448

```

```

<-SCMVA-> <-Sym I''k rms-->
                RE(I)    IM(I)
X----- BUS -----X
                MVA      AMP
  10 [BREED     138.00] 3PH  3087.78  2335.1  -12705.5
                        LG  3592.63  2449.2  -14829.6
THEVENIN IMPEDANCE, X/R (OHM)  Z+:0.577+j6.609, 11.46008  Z-:0.577+j6.609, 11.46008  Z0:0.025+j3.847, 152.43

```

<-SCMVA-> <-Sym I''k rms-->

```

X----- BUS -----X
11 [SOUTHEND 138.00] 3PH
    LG
THEVENIN IMPEDANCE, X/R (OHM)
MVA      RE(I)      IM(I)
1892.22  1335.9    -7803.0
1137.21  547.1     -4726.2
Z+:2.304+j9.468, 4.10869  Z-:2.304+j9.468, 4.10869  Z0:4.312+j28.879, 6.69803
-----
<-SCMVA-> <-Sym I''k rms-->
                RE(I)      IM(I)
X----- BUS -----X
12 [TWINBRCH 138.00] 3PH
    LG
THEVENIN IMPEDANCE, X/R (OHM)
MVA      RE(I)      IM(I)
2288.53  1594.5    -9440.8
1775.33  568.1     -7405.7
Z+:1.942+j7.824, 4.02915  Z-:1.942+j7.824, 4.02915  Z0:0.853+j15.166, 17.7849
-----
<-SCMVA-> <-Sym I''k rms-->
                RE(I)      IM(I)
X----- BUS -----X
13 [CONCORD 138.00] 3PH
    LG
THEVENIN IMPEDANCE, X/R (OHM)
MVA      RE(I)      IM(I)
1563.03  1030.2    -6457.6
932.95   470.2     -3874.8
Z+:2.759+j11.374, 4.12266  Z-:2.759+j11.374, 4.12266  Z0:6.199+j34.898, 5.629
-----
<-SCMVA-> <-Sym I''k rms-->
                RE(I)      IM(I)
X----- BUS -----X
14 [GOSHENJT 138.00] 3PH
    LG
THEVENIN IMPEDANCE, X/R (OHM)
MVA      RE(I)      IM(I)
1618.30  1007.2    -6695.1
1038.12  462.2     -4318.5
Z+:2.664+j10.983, 4.12299  Z-:2.664+j10.983, 4.12299  Z0:4.926+j29.882, 6.065
-----
<-SCMVA-> <-Sym I''k rms-->
                RE(I)      IM(I)
X----- BUS -----X
15 [FTWAYNE 138.00] 3PH
    LG
THEVENIN IMPEDANCE, X/R (OHM)
MVA      RE(I)      IM(I)
2451.25  1725.6    -10109.1
1465.33  686.5     -6091.9
Z+:1.935+j7.151, 3.69534  Z-:1.935+j7.151, 3.69534  Z0:3.786+j22.081, 5.83161
-----
<-SCMVA-> <-Sym I''k rms-->
                RE(I)      IM(I)
X----- BUS -----X
16 [N. E. 138.00] 3PH
    LG
THEVENIN IMPEDANCE, X/R (OHM)
MVA      RE(I)      IM(I)
1729.08  1107.5    -7148.7
1091.15  523.0     -4535.0
Z+:2.439+j10.352, 4.24422  Z-:2.439+j10.352, 4.24422  Z0:4.796+j28.922, 6.030
-----
<-SCMVA-> <-Sym I''k rms-->
                RE(I)      IM(I)
X----- BUS -----X
30 [SORENSEN 138.00] 3PH
    LG
THEVENIN IMPEDANCE, X/R (OHM)
MVA      RE(I)      IM(I)
3382.51  2569.2    -13916.2
1813.29  1364.1    -7462.6
Z+:1.098+j5.463, 4.97692  Z-:1.098+j5.463, 4.97692  Z0:3.893+j19.656, 5.04893
-----
<-SCMVA-> <-Sym I''k rms-->
                RE(I)      IM(I)
X----- BUS -----X
117 [COREY 138.00] 3PH
    LG
THEVENIN IMPEDANCE, X/R (OHM)
MVA      RE(I)      IM(I)
991.12   589.3     -4104.4
647.70   294.0     -2693.8
Z+:4.164+j18.040, 4.33251  Z-:4.164+j18.040, 4.33251  Z0:7.970+j47.336, 5.938
-----
<-SCMVA-> <-Sym I''k rms-->
                RE(I)      IM(I)
X----- BUS -----X
1101 [ 20.000] 3PH
    LG
THEVENIN IMPEDANCE, X/R (OHM)
MVA      RE(I)      IM(I)
518.07   3767.9    -14472.8
0.00     0.0        0.0
Z+:0.197+j0.728, 3.69602  Z-:0.197+j0.728, 3.69602  Z0:0.000+j4000000.0, 9999
-----
<-SCMVA-> <-Sym I''k rms-->
                RE(I)      IM(I)
X----- BUS -----X
1102 [ 20.000] 3PH
    LG
THEVENIN IMPEDANCE, X/R (OHM)
MVA      RE(I)      IM(I)
518.07   3767.9    -14472.8
0.00     0.0        0.0
Z+:0.197+j0.728, 3.69602  Z-:0.197+j0.728, 3.69602  Z0:0.155+j4000000.0, 9999
-----
<-SCMVA-> <-Sym I''k rms-->
                RE(I)      IM(I)
X----- BUS -----X
1103 [ 20.000] 3PH
    LG
THEVENIN IMPEDANCE, X/R (OHM)
MVA      RE(I)      IM(I)
518.07   3767.9    -14472.8
0.00     0.0        0.0
Z+:0.197+j0.728, 3.69602  Z-:0.197+j0.728, 3.69602  Z0:0.155+j4000000.0, 9999
-----
<-SCMVA-> <-Sym I''k rms-->

```

```

X----- BUS -----X
1104 [          20.000] 3PH
                        LG
MVA      RE(I)      IM(I)
518.07   3767.9   -14472.8
0.00     0.0      0.0
THEVENIN IMPEDANCE, X/R (OHM) Z+:0.197+j0.728, 3.69602 Z-:0.197+j0.728, 3.69602 Z0:0.155+j4000000.0, 9999
-----
<-SCMVA-> <-Sym I''k rms-->
                        RE(I)      IM(I)
X----- BUS -----X
1105 [          20.000] 3PH
                        LG
MVA      RE(I)      IM(I)
518.07   3767.9   -14472.8
0.00     0.0      0.0
THEVENIN IMPEDANCE, X/R (OHM) Z+:0.197+j0.728, 3.69602 Z-:0.197+j0.728, 3.69602 Z0:0.310+j4000000.2, 9999
-----
<-SCMVA-> <-Sym I''k rms-->
                        RE(I)      IM(I)
X----- BUS -----X
1106 [          20.000] 3PH
                        LG
MVA      RE(I)      IM(I)
518.07   3767.9   -14472.8
0.00     0.0      0.0
THEVENIN IMPEDANCE, X/R (OHM) Z+:0.197+j0.728, 3.69602 Z-:0.197+j0.728, 3.69602 Z0:0.310+j4000000.2, 9999
-----
<-SCMVA-> <-Sym I''k rms-->
                        RE(I)      IM(I)
X----- BUS -----X
1107 [          20.000] 3PH
                        LG
MVA      RE(I)      IM(I)
518.07   3767.9   -14472.8
0.00     0.0      0.0
THEVENIN IMPEDANCE, X/R (OHM) Z+:0.197+j0.728, 3.69602 Z-:0.197+j0.728, 3.69602 Z0:0.310+j4000000.2, 9999
-----
<-SCMVA-> <-Sym I''k rms-->
                        RE(I)      IM(I)
X----- BUS -----X
1108 [          20.000] 3PH
                        LG
MVA      RE(I)      IM(I)
518.07   3767.9   -14472.8
0.00     0.0      0.0
THEVENIN IMPEDANCE, X/R (OHM) Z+:0.197+j0.728, 3.69602 Z-:0.197+j0.728, 3.69602 Z0:0.310+j4000000.2, 9999
-----
<-SCMVA-> <-Sym I''k rms-->
                        RE(I)      IM(I)
X----- BUS -----X
1109 [          20.000] 3PH
                        LG
MVA      RE(I)      IM(I)
518.07   3767.9   -14472.8
0.00     0.0      0.0
THEVENIN IMPEDANCE, X/R (OHM) Z+:0.197+j0.728, 3.69602 Z-:0.197+j0.728, 3.69602 Z0:0.310+j4000000.2, 9999
-----
<-SCMVA-> <-Sym I''k rms-->
                        RE(I)      IM(I)
X----- BUS -----X
1110 [          20.000] 3PH
                        LG
MVA      RE(I)      IM(I)
518.07   3767.9   -14472.8
0.00     0.0      0.0
THEVENIN IMPEDANCE, X/R (OHM) Z+:0.197+j0.728, 3.69602 Z-:0.197+j0.728, 3.69602 Z0:0.310+j4000000.2, 9999
-----
<-SCMVA-> <-Sym I''k rms-->
                        RE(I)      IM(I)
X----- BUS -----X
1111 [          20.000] 3PH
                        LG
MVA      RE(I)      IM(I)
518.07   3767.9   -14472.8
0.00     0.0      0.0
THEVENIN IMPEDANCE, X/R (OHM) Z+:0.197+j0.728, 3.69602 Z-:0.197+j0.728, 3.69602 Z0:0.310+j4000000.2, 9999
-----
<-SCMVA-> <-Sym I''k rms-->
                        RE(I)      IM(I)
X----- BUS -----X
1112 [          20.000] 3PH
                        LG
MVA      RE(I)      IM(I)
518.07   3767.9   -14472.8
0.00     0.0      0.0
THEVENIN IMPEDANCE, X/R (OHM) Z+:0.197+j0.728, 3.69602 Z-:0.197+j0.728, 3.69602 Z0:0.310+j4000000.2, 9999
-----
<-SCMVA-> <-Sym I''k rms-->
                        RE(I)      IM(I)
X----- BUS -----X
9911 [GAMESAPV MV 20.000] 3PH
                        LG
MVA      RE(I)      IM(I)
603.12   1120.8   -17374.4
0.00     0.0      0.0
THEVENIN IMPEDANCE, X/R (OHM) Z+:0.049+j0.643, 13.20036 Z-:0.049+j0.643, 13.20036 Z0:0.155+j4000000.0, 99
-----
<-SCMVA-> <-Sym I''k rms-->
                        RE(I)      IM(I)
X----- BUS -----X
99111 [COLLECTOR1 20.000] 3PH
                        LG
MVA      RE(I)      IM(I)
561.39   2661.8   -15985.7
0.00     0.0      0.0
THEVENIN IMPEDANCE, X/R (OHM) Z+:0.121+j0.684, 5.66017 Z-:0.121+j0.684, 5.66017 Z0:0.077+j4000000.0, 9999
-----
<-SCMVA-> <-Sym I''k rms-->

```

RE(I) IM(I)

X----- BUS -----X
99112 [COLLECTOR2 20.000] 3PH 561.39 2661.8 -15985.7
LG 0.00 0.0 0.0
THEVENIN IMPEDANCE, X/R (OHM) Z+:0.121+j0.684, 5.66017 Z-:0.121+j0.684, 5.66017 Z0:0.232+j4000000.2, 9999

<-SCMVA-> <-Sym I''k rms-->

RE(I) IM(I)

X----- BUS -----X
99113 [COLLECTOR3 20.000] 3PH 561.39 2661.8 -15985.7
LG 0.00 0.0 0.0
THEVENIN IMPEDANCE, X/R (OHM) Z+:0.121+j0.684, 5.66017 Z-:0.121+j0.684, 5.66017 Z0:0.232+j4000000.2, 9999

<-SCMVA-> <-Sym I''k rms-->

RE(I) IM(I)

X----- BUS -----X
110000 [GAMESAPV 138.00] 3PH 1614.08 1103.6 -6662.0
LG 959.96 501.7 -3984.7
THEVENIN IMPEDANCE, X/R (OHM) Z+:2.621+j11.093, 4.23193 Z-:2.621+j11.093, 4.23193 Z0:5.793+j34.243, 5.911

OPTIONS USED:

- SET PRE-FAULT VOLTAGES AND PHASE SHIFT ANGLES TO POWER FLOW SOLUTION
- SET SYNCHRONOUS/ASYNCHRONOUS MACHINE POWER OUTPUTS TO POWER FLOW SOLUTION
- SET GENERATOR POSITIVE SEQUENCE REACTANCES TO SUBTRANSIENT
- TRANSFORMER TAP RATIOS AND PHASE SHIFT ANGLES UNCHANGED
- LINE CHARGING REPRESENTED IN +/-0 SEQUENCES
- LINE/FIXED/SWITCHED SHUNTS AND TRANSFORMER MAGNETIZING ADMITTANCE REPRESENTED IN +/-0 SEQUENCES
- LOAD REPRESENTED IN +/-0 SEQUENCES
- DC LINES AND FACTS DEVICES BLOCKED
- IMPEDANCE CORRECTIONS NOT APPLIED TO TRANSFORMER ZERO SEQUENCE IMPEDANCES

```

<-SCMVA-> <-Sym I''k rms-->
          /I/      AN(I)
X----- BUS -----X      MVA      AMP      DEG
   2 [POKAGON      138.00] 3PH      974.22    4075.8    -80.50
                               LG      622.05    2602.5    -84.47
THEVENIN IMPEDANCE, X/R (OHM)  Z+:/14.316/74.175, 3.52806  Z-:/14.316/74.175, 3.52806  Z0:/38.750/81.082, 6.
    
```

```

<-SCMVA-> <-Sym I''k rms-->
          /I/      AN(I)
X----- BUS -----X      MVA      AMP      DEG
   3 [HICKRYCK      138.00] 3PH     1289.04   5392.9    -79.00
                               LG      784.04   3280.2    -83.86
THEVENIN IMPEDANCE, X/R (OHM)  Z+:/10.916/73.519, 3.38000  Z-:/10.916/73.519, 3.38000  Z0:/32.140/81.677, 6.
    
```

```

<-SCMVA-> <-Sym I''k rms-->
          /I/      AN(I)
X----- BUS -----X      MVA      AMP      DEG
   4 [NWCARLSL      138.00] 3PH      882.84   3693.5    -82.08
                               LG      559.47   2340.7    -83.96
THEVENIN IMPEDANCE, X/R (OHM)  Z+:/16.011/77.033, 4.34295  Z-:/16.011/77.033, 4.34295  Z0:/43.803/80.276, 5.
    
```

```

<-SCMVA-> <-Sym I''k rms-->
          /I/      AN(I)
X----- BUS -----X      MVA      AMP      DEG
   5 [OLIVE         138.00] 3PH     1703.86   7128.4    -78.32
                               LG      856.20   3582.1    -82.31
THEVENIN IMPEDANCE, X/R (OHM)  Z+:/8.439/75.255, 3.79964  Z-:/8.439/75.255, 3.79964  Z0:/33.564/81.246, 6.49
    
```

```

<-SCMVA-> <-Sym I''k rms-->
          /I/      AN(I)
X----- BUS -----X      MVA      AMP      DEG
   6 [KANKAKEE      138.00] 3PH      802.60   3357.8    -82.59
                               LG      530.67   2220.2    -84.60
THEVENIN IMPEDANCE, X/R (OHM)  Z+:/17.650/76.835, 4.27540  Z-:/17.650/76.835, 4.27540  Z0:/44.822/80.421, 5.
    
```

```

<-SCMVA-> <-Sym I''k rms-->
          /I/      AN(I)
X----- BUS -----X      MVA      AMP      DEG
   7 [JACKSNRD      138.00] 3PH      946.03   3957.9    -81.24
                               LG      619.51   2591.8    -84.42
THEVENIN IMPEDANCE, X/R (OHM)  Z+:/14.950/75.381, 3.83384  Z-:/14.950/75.381, 3.83384  Z0:/38.671/81.013, 6.
    
```

```

<-SCMVA-> <-Sym I''k rms-->
          /I/      AN(I)
X----- BUS -----X      MVA      AMP      DEG
   8 [OLIVE         138.00] 3PH     2098.86   8781.0    -74.60
                               LG      970.39   4059.8    -76.08
THEVENIN IMPEDANCE, X/R (OHM)  Z+:/7.043/76.051, 4.02589  Z-:/7.043/76.051, 4.02589  Z0:/31.622/78.189, 4.78
    
```

```

<-SCMVA-> <-Sym I''k rms-->
          /I/      AN(I)
X----- BUS -----X      MVA      AMP      DEG
   9 [BEQUINE       138.00] 3PH     2053.82   8592.6    -71.25
                               LG     1116.61   4671.5    -75.28
THEVENIN IMPEDANCE, X/R (OHM)  Z+:/7.432/72.275, 3.12878  Z-:/7.432/72.275, 3.12878  Z0:/26.202/78.589, 4.95
    
```

```

<-SCMVA-> <-Sym I''k rms-->
          /I/      AN(I)
X----- BUS -----X      MVA      AMP      DEG
  10 [BREED         138.00] 3PH     2522.08  10551.6    -75.97
                               LG     2932.09  12267.0    -77.09
THEVENIN IMPEDANCE, X/R (OHM)  Z+:/6.607/84.642, 10.66291  Z-:/6.607/84.642, 10.66291  Z0:/3.847/89.624, 152
    
```

<-SCMVA-> <-Sym I''k rms-->

X-----	BUS	-----X		MVA	/I/ AMP	AN(I) DEG	
11	[SOUTHBN	138.00]	3PH	1503.64	6290.8	-78.61	
			LG	886.60	3709.3	-83.16	
THEVENIN IMPEDANCE, X/R (OHM)				Z+:/9.425/74.023, 3.49270	Z-:/9.425/74.023, 3.49270	Z0:/29.200/81.509, 6.69	

				<-SCMVA->	<-Sym I''k rms-->		
				/I/	AN(I)		
12	[TWINBRCH	138.00]	3PH	1832.26	7665.6	-78.40	
			LG	1397.14	5845.2	-85.12	
THEVENIN IMPEDANCE, X/R (OHM)				Z+:/7.742/73.197, 3.31143	Z-:/7.742/73.197, 3.31143	Z0:/15.190/86.782, 17.7	

				<-SCMVA->	<-Sym I''k rms-->		
				/I/	AN(I)		
13	[CONCORD	138.00]	3PH	1230.92	5149.8	-80.01	
			LG	722.64	3023.3	-83.29	
THEVENIN IMPEDANCE, X/R (OHM)				Z+:/11.377/74.536, 3.61473	Z-:/11.377/74.536, 3.61473	Z0:/35.444/79.927, 5.	

				<-SCMVA->	<-Sym I''k rms-->		
				/I/	AN(I)		
14	[GOSHENJT	138.00]	3PH	1275.12	5334.7	-80.76	
			LG	805.05	3368.1	-84.33	
THEVENIN IMPEDANCE, X/R (OHM)				Z+:/10.979/74.490, 3.60332	Z-:/10.979/74.490, 3.60332	Z0:/30.285/80.639, 6.	

				<-SCMVA->	<-Sym I''k rms-->		
				/I/	AN(I)		
15	[FTWAYNE	138.00]	3PH	1952.08	8166.9	-78.95	
			LG	1138.38	4762.6	-83.95	
THEVENIN IMPEDANCE, X/R (OHM)				Z+:/7.097/72.117, 3.09916	Z-:/7.097/72.117, 3.09916	Z0:/22.403/80.270, 5.83	

				<-SCMVA->	<-Sym I''k rms-->		
				/I/	AN(I)		
16	[N. E.	138.00]	3PH	1366.07	5715.2	-80.30	
			LG	848.30	3549.0	-83.61	
THEVENIN IMPEDANCE, X/R (OHM)				Z+:/10.335/74.930, 3.71394	Z-:/10.335/74.930, 3.71394	Z0:/29.317/80.585, 6.	

				<-SCMVA->	<-Sym I''k rms-->		
				/I/	AN(I)		
30	[SORENSEN	138.00]	3PH	2707.03	11325.4	-77.40	
			LG	1425.07	5962.1	-78.40	
THEVENIN IMPEDANCE, X/R (OHM)				Z+:/5.417/77.248, 4.41876	Z-:/5.417/77.248, 4.41876	Z0:/20.037/78.797, 5.04	

				<-SCMVA->	<-Sym I''k rms-->		
				/I/	AN(I)		
117	[COREY	138.00]	3PH	777.00	3250.7	-81.41	
			LG	501.66	2098.8	-84.22	
THEVENIN IMPEDANCE, X/R (OHM)				Z+:/18.109/75.505, 3.86820	Z-:/18.109/75.505, 3.86820	Z0:/48.002/80.442, 5.	

				<-SCMVA->	<-Sym I''k rms-->		
				/I/	AN(I)		
1101	[20.000]	3PH	403.20	11639.5	-73.59	
			LG	0.00	0.0	0.00	
THEVENIN IMPEDANCE, X/R (OHM)				Z+:/0.748/74.339, 3.56696	Z-:/0.748/74.339, 3.56696	Z0:/4000000.0/90.000, 9	

				<-SCMVA->	<-Sym I''k rms-->		
				/I/	AN(I)		
1102	[20.000]	3PH	403.20	11639.5	-73.59	
			LG	0.00	0.0	0.00	
THEVENIN IMPEDANCE, X/R (OHM)				Z+:/0.748/74.339, 3.56696	Z-:/0.748/74.339, 3.56696	Z0:/4000000.0/90.000, 9	

				<-SCMVA->	<-Sym I''k rms-->		
				/I/	AN(I)		
1103	[20.000]	3PH	403.20	11639.5	-73.59	
			LG	0.00	0.0	0.00	
THEVENIN IMPEDANCE, X/R (OHM)				Z+:/0.748/74.339, 3.56696	Z-:/0.748/74.339, 3.56696	Z0:/4000000.0/90.000, 9	

				<-SCMVA->	<-Sym I''k rms-->		

X-----	BUS	-----X		MVA	/I/ AMP	AN(I) DEG	
1104 [20.000]	3PH	403.20	11639.5	-73.59	
			LG	0.00	0.0	0.00	
THEVENIN IMPEDANCE, X/R (OHM)							
Z+:/0.748/74.339, 3.56696 Z-:/0.748/74.339, 3.56696 Z0:/4000000.0/90.000, 9							

				<-SCMVA-> <-Sym I''k rms-->			
				/I/ AN(I)			
X-----	BUS	-----X		MVA	AMP	DEG	
1105 [20.000]	3PH	403.20	11639.5	-73.59	
			LG	0.00	0.0	0.00	
THEVENIN IMPEDANCE, X/R (OHM)							
Z+:/0.748/74.339, 3.56696 Z-:/0.748/74.339, 3.56696 Z0:/4000000.2/90.000, 9							

				<-SCMVA-> <-Sym I''k rms-->			
				/I/ AN(I)			
X-----	BUS	-----X		MVA	AMP	DEG	
1106 [20.000]	3PH	403.20	11639.5	-73.59	
			LG	0.00	0.0	0.00	
THEVENIN IMPEDANCE, X/R (OHM)							
Z+:/0.748/74.339, 3.56696 Z-:/0.748/74.339, 3.56696 Z0:/4000000.2/90.000, 9							

				<-SCMVA-> <-Sym I''k rms-->			
				/I/ AN(I)			
X-----	BUS	-----X		MVA	AMP	DEG	
1107 [20.000]	3PH	403.20	11639.5	-73.59	
			LG	0.00	0.0	0.00	
THEVENIN IMPEDANCE, X/R (OHM)							
Z+:/0.748/74.339, 3.56696 Z-:/0.748/74.339, 3.56696 Z0:/4000000.2/90.000, 9							

				<-SCMVA-> <-Sym I''k rms-->			
				/I/ AN(I)			
X-----	BUS	-----X		MVA	AMP	DEG	
1108 [20.000]	3PH	403.20	11639.5	-73.59	
			LG	0.00	0.0	0.00	
THEVENIN IMPEDANCE, X/R (OHM)							
Z+:/0.748/74.339, 3.56696 Z-:/0.748/74.339, 3.56696 Z0:/4000000.2/90.000, 9							

				<-SCMVA-> <-Sym I''k rms-->			
				/I/ AN(I)			
X-----	BUS	-----X		MVA	AMP	DEG	
1109 [20.000]	3PH	403.20	11639.5	-73.59	
			LG	0.00	0.0	0.00	
THEVENIN IMPEDANCE, X/R (OHM)							
Z+:/0.748/74.339, 3.56696 Z-:/0.748/74.339, 3.56696 Z0:/4000000.2/90.000, 9							

				<-SCMVA-> <-Sym I''k rms-->			
				/I/ AN(I)			
X-----	BUS	-----X		MVA	AMP	DEG	
1110 [20.000]	3PH	403.20	11639.5	-73.59	
			LG	0.00	0.0	0.00	
THEVENIN IMPEDANCE, X/R (OHM)							
Z+:/0.748/74.339, 3.56696 Z-:/0.748/74.339, 3.56696 Z0:/4000000.2/90.000, 9							

				<-SCMVA-> <-Sym I''k rms-->			
				/I/ AN(I)			
X-----	BUS	-----X		MVA	AMP	DEG	
1111 [20.000]	3PH	403.20	11639.5	-73.59	
			LG	0.00	0.0	0.00	
THEVENIN IMPEDANCE, X/R (OHM)							
Z+:/0.748/74.339, 3.56696 Z-:/0.748/74.339, 3.56696 Z0:/4000000.2/90.000, 9							

				<-SCMVA-> <-Sym I''k rms-->			
				/I/ AN(I)			
X-----	BUS	-----X		MVA	AMP	DEG	
1112 [20.000]	3PH	403.20	11639.5	-73.59	
			LG	0.00	0.0	0.00	
THEVENIN IMPEDANCE, X/R (OHM)							
Z+:/0.748/74.339, 3.56696 Z-:/0.748/74.339, 3.56696 Z0:/4000000.2/90.000, 9							

				<-SCMVA-> <-Sym I''k rms-->			
				/I/ AN(I)			
X-----	BUS	-----X		MVA	AMP	DEG	
9911 [GAMESAPV MV	20.000]		3PH	469.83	13562.7	-84.55	
			LG	0.00	0.0	0.00	
THEVENIN IMPEDANCE, X/R (OHM)							
Z+:/0.638/85.166, 11.82370 Z-:/0.638/85.166, 11.82370 Z0:/4000000.0/90.000, 9							

				<-SCMVA-> <-Sym I''k rms-->			
				/I/ AN(I)			
X-----	BUS	-----X		MVA	AMP	DEG	
99111 [COLLECTOR1	20.000]		3PH	437.38	12626.0	-78.73	
			LG	0.00	0.0	0.00	
THEVENIN IMPEDANCE, X/R (OHM)							
Z+:/0.689/79.459, 5.37418 Z-:/0.689/79.459, 5.37418 Z0:/4000000.0/90.000, 9							

				<-SCMVA-> <-Sym I''k rms-->			

```

X----- BUS -----X
99112 [COLLECTOR2 20.000] 3PH
      LG      MVA      AMP      AN(I)
              437.38  12626.0  -78.73
              0.00    0.0    0.00
THEVENIN IMPEDANCE, X/R (OHM)  Z+:/0.689/79.459, 5.37418  Z-:/0.689/79.459, 5.37418  Z0:/4000000.2/90.000, 9

```

```

-----
<-SCMVA-> <-Sym I''k rms-->
          /I/      AN(I)

```

```

X----- BUS -----X
99113 [COLLECTOR3 20.000] 3PH
      LG      MVA      AMP      DEG
              437.38  12626.0  -78.73
              0.00    0.0    0.00
THEVENIN IMPEDANCE, X/R (OHM)  Z+:/0.689/79.459, 5.37418  Z-:/0.689/79.459, 5.37418  Z0:/4000000.2/90.000, 9

```

```

-----
<-SCMVA-> <-Sym I''k rms-->
          /I/      AN(I)

```

```

X----- BUS -----X
110000 [GAMESAPV 138.00] 3PH
      LG      MVA      AMP      DEG
              1274.64  5332.7  -79.29
              745.66  3119.6  -82.67
THEVENIN IMPEDANCE, X/R (OHM)  Z+:/11.082/74.858, 3.69530  Z-:/11.082/74.858, 3.69530  Z0:/34.729/80.398, 5.

```